Master's thesis

NTNU
Norwegian University of Science and Technology
Faculty of Natural Sciences
Department of Materials Science and Engineering

Ronald Reagon Ravi Kumar

Modeling and Analysis of vertical bifacial agrivoltaic test system at Skjetlein high school, Norway

Master's thesis in Innovative Sustainable Energy Engineering
Supervisor: Marisa Di Sabatino Lundberg (NTNU), Sune Thorsteinsson (DTU)
Co-supervisor: Gaute Stokkan (SINTEF), Gabriele Lobaccaro (NTNU), Ashok Sharma (MNIT)

June 2022

NTNU
Norwegian University of Science and Technology

DTU

Ronald Reagon Ravi Kumar

Modeling and Analysis of vertical bifacial agrivoltaic test system at Skjetlein high school, Norway

Master's thesis in Innovative Sustainable Energy Engineering
Supervisor: Marisa Di Sabatino Lundberg (NTNU), Sune Thorsteinsson (DTU)
Co-supervisor: Gaute Stokkan (SINTEF), Gabriele Lobaccaro (NTNU), Ashok Sharma (MNIT)
June 2022

Norwegian University of Science and Technology
Faculty of Natural Sciences
Department of Materials Science and Engineering

NTNU
Norwegian University of
Science and Technology

Preface

This thesis is being delivered in partial fulfillment of a Joint Nordic MSc. in *Innovative Sustainable Energy Engineering and the Study track is Solar Cell Systems and Materials.* It was carried out in the spring semester of 2022 at *The Department of Material Science and Engineering, NTNU* in collaboration with SINTEF. This body of work corresponds to 30 ECTS. It was supervised by Marisa Di Sabatino Lundberg at NTNU and Gaute Stokkan at SINTEF. The co-supervisor from the Nordic Five Tech. partner university was Sune Thorsteinsson at DTU. Other co-supervisors are Gabriele Lobaccaro at NTNU and Ashok Sharma at MNIT.
This Master's thesis builds upon the work done in the fall semester of 2021 as part of a specialization project corresponding to 15 ECTS. Overlapping content has been amended accordingly.

June 2022
Trondheim, Norway
Ronald Reagon R

Acknowledgements

It would have been impossible to complete this thesis without God's blessings of health and wellbeing. In addition, the support and help of many people have made this thesis possible.

I want to begin by thanking my supervisor, Professor Marisa di Sabatino, Department of Materials Science and Engineering, NTNU, for her excellent guidance, support, and dedication throughout the thesis research. She was a great mentor and advisor during this journey. I would also like to thank Gaute Stokkan, my co-supervisor at SINTEF, who gave me this opportunity to work on this topic, provided me with invaluable guidance and feedback and challenged me to grow as a researcher.

My sincere thanks go out to my co-supervisor Sune Thorsteinsson, Project Manager, Department of Photonics Engineering Photovoltaic Materials and Systems, DTU, who was always available for online meetings and essential insights into the project.

Special thanks to Gabriele Lobaccaro, Associate Professor, Department of Civil and Environmental Engineering, NTNU, for guidance in microclimate trial studies and providing a study desk to write my thesis report. Your constant interest and enthusiasm in the project are greatly appreciated.

My special gratitude also goes to Ashok Sharma, Professor & Head (Formerly), Department of Metallurgical and Materials Engineering, Malaviya National Institute of Technology, Jaipur, India, for his fruitful collaboration, advice, and study guidance.

A special thank you goes to my dear friend and thesis partner Erlend Hustad Honningdalnes for long discussion hours, corrections, and suggestions during this thesis work. I respect his supervisor, Steve Völler, Associate Professor, Department of Electric Power Engineering, NTNU, for his constant guidance and support.

I thank all the teachers and administrative staff from Skjetlein videregående skole, Trondheim. Thanks to Stefan N Preisig, Assistant Principal, for his continuous support during site visits.

To conclude, and perhaps most importantly, I would like to express my deepest gratitude to my family, my wife, and my daughter for their love, support, and patience during my extended absence over the past two years.
To them, I dedicate this thesis.

I can do all things through Christ who strengthens me. Philippians 4:13

Abstract

The agriculture sector is facing three significant challenges: i) food production must double by 2030 in order to feed an ever-growing population, ii) decrease in the amount of arable lands and iii) accelerating climate change. Agricultural crop is exposed to extreme climate events and lacks water due to heat stress. With frequent drought and growing unpredictability in climate, it has become the need of the hour to have systems running on fully-renewable energy sources, not to mention the urgent need to preserve, rather than deplete, ever-scarcer water resources. Systems of this nature enable us to work towards increased crop productivity by making farmlands more resilient to climate extremities/change.

Innovative solution like agrivoltaics can address these problems. They adapt photovoltaic(PV) technology so as to coexist with crop cultivation. Agrivoltaics are attracting a lot of attention across the globe, especially in regions where PV power plants and agricultural practices are common. As of this writing, there have only been two agrivoltaic studies in continental climate zones.

Norway has been doing well in terms of its renewable energy mix by fully utilizing its hydro energy resources. Norway was previously classified as a country with low PV potential, but as of 2021, it has a total installed PV capacity of 216.8 MW. Norway's agriculture sector is doing fairly well, especially when you consider the challenges involved: cold winters, hilly mountain areas, and high relative humidity. The backbone of Norwegian agriculture is grasslands and livestock, i.e., grassland covers 70% of Norwegian agricultural land

The potential usage of agrivoltaics in Norwegian conditions has not been researched so far. This thesis aims to find a suitable modelling procedure to model a vertical bifacial East/West oriented agrivoltaic system. This model uses a 53.3 kWp agrivoltaic system, located at Skjetlein videregående skole, Trondheim (N63°41.06′ E10°45.39′) with 'timothy grass' as a crop. Crop yield will be estimated using the CATIMO crop model.

The energy analysis results agree well with the literature concerning the performance of vertical bifacial systems in Norwegian conditions. In an agrivoltaic scenario, vertically East/West oriented PV systems provide a homogeneous light distribution compared to conventionally oriented South-facing PV systems. Sun hour analysis reveals different shading patterns on crops near the edges of PV modules compared to internal rows. Estimated land-use efficiency of agrivoltaic systems is 79% higher than the efficiency of conventional land use, either for PV power plants (100% energy) or for the cultivation of crops (100% crop).

Overall, the methodology developed in this thesis is an effective modelling tool that can be used for other agrivoltaic configurations, crops, and climate zone.

Nomenclature

AVS Agrivoltaic System

CAPEX Capital expenditure

CSV Comma separated value

DLI Daily light integral

ECMWF European Centre for Medium-Range Weather Forecasts

EPW EnergyPlus weather file

LCP Light compensation point

LSP Light saturation point

NREL National Renewable Energy Lab

NSRDB National Solar Radiation Data Base

PAR Photosynthetic active radiation

PPFD Photosynthetic photon flux density

PV Photovoltaics

PVPP Photovoltaic power plants

TMY Typical meteorological years

Table of Contents

List of Figures

List of Tables

1 Introduction

Global challenges such as climate change, geopolitical crises, extreme poverty, food demand, and pandemics, are large, complex, and intractable. This is especially true in densely populated emerging countries, where addressing these problems is becoming increasingly crucial. Problems like increase in population, decrease in groundwater level, and increases use of chemical fertilisers are prevalent at local scale. However, a local problem can affect people across borders due to the effect of globalization. It is the responsibility of an engineer to look at micro and macro problems holistically.
The recent geopolitical crisis between Russia and Ukraine has revealed just how many countries depend on fossil fuels to meet their energy demands. This has motivated the European commission to speed up the roll-out of renewable energy projects and to be independent of Russian fossil fuels well before 2030 [1]. The success of such bold decisions hangs on robust planning, and implementing those plans via changes in policy. Furthermore, there are plans to bring photovoltaic (PV) module manufacturing back to Europe from China in order to boost Europe's manufacturing capacity for solar energy [2]. It is estimated that by 2030, 480 GW of wind energy and 420 GW of solar photovoltaic (PV) energy will be able to replace 170 billion cubic metres (bcm) of Russian gas. This is just one of many examples showing increased demand for renewable energy systems. However, the question is whether or not we have enough land area to install such massive solar PV projects? Based on data from 2018, 40.9% of land in the European Union is agricultural and 24.7% of land area is arable [3]. These percentages are in decline due to rapid urbanisation, farming policies, and land abandonment. All fertile and profitable arable land is precious and must be safeguarded so as to meet agricultural demands. This causes issues sharing land between solar PV projects and agricultural areas.
Solar and wind resources are intermittent sources of energy and their potential varies based on geographical location. There are no universal solutions - each country must to develop or adapt renewable energy technologies based on their available resources. For example, the PV power potential of Southern Norway is in the range of 730-1095 kWh/kWp [4] whereas it is 949-1168 kWh/kWp [5] and 1095-1972 kWh/kWp [6] for Southern Sweden and the whole of Spain respectively.
With climate change becoming a more pressing concern, the demand for cleaner and affordable energy has been on a rise. In parallel, we also see an increasing demand for food production techniques that are less resource-intensive, especially in reference to water usage. It remains an ongoing challenge for the scientific community to collectively address such challenges. In most cases, clean energy comes from setting up renewable energy networks, while sustainable agricultural practices lead to reduced food and water waste. These challenges have independent solutions, and so can be tackled concurrently. As a result of extensive research [7] and testing in recent years, agrivoltaic technology has already demonstrated that it is capable of collectively addressing the issues discussed above. Agrivoltaics involve growing food crops under or between solar panels in order to increase land use efficiency. In other words, agricultural land will be used to install solar PV power plants and generate electricity without decreasing the agricultural output of that land. Agrivoltaics map cleanly to several of the UN's Sustainable Development

Goals (SDGs), shown in Figure 1. Agrivoltaics are a win-win for clean energy and sustainable agriculture, and have the potential to meet the demand for clean & affordable energy [SDG-7] and food [SDG-2], as well as to reduce water wastage in agriculture [SDG-6].

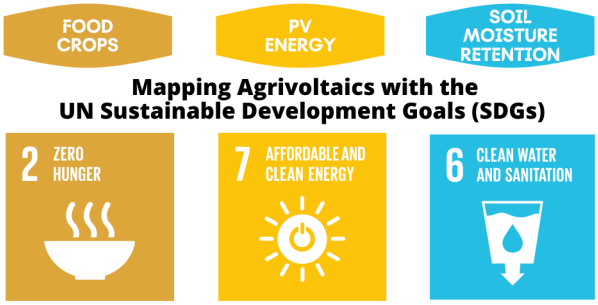

Figure 1: Agrivoltaics mapped against a few of the UN's Sustainable Development Goals.

Combining solar PV and agriculture leads to a wide range of positive effects, including improved crop production [8], better water retention in the soil beneath a PV array [9], and lower maintenance costs. Moreover, it can increase revenue for all parties involved. However, these systems haven't yet been specifically designed for Norwegian weather conditions and food crop types.
This thesis attempts to fill that gap by designing, modelling, and analyzing a vertical bifacial agrivoltaic test system. The modelled system is located at Skjetlein videregående skole (N63°20.27′ E10°18.8′) a school in the South of Trondheim, Norway. Students learn both conventional and organic farming at this school. The school's educational activities include the cultivation of organic grass, grains, vegetables, fruits, berries, and herbs. Moreover, the school has renewable energy systems, a compositing reactor, and sheep farming. This would be an ideal place to implement the designed model in practice.

1.1 Background

In 1982, Goetzberger and Zastrow, developed the concept of co-producing PV energy and food on the same plot of land [10]. The first field test was carried out in Japan [11] in 2004, and was called "solar sharing". In 2011, Dupraz C et al. coined the term 'agrivoltaics' and further developed the concept of producing PV energy and food crops on same land area in order to enhance land use efficiency [8]. The primary objective of early agrivoltaic research was to solve the land constraint problem encountered during the installation of ground-mounted PV systems. Increasing research in agrivoltaics has revealed that it can provide other benefits, such as retaining soil moisture, reducing heat stress on crops, increasing revenues for farm owners, and creating microclimate.

Figure 2 illustrates land use efficiency with and without agrivoltaics. Note that the percentages shown are an assumption. The increase in land use efficiency is usually quantified using the land equivalent ratio (LER).

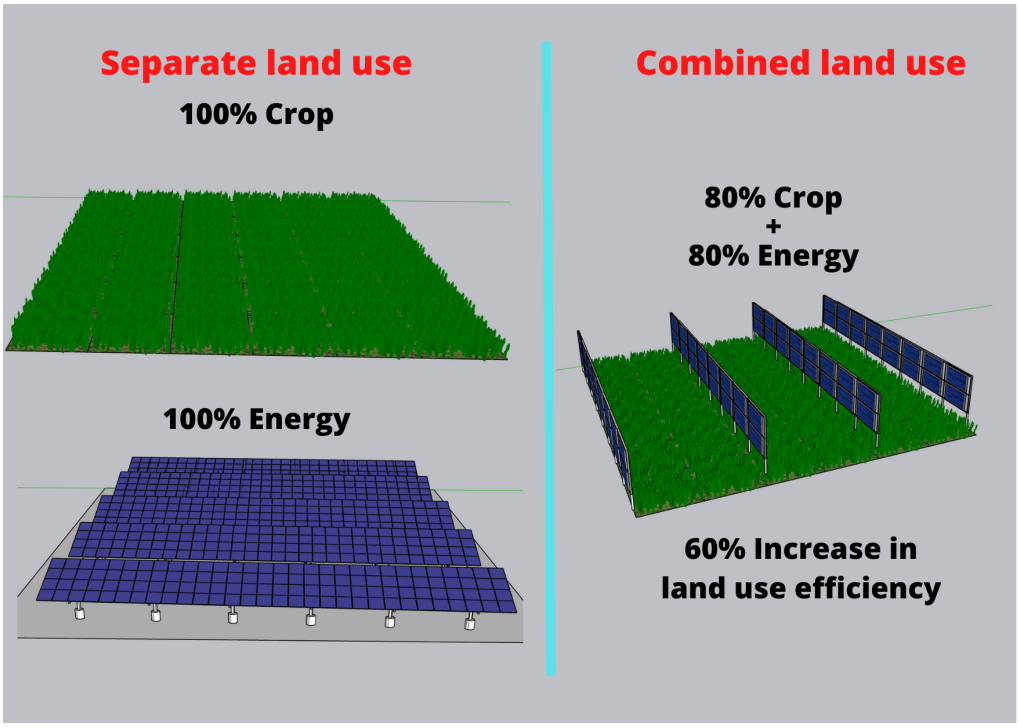

Figure 2: Comparison of separate land use and combined land use.

The concept of LER can be applied to any system that combines two or more types of production on the same land unit. This was first proposed for agrivoltaic systems by Dupraz et al. in 2011[8]. LER is represented by a simple equation:

$$LER = \frac{Y_{cropAVS}}{Y_{monocrop}} + \frac{Y_{electricityAVS}}{Y_{electricityPV}} \tag{1}$$

where the monocropping system refers to growing crops in open field; PV refers to a conventional ground mounted PV plant, and AVS refers to the dual-use agrivoltaic system. If the land productivity of the agrivoltaic system increases as compared to separate PV and agriculture usage, then LER value will be greater than 1[12]. Nassar et al.,[13] reported that the LER approach ignores other important factors, such as initial investment, maintenance cost, and soil condition. LER only considers system revenues and excludes expenditures.
The growth rate of agrivoltaic research publications was 80% in 2021 compared to 2020. The current total worldwide installed capacity of agrivoltaic systems has increased to 14 GW [14] from just 5 MW in 2012 [15]. With that said, there has not been as much research on the East/West (E/W) vertical bifacial PV system and in countries that sit at higher latitudes, like Norway.

1.1.1 Literature review on vertical bifacial agrivoltaic systems

Hassan Imran et al.(2021) [16] have modelled East/West vertical bifacial PV systems for á location in Pakistan (Lahore, N31°53.03′ E74°35.77′). They computed the PV energy output and ground irradiance available to the crops. Among the rows of vertical bifacial panels at certain pitch-to-height ratios, they suggest a design that provides equally homogeneous ground irradiance to crops.
For same location, studies by Zamen Tahir et al.(2022) [17] also proved that for any given row to row PV module spacing, vertical PV modules facing East/West produce the greatest spatial homogeneity and intensity of photosynthetically active radiation (PAR).
Ramachandran A V et al.(2021) [18] modelled vertical bifacial agrivoltaic farms and compared two different bifacial PV panel technologies for the South-Eastern part of India (Chennai, N13°8.27′ E80°27.07′). It appears that silicon heterojunction (SHJ) technology is more efficient in terms of energy yield compared to passivated emitter rear contact (PERC). In conclusion, an optimal sharing of the solar spectrum between crops (in this case rice) and PV panels could result in a win-win scenario.
Pietro Elia Campana et al.(2021) [19] developed an optimization model to evaluate vertically mounted agrivoltaic systems with bifacial PV in Sweden. The outcome showed that the lower pitch values between rows of PV arrays could reduce crop (in this case potato and oat) yield upto 50%. A land equivalent ratio (LER) of 1.2 was estimated for a location in Sweden (Västmanland, N59°55.49′ E16°75.85′). This study used Environmental Policy Integrated Climate (EPIC) crop model for estimating crop yields. Further, they evaluated the temperature distribution and energy performance of a vertical bifacial PV module for agrivoltaic applications, using a 3D computational fluid dynamic model [20].
Odysseas A K et al.(2022) [21] studied limitations and potential synergies associated with agrivoltaic system. The multi-scale modelling of agrivoltaic system for a location in USA (Boston, N42°36.98′ E−71°1.63′) suggested that, for permanent crops, a vertical East/West orientation is more appropriate than South-North(S/N).
Hassan Imran et al.(2022) [22] group developed a new approach 'light productivity factor (LPF)' to optimise vertical bifacial agrivoltaic system. Based on this approach, a given crop type and PV array design can together be evaluated for their effectiveness at sharing irradiance.
In conclusion, there has been no crop-specific optimisation of the system, except one study from Sweden [19]. It is imperative that we start desigining agrivoltaic systems that are well-suited to local weather conditions (solar potential) and crops that are popular in the region.This thesis approaches the concept of agrivoltaics by combining a locally popular crop with most suited PV systems configuration in Norway.

1.1.2 Modelling approaches

There are various approaches followed when designing and optimizing different types of agrivoltaic system configurations. Modelling approaches are usually used to arrive at

good designs that enable optimal sharing of light between crop and PV panels. Table 1 provides selected examples of modelling tools/approaches used for a sampling of prior work in this area. These were selected based on the diversity of tool being used, and the type of agrivoltaic system. "PV" tools are mainly used for energy yield estimation of the PV systems. Similarly, "crop" tools are either used for crop yield estimation or to estimate photosynthetically active radiation(PAR) and sunlight hours available to the crops.

Table 1: Selected examples of modelling tools used in agrivoltaic research

Reference	Agrivoltaic system	Tools used	
		PV	Crop
Vijayan et al. (2021) [18]	Vertical bifacial East/West oriented	Energy3D	WARM rice yield model
Max Trommsdorff et al. (2021) [23]	Fixed tilt,elevated, bifacial, South/West oriented	ZENIT	-
Joshua M Pearce et al. (2017)[24]	Fixed tilt, elevated, monofacial, South oriented	SAM-NREL	-
Harinarayan T et al. (2014)[25]	Fixed tilt, elevated, monofacial, South oriented	PVsyst	-
Deng Wang et al.(2017)[26]	Fixed tilt, ground mounted, monofacial South oriented	PVsyst	Ecotect
Atsutaka Yamada et al. (2021)[27]	Missing information	SketchUp	Sunhour plugin
Martin Elborg (2017)[28]	Fixed tilt, ground mounted & elevated, monofacial South oriented	-	Mathematica
Riaz, Muhammad Hussnain, et al. (2021) [29]	Vertical bifacial East/West oriented	Sandia PV library	MATLAB, Mie scattering theory
Alexander Nassar et al. (2020)[13]	Fixed tilt, ground mounted, monofacial South oriented	SAM-NREL	-
David Jung et al. (2021)[30]	Fixed tilt, elevated, monofacial, South oriented	SAM-NREL	-
Pietro Elia Campana et al.(2021) [19]	Vertical bifacial East/West oriented	OptiCE	EPIC growth model
Odysseas A K et al.(2022)[21]	North/South facing, East/West wings, and East/West vertical bifacial systems	Radiance ray-tracer	PAR based model

1.1.3 Bifacial solar cell technology

Bifacial PV technology's share of the PV market has rapidly risen in recent years, which has helped unlock new possibilities for performance improvements, not to mention solving new problems [31]. Figure 3 describes the projected market share of technologies with the capability of absorbing light both from the front and rear side of the panel, if suitable electrical contacts are designed. The market share of bifacial cell technology will likely hit 85% in 10 years as compared to 50% in 2021 (Figure 4). Therefore, it is right time and direction to look into the application of bifacial cell technology in agrivoltaics. As mentioned above, researchers across globe are already exploring synergies of bifacial agrivoltaic systems, especially in the area of vertical configuration systems.

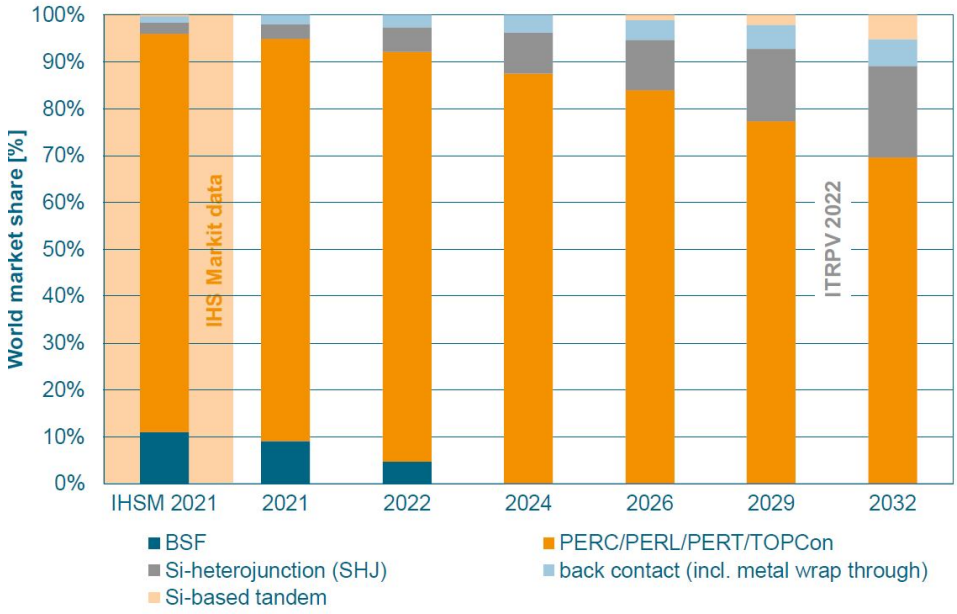

Figure 3: Projected market share by solar cell technology [32].

The acceptability of bifacial PV systems for electricity generation is influenced mainly by installation location, weather condition, and albedo number. According to studies by Guo et al., vertical bifacial PV panels receive higher irradiation than monofacial PV panels at higher latitudes (where the sun's altitude angle is lower) and higher albedo (subtropical regions) [33]. This implies that bifacial PV could perform well in Nordic countries, potentially spurring further research on this topic. Jouttijärvi, Sami, et al. [34] highlighted the benefits of vertical East-West mounted bifacial PV systems: a) generating electricity in the mornings and evenings, instead of noontime b) better symmetry between production and load profiles c) increased self-consumption and reduced grid interaction, and d) increased profitability. Even though while conventional South oriented bifacial PV systems provide better electricity production than vertical East-West mounted bifacial PV systems, the economic and utilisation benefits of the latter are hard to ignore.

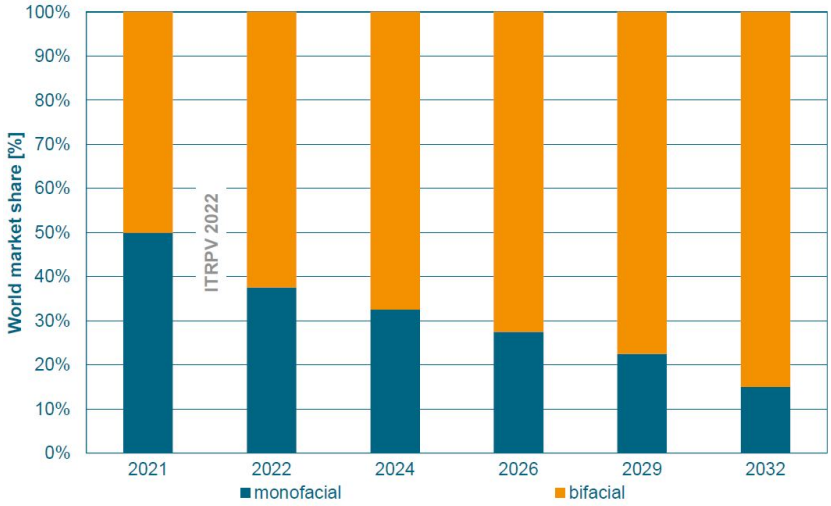

Figure 4: Projected market share by solar cell type [32].

1.1.4 Specialization project

I learned a lot about agrivoltaics during a detailed literature review I carried out as a part of specialisation project in a previous semester. The main objective of the project was to understand worldwide research trend on agrivoltaics and to identify the research gaps. Critical research findings that were extracted during this period is tabulated as matrices such that it can easily read and understood by anyone who is interested to start their research in the field of agrivoltaics. Before 2016, the agrivoltaic research studies were based on theoretical modeling of PV system such that enough light is available for crop growth and yield [8], microclimate studies [35] [36], and validation with real time data was carried by [37]. Most of them used the prior knowledge of PV system design to optimise the agrivoltaic design. However, the prediction of crop yield was purely based on PAR values that are obtained using theoretical models except study by [37] where they used a crop model to estimate crop yield. That means, only few used exclusive crop models to estimate crop yields.
There are countable number of studies till date that uses both energy and crop models in agrivoltaic research. However, modeling is powerful tool that saves you from bad designs, wrong assumptions, predicts close enough end results, and progresses your research. After 2017, agrivoltaic researchers have started to validate their modeling results with real time data especially crop yield [38], light management studies have become priority [26], soil moisture retention due to shade from PV panels has been extensively studied [9], different solar cell technologies were tried out [39], new approaches to explore more synergies of agrivoltaics [40] are common focus, and giant agrivoltaic systems have been installed [41].
It was noticed that, the research until recent years was focused on Northern hemisphere, optimising PV system design in order to share the sun light between PV panels and crops. Only a few studies on different solar cell technologies, and majorly shade tolerant crops

have been published. Looking at 2021 specifically, there were only three groups [42][19] [18] focusing on vertical bifacial agrivoltaic systems and they remained at the modelling stage at the end of the year. However, the corporation Next2Sun has developed patented vertical bifacial agrivoltaic systems [43] [44] and such systems have been installed in Sweden, France, Germany, South Korea, and Austria between 2019-2021 [45].
The research gaps identified during this study are listed below; note that the highlighted entries are relevant to Norway.

- Bifacial PV panels can used instead of monofacial panels, since solar energy is shared between crops and monofacial PV. Losses due to sharing can be recouped using bifacial panels.
- Lack of scientific evidence for vertically mounted agrivoltaic systems
- More research is required to arrive at an optimal solution for light sharing between PV panels and crops. One area that shows promise is the use of semitransparent PV modules.
- Establishing a relationship between microclimate and crop morphology & physiology, for specific crops.
- For agricultural practices with agrivoltaics, more research is needed on the morphology, yield, and nutritional value of crops grown by an agrivoltaic system.
- Many crops are studied in just a single climate zone. Cucumbers and grapes are studied once each in dry and temperate climate zones. It is necessary to cultivate the same crop several times in these climate zones and also in other climate zones (Polar and Continental climate zones), to understand crop morphology.

1.1.5 Solar potential and PV systems in Norway

In the report published by the energy sector management assistance program (ESMAP), Norway is 3rd-from-last in a listing of countries ranked according to their practical PV potential [46]. Figure 5 compares the average solar radiation between a summer month (July) and a winter month(January) in Norway [47]. It can be observed that there is large difference between summer and winter month's solar radiation values. In Skjetlein (N63°34.12′ E10°30.16′), Trondheim, values of around 150-200 Whm^{-2} per day are expected in January, and 4000-4500 Whm^{-2} per day in July. It follows that, there is enough solar energy available to be harnessed during summertime by utility scale PV power plants (PVPP) in Norway. Utility scale PVPP require relatively flat land without mountainous sections. However, due to increase in energy and power densities in recent years, PVPP are not as land intensive as they were 10-15 years ago [48]. Even so Norway does not have too much land suitable for utility-scale PVPP, most candidates are either already being used for farming or to build urban landscapes. As per data from 2019 the share of installation capacities in different sectors in Norway are: Residential ($\leq$15 kWp) 36 %, Commercial (15-250 kWp) 23 %, Industrial ($\geq$250 kWp) 35 %, Off grid 4 %, and building integrated PV(BIPV) 2 % [49]. The higher percentage in residential sectors indicates the climate cautiousness of people and the potential to integrate PV systems into Norwegian power systems.

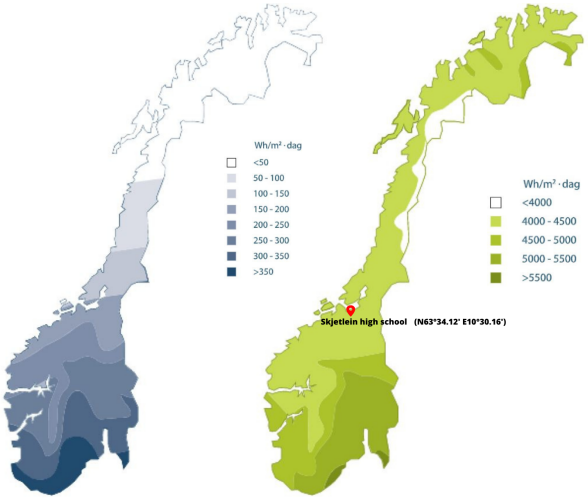

Figure 5: Average daily solar radiation received by a horizontal surface in Norway, in January (left) and in July (right) [47].

Figure 6 shows total installed solar PV capacity in Norway from 2011 to 2021, and is based on various reports [50] [51] [52] and article [53]. It can be observed that at the beginning of 2021, the installed photovoltaic capacity in Norway was 152 MWp with just $\approx$ 28Wp/capita, contributing only 0.02% of world's total installed capacity. However, the growth rate between 2020-2021 was around 42% as compared with 21% between 2019-2020. The trend shows the potential for a PV market in Norway. Being a country that lacks large flat areas, the increasing trend of PV capacity is very promising and motivational.

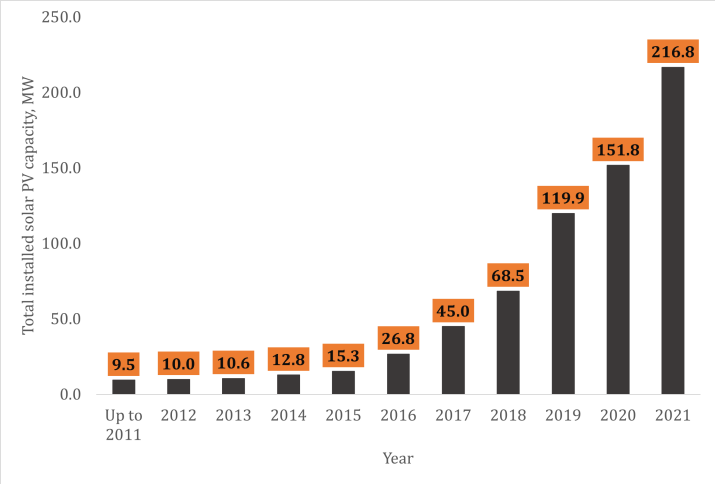

Figure 6: Total installed solar PV capacity in Norway from 2011 to 2021

1.1.6 Agriculture sector in Norway

Norway may appear to be unsuitable for active farming across the country because of the high mountains, limited arable land, fjords, severe winters, and short summers. However, traditional family farming is keeping the country's agricultural sector alive. Productive or fertile land area available for growing many important crops is around 3% in Norway. A third of this land is used to grow food grains, and the rest is used as grasslands. Therefore Norway is classified under the category of European countries where sugar crops like sugarcane or sugar beet cannot be produced. It is a well known fact that the soil quality needed for farming is determined by topography, geology, and biology. Further, the type of crops that can be grown is determined by climate, irrigation facilities, and geographical location [54]. For example, dates are usually grown in dry arid zones with irrigation. Northern Norway is classified as a cold polar zone, while Southern Norway is more temperate. In comparison with other European countries, Norway's grain output per hectare is lower. Growing fodder crops like grass is the only alternative in most areas of Norway.
The success of Norwegian agriculture is mainly due to high quality fodder that in turn contributes to livestock production. The quality of fodder is maintained due to the cold climate that prevents the spread of grass diseases and pests. Figure 7 and 8 show that cultivated grasslands are the major crop in every region of Norway. There are three dominant grassland species in most parts of the country, timothy (*Phleum pratense L.*), meadow fescue (*Festuca pratensis Huds.*) and red clover (*Trifolium pratense L.*). However, the production of ryegrass (*Lolium perenne L.*) has been increasing in Southern areas of Norway [55].

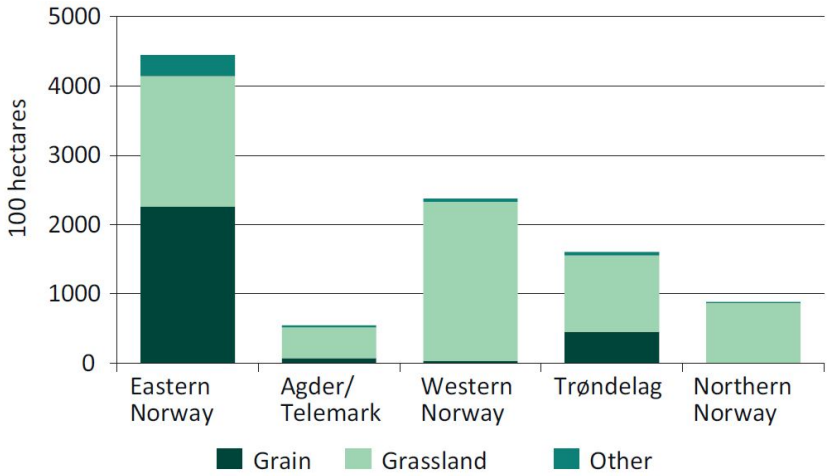

Figure 7: An overview of the main crops in Norway by region. Source: Statistisk sentralbyrå (2019a), preliminary figures[56].

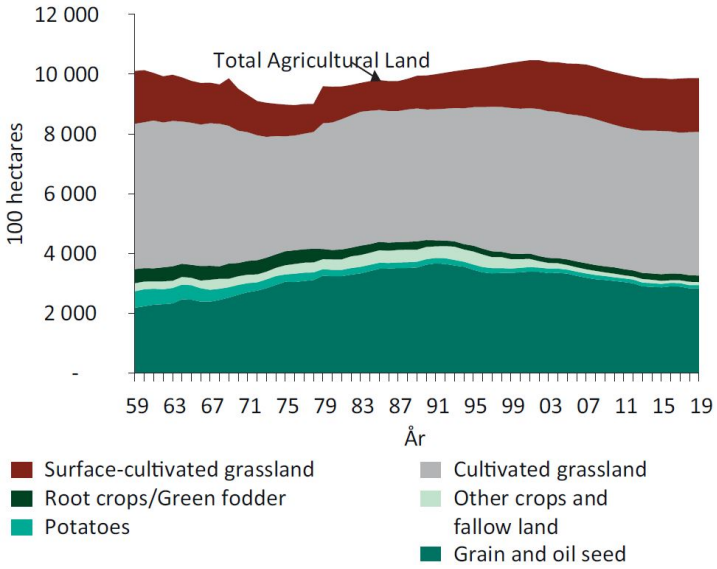

Figure 8: Norway's agricultural area by main crops, 1959-2019. Source: Budsjettnemnda for jordbruket (2019a)[56].

1.1.7 Norway in 2030

As on 2020, Norway is the 2^{nd} country in the world after Iceland in terms of electricity consumption per capita [57]. Based on population forecast data [58] [59] [60], Figure 9 estimates population growth and the corresponding growth in electricity consumption by the year 2030. The numbers indicate that food and energy production will be in demand in the near future. As Norway aims towards being carbon neutral by 2030, energy and food demands will have to be met with renewable energy sources and sustainable agricultural methods.

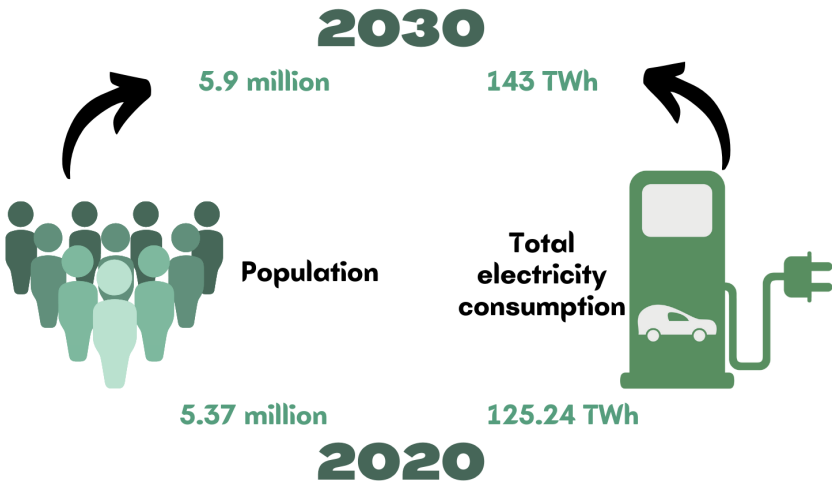

Figure 9: Norway's estimated population growth and associated electricity consumption by 2030

1.2 Thesis Objectives

Various subsections of Section 1.1 described the potential of agrivoltaic systems to solve societal needs like energy and food demands. As a sustainable energy engineering students, it is our responsibility to find newer solutions for these modern problems. The solutions must be sustainable & economically viable, work on global and local scales, allow implementation without political barriers. Agrivoltaics is one among several solutions, that address food and energy demands at global and local levels.
In order to explore the potential of agrivoltaics that could meet the future food-water-energy demands of Norway, a detailed theoretical and practical study has to be carried out. So far there are different modelling approaches followed in the literature. In this thesis, we have tried to develop a new modelling approach to quantify the availability of light energy to the crops in an vertical PV system set up. This also includes optimisation of certain parameters. This is will be our first main objective.
As a next step, finished model will be applied to a 53.3 kWp vertical bifacial agrivoltaic system at a selected test site in the region of Trondheim (N63°43.39′ E10°39.65′), Norway. This is done by combining the PV potential described in section 1.1.5 with timothy grass fodder in section 1.1.6.
To fulfil above said main objectives, following sub-objectives have been listed.

- Exploring various software in order to understand the functionalities that could suit agrivoltaic system modeling.
- Theoretically checking the performance of vertical bifacial systems for Norwegian condition and also in an agrivoltaic scenario.
- To determine the impact of edge effect of PV arrays on the crops using Grasshopper-Ladybug tool and ClimateStudio.
- Radiation map analysis to determine homogeneity and percentage light available to the crops due to PV array shading using Rhino3D-Climate Studio.
- Modeling of 53.3 kWp vertical bifacial agrivoltaic test system for the location of Skjetlein videregående skole (N63°34.12′ E10°30.16′) and estimation of crop yield using timothy crop model.
- Estimation of land equivalent ratio for the test system.

1.3 Thesis structure

The summary of each chapter is as follows:
Chapter 1: A general introduction and background to the thesis that acts as supporting literature for the problem statement. What are the current issues that need immediate attention, what is the proposed solution in this thesis, and what is developed in the Norwegian context?. This leads to a brief section on vertical bifacial agrivoltaic systems, growth of bifacial solar cell technology, overview of the specialization project, the solar potential of Norway, Norway's agriculture sector, and future demands.
Chapter 2: Here theories that are required for the discussion of results are presented. There are three major sections in this chapter: Crops, solar PV technology and agrivoltaics. This includes all the basic definitions, theories, terminologies, related facts,

and illustrations. All the illustration and graphical images (except the images of crops) in this chapter have been created using *Canva* and *SketchUp Pro*.
Chapter 3: A detailed description of all the processes and procedures followed in this thesis is presented. Initially, vertical bifacial PV systems' energy yield is estimated, and its adaptability is verified in an agrivoltaic scenario. Later suggested design from this step is modelled and verified whether the required light is available to the crops. Further, this procedure is implemented to a 53.3 kWp agrivoltaic system case study and estimates crop yield using a crop model.
Chapter 4: All the results obtained so far are presented here. The results are presented in same order as methodology.
Chapter 5: The results presented in Chapter 4 are compared with literature. This is the hardest part of the report because some of the procedures have never been tried in a research setting before. Even so, present a discussion on the case study that validates our newly developed procedure for agrivoltaic system designs.
Chapter 6: Lessons learnt in this thesis and overall observation are presented as concluding remarks in this chapter.
Chapter 7: At the beginning of this thesis, there was a plan to setup a test site in the Trondheim region. Due to certain practical issues, this didn't pan out. However, the project received a grant from the Regional Research Foundation Trøndelag (Regionalt Forskningsfond Trøndelag) to carry out agrivoltaic research under name 'Soldeling i Trøndelag' solar sharing in Trondelag region. The procurement of vertical bifacial system is underway and the next batch of students will carry out data collections from this facility. This chapter discusses certain details about potential future projects.

2 Theory

This chapter will present the theory necessary to understand this thesis. The theory is mainly related to solar cells and food crops. The discussion begins with brief theory on monofacial and bifacial PV panels , and then move onto more advanced topics such as azimuth angle (horizontal angle), tilt (vertical angle), albedo, bifaciality gain, and weather data. A detailed description of conversion of sunlight into crop biomass is included as well.

2.1 Solar cells

2.1.1 Difference between monofacial and bifacial PV panel

Monofacial solar panes convert solar energy to electricity only on their top faces, as shown in shown in Figure 10. Bifacial panels produce electricity on both sides, both from the direct sunlight and reflected light that rebounded from the ground. The rear side also produces electricity when diffused light strikes it from clouds, buildings, and other objects. Yield can be optimized based on the albedo of ground and surrounding (Section 2.1.3).

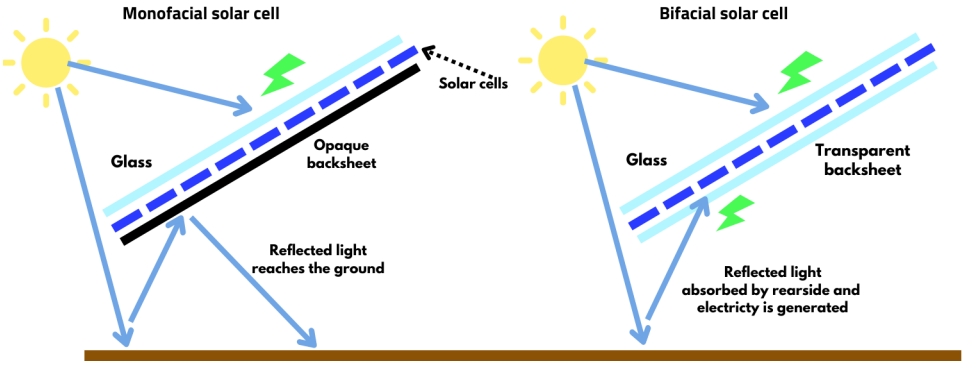

Figure 10: High-level overview of monofacial vs. bifacial solar cells

2.1.2 Bifaciality

Bifacial solar cells are the result of the ever-present need to generate as much energy as possible from the same surface area. Bifacial solar panels can collect direct-incident light and albedo radiation on both sides. They are now available at a similar price per Watt as conventional monofacial panels, which makes for a lower levelised cost of energy (LCOE). They are currently used as sound barriers on highway roads, fences for farmland, floating systems and even in large scale PV systems. Advantages vary according to the type of mounting configuration, as shown in Figure 11. For example, in vertical East/West mounting systems, it is possible to generate electricity during times of peak demand while avoiding the issue of snow settling on panels.

However, the selection of mounting configuration depends on geographical location (latitude, cost of electricity), sun's altitude (It will be studied in later part of the thesis), and economies of scale.

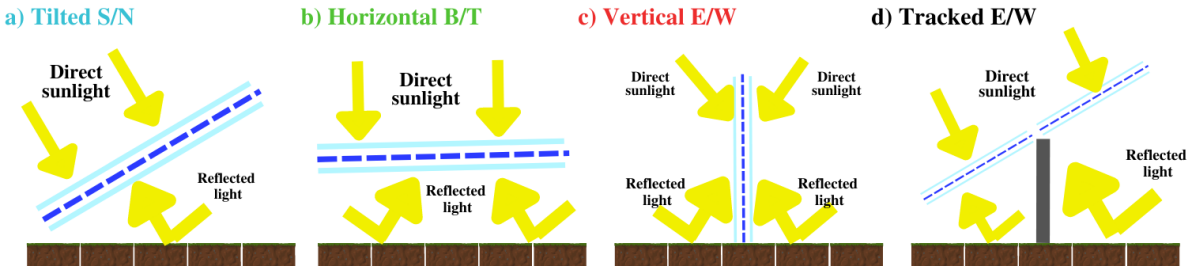

Figure 11: The ways a bifacial solar panel can be mounted: a) Tilted South/North(S/N), b) Horizontal bottom/top (B/T), c) Vertical East/West (E/W) and d) Tracking East/West

For the Skjetlein (N63°34.12′ E10°30.16′) location, the configurations from Figure 11 gives annual energy output as shown in the Figure 12. The North/South configuration is tilted at 49° which is the optimal tilt for Skjetlein. The tracking system used a PV array oriented to Southwards with a fixed tilt of 49° and was tracked about its vertical axis from East to West.
Simulations was performed with PVsyst, with a system size of 5 kWp. Output values depend on the type of PV panel chosen: specifically the panel's efficiency and the bifaciality factor(BF). Configurations are compared using the same front-side efficiency and bifaciality factor.
Bifacial gain (BG) and BF are two significant criteria for bifacial PVs' performance that are frequently explored in research. The ratio of rear to front side efficiencies is represented by BF. Bifaciality gain is the extra energy yield that bifacial PV panels have over monofacial PV panels [34].
Bifaciality factor is typically less than 1 and is specified by the product manufacturer. Bifaciality gain is location- and design-specific. Back in Figure 12, 17% bifaciality gain can be observed for BF=0.85 and albedo=0.3. In all the mounting configurations presented here, bifacial panels yield more energy than monofacial panels. As it is expected, bifaciality gain varies by configuration. While energy is always generated from both sides of the bifacial panels, they will not always contribute to the efficiency output of the cell in the same proportion. The front side is usually textured to trap more light by causing total internal reflection, while rear side is untextured and so reflects more light.

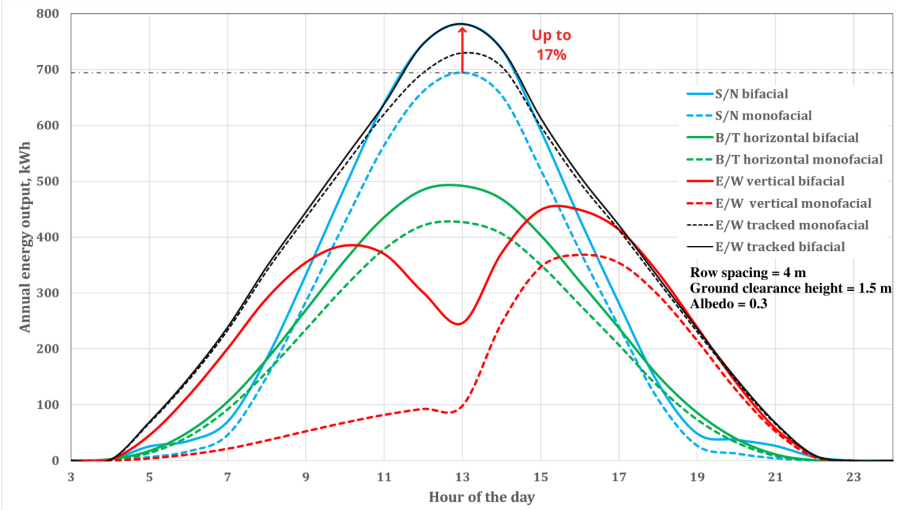

Figure 12: Annual energy output for each hour of the day for a 5 kWp system in different mounting configurations.

2.1.3 Albedo

As discussed above, the rear-side of a bifacial PV panel absorbs light that is reflected from the ground. The quantity of light reflected depends on reflection coefficient of the ground, also known as 'albedo'. If all the light is absorbed then albedo=0, and albedo=1 if all the light is reflected. The average value of Earth's albedo is ≈ 0.2, but outliers are not uncommon. For example, the albedo can be 0.9 for freshly fallen snow. Albedo coefficients is more important in vertical mounting configurations because a larger surface area of the PV panel is exposed to the ground.
In conventional PV systems (South-oriented fixed tilt systems with monofacial PV panels), the albedo of the ground is not as significant and is assumed to be constant in energy yield simulations. The albedo of a surface is not constant, however: it depends on the season, the impact of rain, and reflective properties of the ground. Ground albedo becomes significant when bifacial PV panels are used. The percentage difference of various components of light between the front and rear sides of PV panels is clearly visible in Figure 13 and 14. In Figure 14, ground-reflected light has a significant share in yearly irradiance for the rear-side, while on the front side, beam irradiation has a significant share as shown in Figure 13 [61].

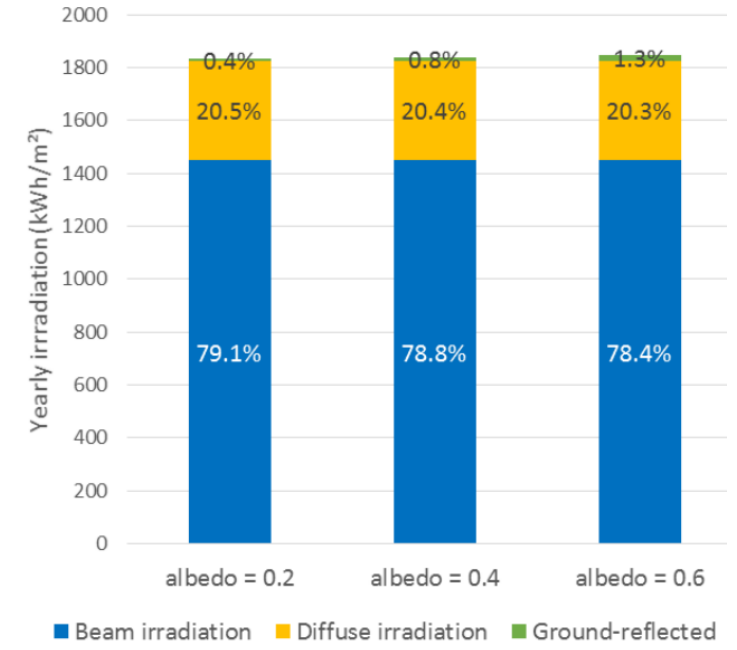

Figure 13: For different albedo values, contributions of various components of light to the yearly irradiance received on a PV panel's front-side [61].

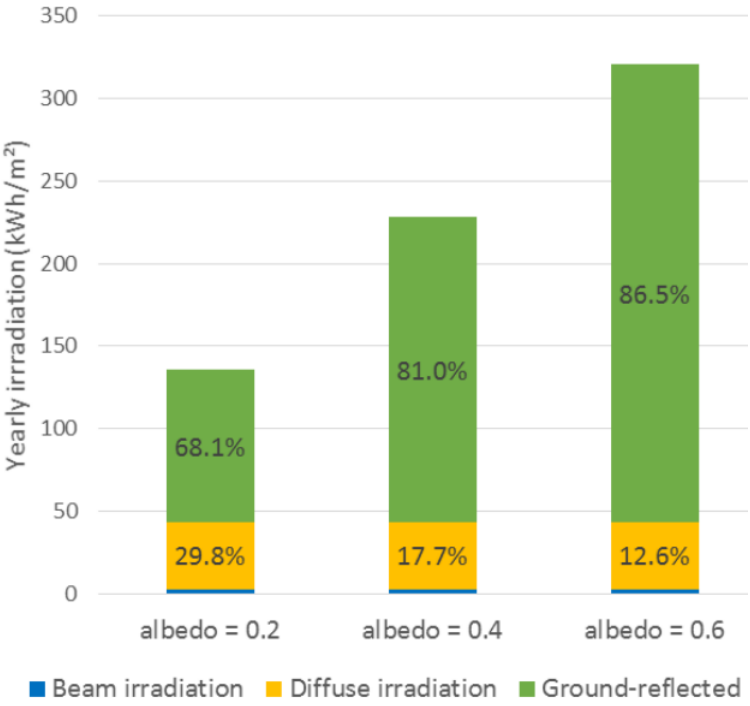

Figure 14: For different albedo values, contributions of various components of light to the yearly irradiance received on a PV panel's rear-side [61].

Table 2 shows albedo numbers for various surfaces.

Table 2: Albedo values of various surfaces [62]

Surface	**Albedo**
Grass	0.15-0.25
Fresh grass	0.26
Lawn	0.18-0.23
Dry grass	0.28-0.32
Soil	0.17
Gravel	0.18
Fresh/clean concrete	0.3
Old/dirty concrete	0.2
Red tiles	0.33

Surface	**Albedo**
Cement	0.55
Asphalt	0.15
Forest	0.05-0.18
Sand	0.1-0.25
Water	0.05-0.22
Fresh snow	0.8-09
Old snow	0.45-0.7
Alumimium	0.85

2.1.4 PV performance

In general, PV power plants' performance degrades over time, especially after ten to fifteen years. Installation quality will determine future performance, but operations and maintenance practices will also affect PV performance to some degree as well. PV performance can be assessed using three parameters: Performance Ratio (PR), Specific Yield/Production, and Capacity Factor (CF).

Performance Ratio (PR)

Performance ratio is a measurement standard for determining how well PV plants perform during actual operations. This is done by tracking actual performance and benchmarking it against the theoretical performance estimated during modelling stage. It is calculated using following expression.

$$\text{PR} = \text{Actual output in kWh} \;/\; \text{Theoretical output in kWh} \tag{2}$$

Where,

$$\text{Theoretical output} = \text{Solar irradiation} * \text{PV module area} * \text{Module efficiency} \tag{3}$$

PV plant performance and PR can be affected by a few factors: operating temperature, shading losses, module orientation (azimuth), DC/AC wiring losses, inverter efficiency, O&M practices like cleaning, and predictive maintenance.

Specific yield

Performance metrics for PVPP are commonly measured in terms of Specific Yield (kWh/kWp). Different locations and designs can be compared using this metric. The specific yield is the ratio of the annual energy produced to the installed PV capacity. Specific yield can be affected by a few factors: location, weather, design, and quality of PV modules.

Capacity Factor (CF)

In a PV plant, the Capacitor Factor is the ratio of actual output (kWh) to a theoretical maximum output assuming the PV plant runs at full capacity all year round, which is not possible in practice.

2.1.5 Solar geometry

There are certain solar angles used in this thesis work while designing PV systems. Definitions are presented below, and Figure 16 contains a visual representation of each type of solar angle.

PV collector tilt (β)

The angle between the PV collector surface and the horizontal plane. It is denoted by the symbol β and usually varies from 0° (horizontal) to 90° (vertical). The term 'tilt' used in this thesis refers to PV collector tilt.

PV collector azimuth (γ)

The angle between the direction the surface is facing and South. The direction a surface is facing is a vector normal to the surface. The azimuth of a PV collector can vary from -180° to +180°, where the azimuth is 0 when the collector is facing due South, and has negative values to the East and positive values to the West. Figure 15 (left) shows azimuth values in relation to the points of the compass. As an example of the azimuth of a surface, a surface and its normal (projected horizontally) have been drawn in blue on the same figure (right). This allows, the azimuth of this surface to be computed, as shown in Figure 15 (right).

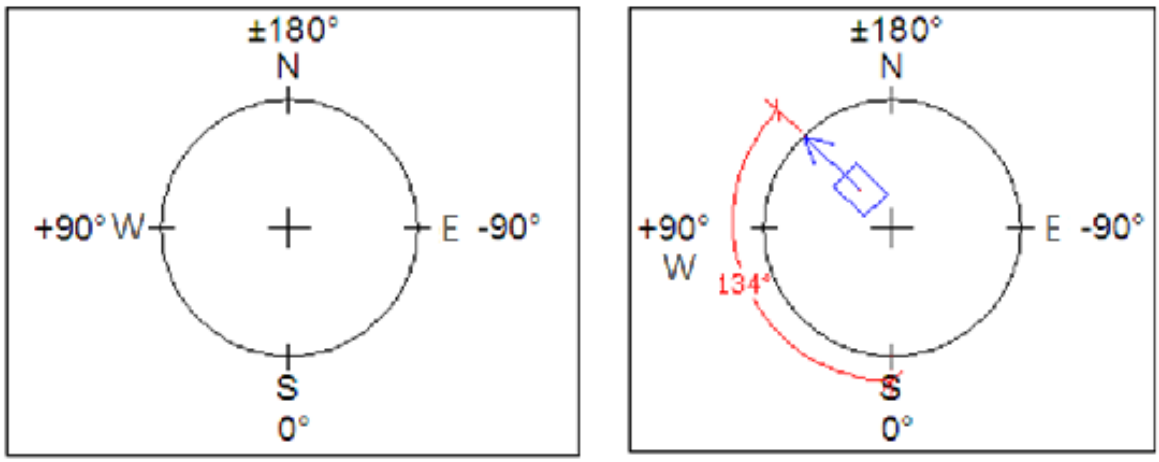

Figure 15: The range of values for the azimuth of a surface (left) and an example (right) [63]

Solar zenith angle (θ_z)

The angle between a vertical line and the Sun.

Solar altitude angle (α_s)

The complement of the solar zenith angle. Altitude = 90 - zenith angle.

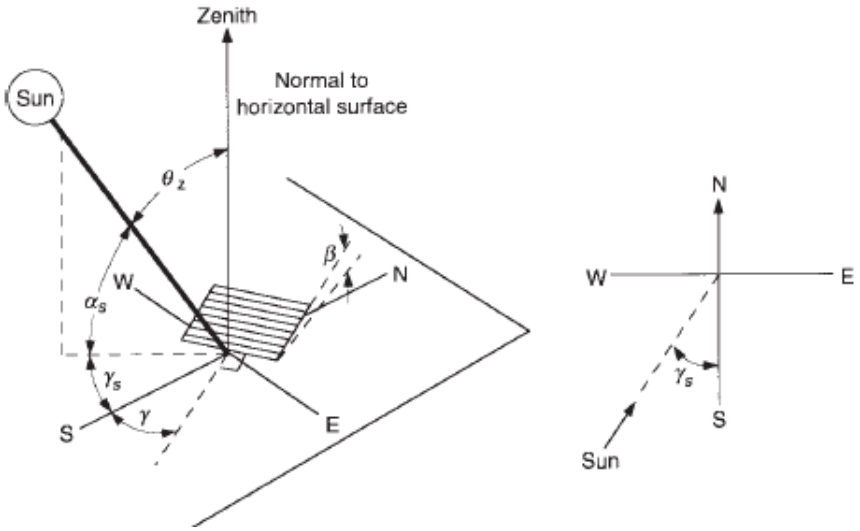

Figure 16: Angles of the sun relative to a horizontal surface (Duffie & Beckman, 2013)

2.1.6 Components of solar radiation

Direct/Beam radiation

Radiation that strikes a given object directly from the Sun, i.e. without being filtered by clouds. A clear sky will allow more beam radiation to pass through a cloudy sky. On an overcast day, there is no solar beam radiation.

Diffuse radiation

Diffuse radiation, also known as diffuse skylight or sky radiation, is a type of radiation that is scattered by the atmosphere. If the sky is cloudless, diffuse radiation will be low, and if it is overcast, diffuse radiation will be higher.

Ground-reflected radiation

A portion of beam or diffuse radiation will be reflected from the surrounding area of the surface being considered. Albedo determines the quantity of ground reflected radiation available for PV energy conversion.

Total radiation

The solar radiation incident on a sloping surface includes beam radiation, diffuse radiation, and reflected radiation as shown in Figure 17. Total radiation is the amount of solar radiation that falls on a sloped surface.

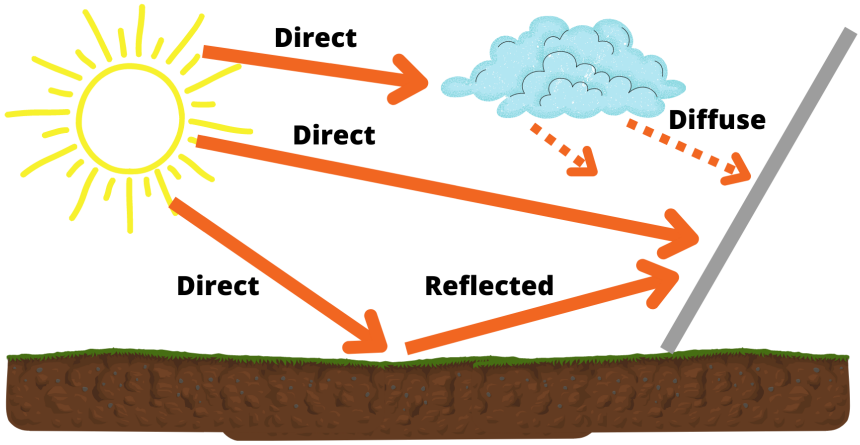

Figure 17: Graphical illustration of of the three types of solar radiation that make up total radiation

2.1.7 Sun's Path

Sun path is the path followed by sun from sunrise to sunset on a particular day. The sun path in a location changes every day due to the Earth's tilt. A collection of these paths recorded for a full year and drawn against the azimuth of the sun is a sun path diagram or an analemma. Sun paths are location specific and vary by season. The sun's path at a given location is a crucial piece of information while planning PV installations. In an agrivoltaic setup, solar energy or radiation is needed for both crops and PV systems. The availability of this energy entirely depends on sun positions throughout the year.
Figure 18 shows the sun path diagrams for four seasons of a single year in Trondheim, Norway (N63°42.3′ E10°38.86′). During spring (Figure 18a & 18b) and summer seasons (Figure 18c & 18d) the sun's azimuth is spread from North/East (N/E) to North/West (N/W) and the sun's altitude (elevation) is quite high above the horizon. Longer azimuths during these seasons can be advantageous to East/West bifacial PV systems and also for crops. Also, there is an advantage of harnessing more energy due to the long daylight hours during the summer.
In autumn (Figure 18e & 18f), the sun's altitude gets lower & lower each day as the season progresses towards winter. The azimuth is oriented from East to West. The winter (Figure 18g & 18h) sun's altitude is start depressed and remains very low. The azimuth oriented from East/South/East (ESE) to West/South/West (WSW).

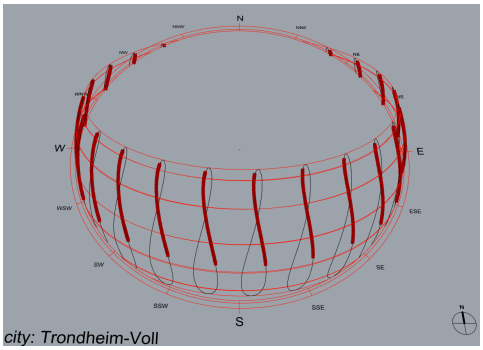

(a) Spring (March-May) Isometric view

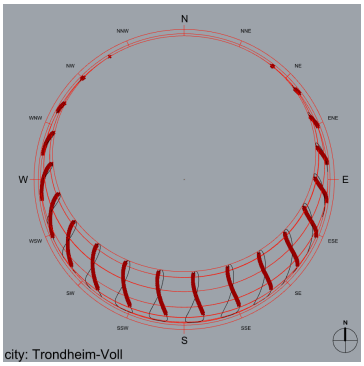

(b) Spring (March-May) Top view

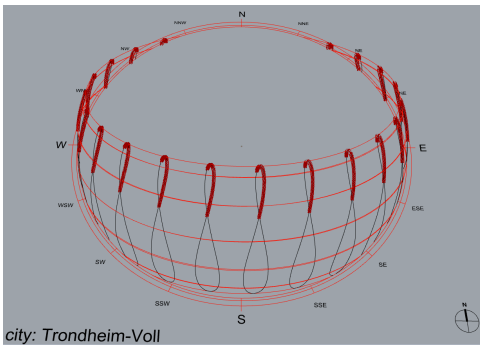

(c) Summer (June-August) Isometric view

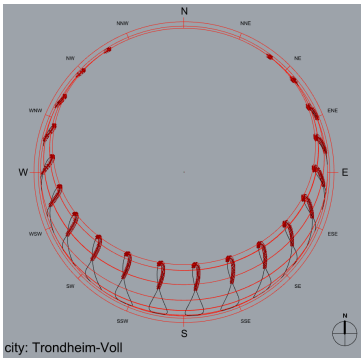

(d) Summer (June-August) Top view

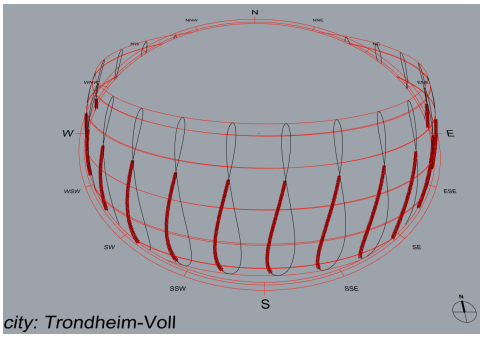

(e) Autumn (September-November) Isometric view

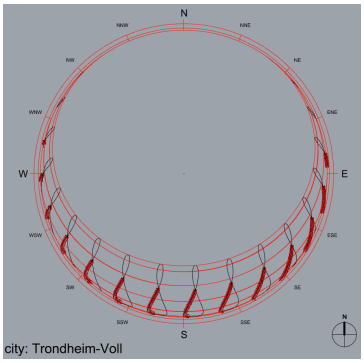

(f) Autumn (September-November) Top view

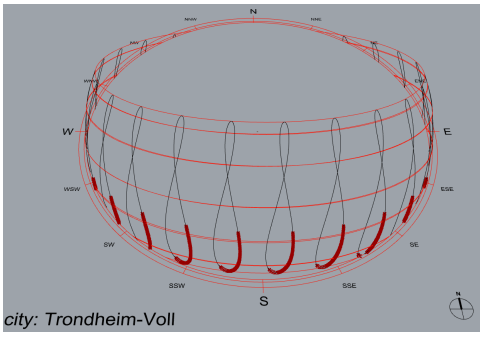

(g) Winter (December-February) Isometric view

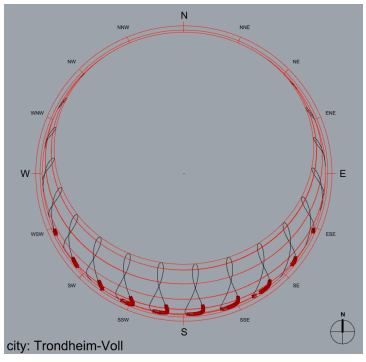

(h) Winter (December-February) Top view

Figure 18: Sun path diagrams for four seasons of a single year in Trondheim, Norway using ladybug sunpath tool.

2.2 Bifacial modelling techniques

Modelling a bifacial PV systems are becoming very crucial due their increase in market share, which has lead to a rapid penetration into the energy market. What does modelling a bifacial system mean to an PV engineer or a solar researcher?. It provides a means to accurately predict energy yields and match the price profiles at which electricity is sold. Any inaccuracies in prediction could affect project's finances. Monofacial system modelling matured and therefore provides an accurate prediction of front-side irradiance is possible.
There are two popular methods used to model rear-side irradiance in a bifacial system: the view factor method and the ray-tracer method.

2.2.1 View factor method

Ground-reflected irradiance is used in the view factor method, along with a configuration factor called the view factor. The view factor is a fraction of the irradiance leaving a point on the ground and being intercepted by an object (PV panels) on the way. The view factor considers reflected irradiance from shaded as well as non-shaded areas on the ground. This in turn depends on ground albedo. Commercial PV performance modelling tools like PVsyst, SAM and the open source tool *bifacialvf* use this method. It is fast and computationally inexpensive, and is suitable for simple geometries. Note that edge effects are neglected. An example from the PVsyst tool is shown in Figure 19. Rear-side irradiance is estimated at five points on the ground and the mean of these points is added to front-side irradiance to calculate total energy yield [64]. The diffuse irradiance from the sky is estimated in two dimension by integrating over the region of sky that is viewed from the rear-side of the PV panel. The integration procedure considers limit angle and incident angle modifier (IAM) losses. PVsyst assumes an isotropic distribution of diffuse and ground reflected irradiance.

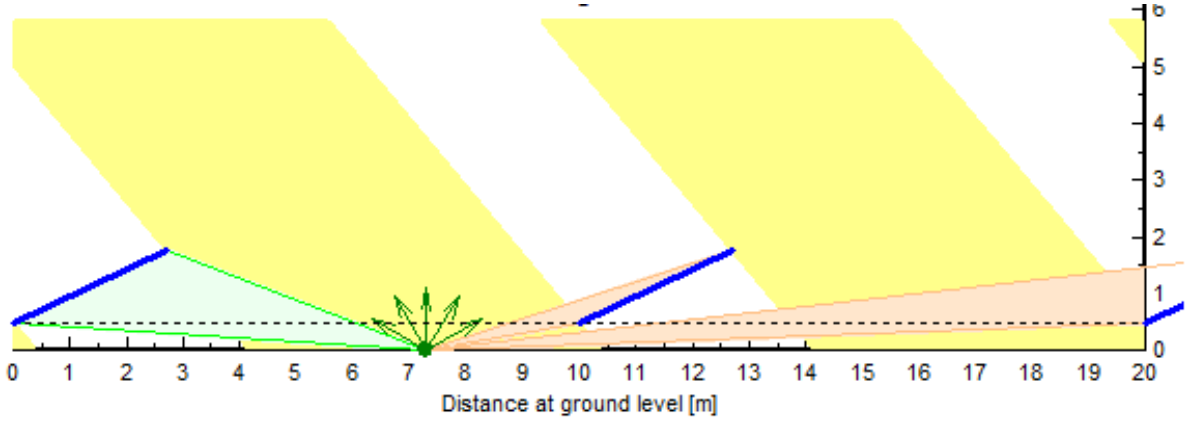

Figure 19: Example of how irradiance from the rear being estimated in PVsyst using the view factor method(limit angle = 9.9°).

2.2.2 Ray tracing method

A ray is defined by two things, origin and direction. The origin is some point in space in the 'x,y,z' coordinate system. Ray casting is the process of shooting this ray along its direction to determine what objects it strikes on its way. Ray casting is used for various purposes like radiation study, rendering computer games, shadow studies between two surfaces, creating an image using pixel screen etc.
To estimate the positive and negative impacts of solar irradiance in complex environment like agrivoltaic systems, it is crucial to evaluate the actual solar radiation on every point on the ground where crop will be grown. This estimation has to be performed for every hour of the day, season, and climate zone, while considering mutual shading, reflections, and diffuse scattering effects. This kind of complex scene can be computed using the ray tracing (RT) method [65].
This method is more accurate than the view factor method. It considers edge effects, evaluates electrical mismatch, complicated geometries and any array size. Most programming tools used for urban environment analysis use the RT method to evaluate microclimate conditions, render solar radiation maps, identify urban heat islands, etc. ClimateStudio, Honeybee-Radiance, bifacial_radiance, and EnviMet are some of the programs which incorporate the RT algorithm.
Dupraz C et al., [8] have used the RT algorithm to estimate direct and diffuse radiation available to the crops at ground level below the PV arrays in an agrivoltaic set up.
Zheng J et al., [38] estimated illuminance results by implementing the RT algorithm. Illuminance results were obtained for grooved glass, but this can be used for even-light distribution in agrivoltaic applications instead of plane glass.
There are two RT techniques: forward and backward (reverse) ray tracing. In forward RT, light particles travel from light source onto the object and bounce the shadow ray towards the observer. In reverse ray tracing, an eye ray passes onto the object and bounces towards light source. Backward ray tracing is more efficient than forward ray tracing [66].

2.2.3 Radiance

Radiance is a backward ray tracing model initially developed for designing building lighting. It renders physical realistic images and performs illuminance mapping. Nowadays, radiance models are used in a variety of applications, for example in the modeling of bifacial PV installations [65].

2.3 Climate data

Climate or weather data is crucial to the modelling of an energy system, as the accuracy of predicted energy yields depends on the accuracy of weather data and sources. Most of the PV energy modelling and other software programs used in this thesis use different weather data file formats.

2.3.1 Typical Meteorological Years(TMY)

Typical meteorological year data (TMY) is used most often to describe the local solar climate. TMY data is prepared by collecting hourly meteorological measurements for several years. From this data, the month with the least variability is selected instead of the yearly average of a particular location. For each month, the mean radiation over the entire data collection duration is estimated, along with the mean radiation in each month during the data collection duration. A given month's mean radiation data with the least deviation from the monthly mean over the entire data collection duration is selected as TMY data for that month. Hourly data for the entire year is prepared as well [67].
The first TMY dataset for 248 locations of USA was developed in 1978. Later it was updated to TMY2 and TMY3 in 1994 and 2008 respectively [68]. TMY and TMY2 used columnar or positional formats which is quite difficult to read and understand. Hence the TMY3 dataset uses the comma separated value (CSV) format due to the fact that many existing pieces of software have in-built functions to read CSV files. The data to prepare all these files are collected from weather stations using certain satellites , but this is out of scope for this thesis. The contents and headers of TMY3 files in the CSV format is explained in Figure 20.

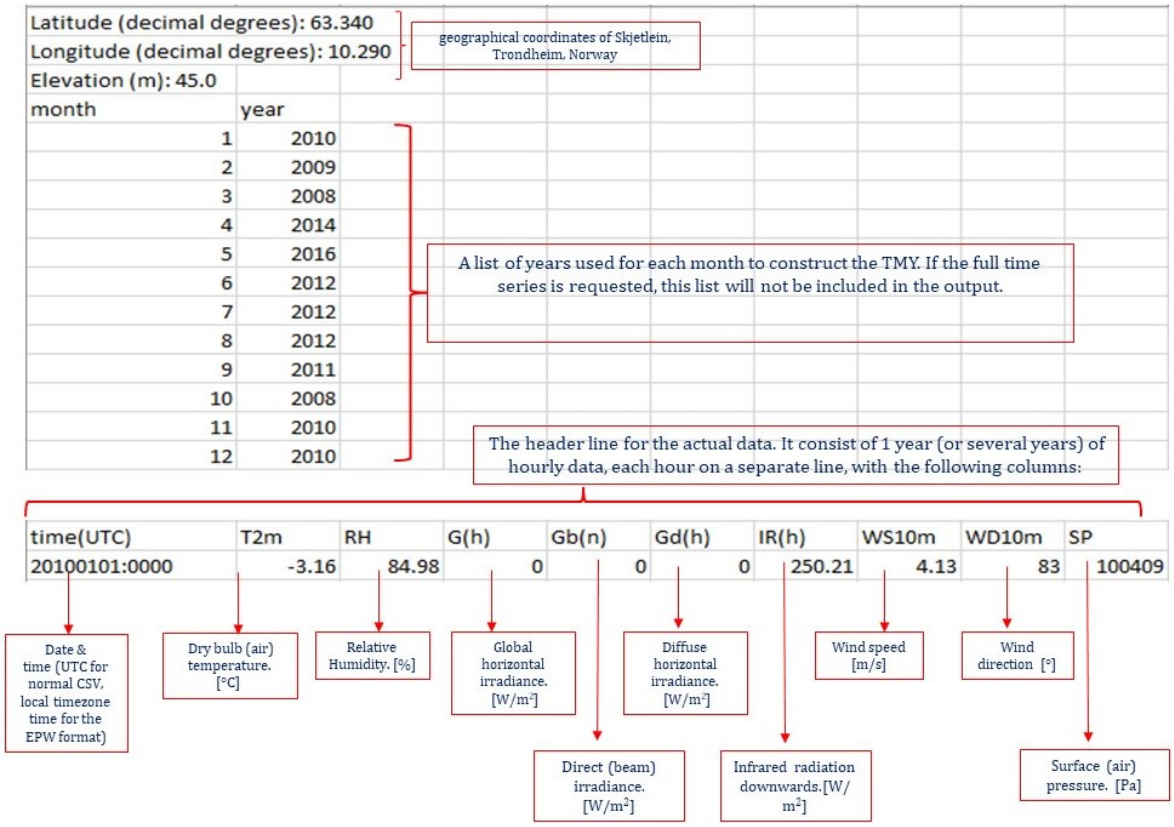

Figure 20: CSV headers in a TMY3 file

2.3.2 EnergyPlus Weather File (EPW)

EnergyPlus and Environmental Systems Performance - Research (ESP-r) are the two main simulation programs where EPW files were originally used. It was developed mainly for energy modeling (heating and cooling loads, daylight, etc) of buildings. EPW data is derived from TMY2 and modified s0 that it can be easily read in spreadsheet programs. In addition to the data fields available in TMY2, an EPW file will have minute and infrared sky data fields also. These fields allow calculating the energy efficiency of a building and the effective sky temperature for irradiation during night respectively [69]. For a selected location, the data in TMY and EPW files are the same.

2.4 Agrivoltaics

Agrivoltaic systems(AVS) are a synergistic technique for combining renewable energy with agricultural products in one system. This is especially prevalent in highly populated emerging countries and as well as in developed countries, where renewable energy production is becoming increasingly crucial; nonetheless, fertile farmland must be safeguarded.

2.4.1 Graphical views of typical agrivoltaic system configurations

To visualise different types of agrivoltaic systems, illustrations have been created in SketchUp. In ground mounted agrivoltaic systems (GMAPV), arrange food crops in the space between rows and sometimes below the PV arrays. These systems have larger row spacing compared to conventional ground mounted PV systems. Figure 21a shows different dimensions that are typically important along with tilt and azimuth of the GMAPV system. If the food crops grow tall and cause shade on PV arrays, then elevated agrivoltaic systems(EAPV) as shown in Figure 21b are used. In both types of systems, sun tracking mechanisms can be incorporated to maximise the energy available to the PV arrays and crops. The third type of system that has been popular in recent times is vertical agrivoltaic system(VAPV) as shown in Figure 21c. These kind of systems are typically used as fencing in sheep and other livestock farming. These systems are fitted with bifacial PV panels if there is an advantage of ground albedo(for example: Snow) in certain geographical locations.

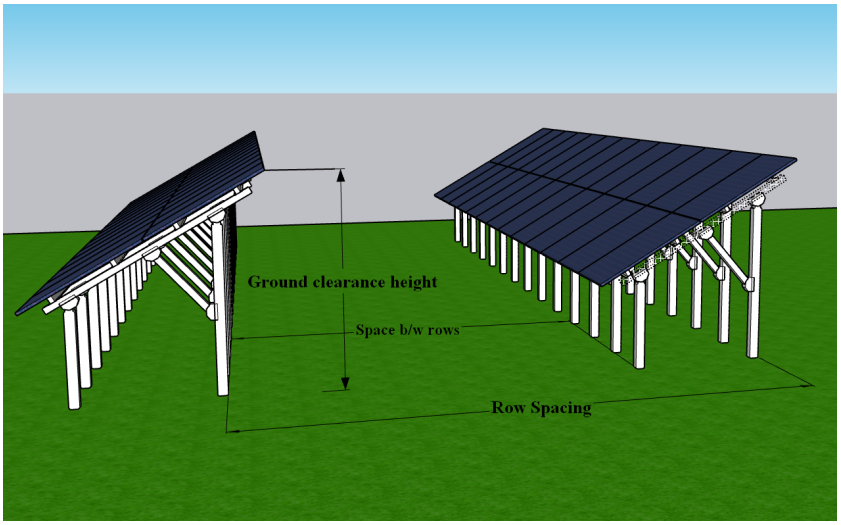

(a) Ground mounted agrivoltaic system (GMAPV)

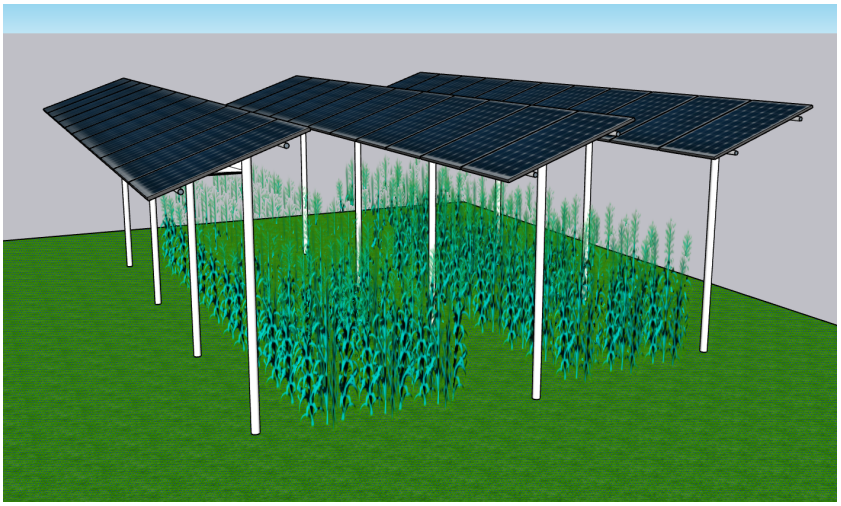

(b) Elevated agrivoltaic system (EAPV)

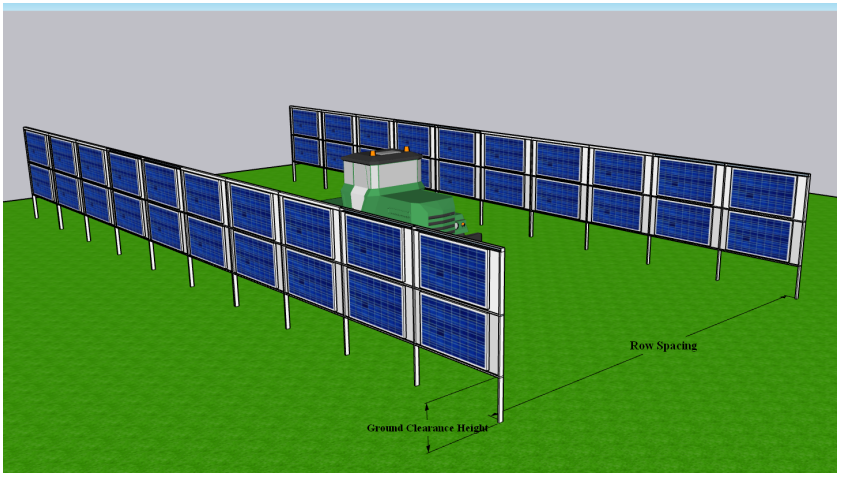

(c) Vertical agrivoltaic system (VAPV)

Figure 21: Graphical representation of different agrivoltaic concepts.

2.5 Crops

Crops are plants that are usually grown at a large scale to provide food to humans and animals. Crops can either be directly consumed or indirectly used in other form. For example, aloe vera a crop mainly grown for use in cosmetic products.
To grow and develop optimally, crops require sunlight. That's not all ,though: the quality, quantity, and duration of sun light significantly influence their growth. These factors depend on the location, season of the year, hour of the day, and weather. Crops use photosynthesize light and store it as biomass. The 400-700 nm range of the solar spectrum is useful for photosynthesis and is known as photosynthetic active radiation (PAR).
Chlorophyll, the green pigment in leaves responsible for absorbing the PAR, has two peaks of absorption: blue and red light. Each crop type begins the process of photosynthesis at different light energy level, this limit is called as the light compensation point(LCP)[70]. At this point light energy is sufficient for photosynthetic activity to produce more oxygen than is required by the plant for respiration.
As shown in the Figure 22, light intensity proportionally increases with rate of photosynthesis up to certain maximum limit. This limit is known as light saturation point(LSP) and after this limit crops doesn't utilise light energy or photosynthesis stops. The number of active photons that fall on a given surface per second including photons in 400-700 nm range of the solar energy spectrum is called photosynthetic photon flux density (PPFD) [Units: moles of light per square meter per second]. PPFD constitute about 42-49% of the total energy of the whole solar spectra. PPFD is expressed as PAR and its collective availability is known as the daily light integral (DLI) [Units: moles of light per square meter per day]. Based on quantity of available PAR in an agrivoltaic design, researcher are computing crop growth parameters like lead area index (LAI), radiation use efficiency (RUE), daily crop growth rate, and crop dry matter weight.

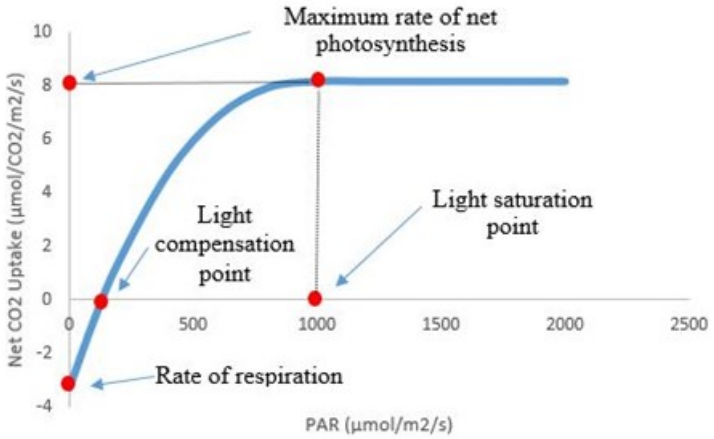

Figure 22: Graph of the light compensation point and the light saturation point [70].

Each crop has a different light saturation point. For some crops like green vegetables,

berries and tomatoes, the LSP indicates that sunlight is not being utilized for about half the day. Such conditions contribute to lower water consumption and higher crop production in high solar insolation locations [9]. The growing environment of some cereal crops, like corn and wheat, are highly optimised and any shortage in light intensity will inhibit crop yield. Hence, it is very important to understand the biological processes responsible for the growth, development, and production of economic yield i.e., crop physiology.
Figure 23 shows how plants selectively utilise the solar spectrum for photosynthetic process. It is very clear that, plants absorb sunlight in the wavelength range of 400-700 nm of the solar spectrum.

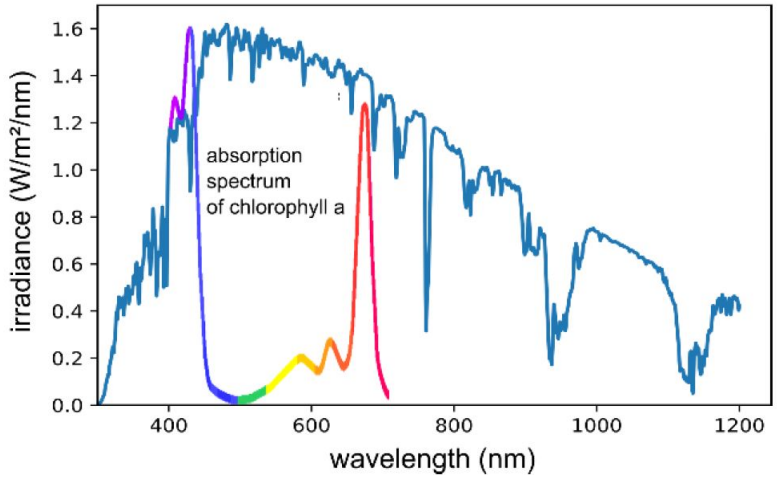

Figure 23: Absorption of 'chlorophyll a' compared to the irradiance in the solar spectrum.[71]

2.5.1 Types of grass grown in Norway

Figure 24 shows pictures of major grass types that are grown in Norway for livestock fodder. Among these, timothy grass is most widely grown for silage and hay production. The cold maritime climate helps in good quality production of timothy. It is very tasty and nutrient rich for domestic animals.

Figure 24: Pictures of major types grass grown in Norway for fodder [72] [73] [74] [75].

2.6 Microclimate

A climate in a localised or restricted area which is different from the climate in surrounding areas is microclimate. It is formed by complex interactions between a few variables: temperature, humidity, intensity of solar radiation, and wind[76].
In an agrivoltaic system, the area below and between the PV arrays have varied shade durations. This creates a difference in temperature, solar intensity and wind speeds, which manifests as a microclimate in those open areas. PV greenhouses are an example of microclimates in a controlled area. A change in one variable causes a proportional shift in the others, which could influence crop yield or growth below and between the PV arrays. The productivity of crops is eventually dependent upon the impact of the microclimate on the crop processes: photosynthesis, respiration, transpiration, and translocation.

3 Methodology

This section lists the steps that were followed to achieve the objectives of this thesis. Every section acts as a recipe for someone who would like to use these tools to model any type of agrivoltaic system configuration. The PV system configuration discussed in this thesis is a vertical bifacial East/West oriented agrivoltaic system.
After setting on an objective for the thesis, it was found that following end results have to be obtained to determine the feasibility of agrivoltaic systems in Norway.

- Energy yield of PV systems
- Light energy available to the crops with and without shade from the PV systems
- Number of hours of sunlight available for different values of various agrivoltaic settings.
- Effect of PV array's row edges on crops
- Radiation maps of various configurations of agrivoltaic systems

To obtain these results and achieve the overall objective i.e. modelling of an agrivoltaic test system at Skjetlein videregående skole (N63°34.12′ E10°30.16′), this methodology section has been divided into four parts. In Section 3.1 a suitable modelling tool is selected, section 3.2 will show that vertical bifacial system suit Norway well, section 3.3 will check whether sufficient light energy is available for the crops during growth season in an vertical PV system, and section 3.4 will finally incorporate the methodology at Skjetlein videregående skole (Skjetlein high school).

3.1 Modelling tool selection and overview

There is no single piece of software that could be used to determine the above targets. Various software packages were trialled as an initial step. A key observation here is that all these pieces of software use different sources and formats for weather data. Section 3.1.1 will briefly dig into this issue before diving into the details of the software.

3.1.1 Weather data sources and formats

Typical Meteorological Years (TMY) (described in Section 2.3.1) and EnergyPlus Weather File (EPW) (Section 2.3.2) are two weather file formats used in this thesis. Table 3 provides an overview of the sources and formats that each software program is compatible with. Even though each program accepts different formats, there are external websites and procedures to convert an EPW file to TMY file or TMY to EPW. For location of Skjetlein, TMY and EPW files can be downloaded from PVGIS but this does not include the location name. Therefore, a separate weather file available for 'Trondheim-Voll (N63°41.06′ E10°45.39′)' from a different website was downloaded and used it in ClimateStudio, Labybug and SAM. For PVsyst, it is recommended (to avoid mismatch

in the weather file structure) that you use the weather data downloaded directly by the software.

Table 3: Weather data sources and accepted file formats for various software programs

Software	Source for downloading weather files	Accepted formats
SAM(version 2021.12.02) [77]	National Solar Radiation Data Base (NSRDB), European Centre for Medium-Range Weather Forecasts (ECMWF/ERA)	TMY, EPW
PVsyst(version 7.2)	Built-in function downloads weather data either from PVGIS TMY or NASA-SSE or Meteonorm or NREL/NSRDB or Solcast TMY using geographical coordinates as input. If data from local weather stations are available, there is a built-in function that converts the data into a TMY file.	TMY
ClimateStudio (Institute license)	Built-in weather browser consisting of 30,000 TMY files sourced from EnergyPlus and climate one building	TMY
Ladybug tool (Version 1.4.0) [78]	Data can be downloaded from EPW map link [79]. This map has data for most locations however if a particular geographical coordinate is not available an EPW file can be download and imported from PVGIS.	EPW

3.1.2 Modelling tools

The fundamental theory based on which the software tools listed in Table 4 work is described in Section 2.2. A number of software programs were evaluated so as to understand their overall functionality and user friendliness, to compare their compatibility with similar tools, and to assist future researchers in agrivoltaic system modelling. A brief overview is given in tables 4 & 5.

Table 4: General overview of the software tools used in this thesis work

Software	Core functionality	Usage for this thesis	Remarks
PV energy estimation			
System Advisor Model (SAM) (version 2021.12.02)	Complete PV system optimisation and energy system modelling.	Parametric modelling, rear side bifacial gain percentage versus azimuth and tilt.	It is possible to use SAM instead of PVsyst for complete PV energy estimations. However PVsyst is widely used at industries as well as found in agrivoltaics literature.
PVsyst (version 7.2)	PV system design, modeling and optimisation.	Optimisation of vertical bifacial system.	Prediction of PV performance according to agrivoltaic set up geometry. The main goal is to measure crop energy and yield. The energy from PV is an bonus farmers' revenue.
Energy available to the crop(grass) & shade analysis			
ClimateStudio (Institute license)	Energy modelling, daylight access of urban landscapes, buildings, etc.	To estimate solar exposure on surfaces where the crop will be cultivated. ClimateStudio estimates energy values after considering shade from the surrounding objects. This is used as energy input in crop model.	The crop model is developed in Python. The energy to crop is then converted into biomass.
Ladybug (Version 1.4.0)	Daylight and radiation analysis, analyse weather data, and shadow studies. This is a plugin to the GrassHopper tool. Which is itself a plugin to Rhino3D	Sun hour analysis, sky dome analysis.	Wind rose, heat maps are the other functionalities tried during learning. Honeybee is an advanced version of Ladybug which uses ray-tracing algorithms for similar analysis.
Rhino3D (Trial Version 7)	CAD modelling software	Used for drawing PV system geometry and visualizing results from Ladybug and ClimateStudio	Ladybug and ClimateStudio are plugins to Rhino3D

Table 5 shows software tools that were evaluated and rejected during this thesis. Reasons range from limited accessibility under trial versions to steep learning curves. In addition, the WOFOST and DSSAT crop modelling tools were evaluated to in reference to specifically modelling

Table 5: General overview of other software tools tried during the thesis period.

Software	Core functionality	Usage for this thesis	Remarks
EnviMet (Trial version)	Primarily used for urban heat island estimations, microclimate studies. It considers reflectivity of surrounding objects, wind circulations, and other microclimate properties while estimating urban heat islands. [65]	To estimate temperature, relative humidity at the space between two vertical PV panels	This has never been used for microclimate studies w.r.t agrivoltaic systems. The trial version has very limited grid (geometry) size so it was not possible to achieve intended outcomes.
bifacial_radiance	Open source bifacial PV system modeling	To estimate and optimise vertical bifacial agrivoltaic system. This was evaluated as an alternative to PVsyst and ClimateStudio.	Very good open-source tool. However, it requires programming skills, which was out of scope here.
ArcGIS	An integrated geographical information systems (GIS) program that allows you to create, analyze, manage, edit, and visualize geographic data.	Tried to estimate soil(land surface) temperature using satellite images and certain formulas provided in [80]. This was required in the thesis to understand change in crop yield due to soil temperatures.	The results obtained were decent but the program did not provide a way to narrow the study area. This tool is mainly useful in the context of global crop yield estimations.

3.2 Vertical bifacial system

Bifacial PV technology's share of the PV market has rapidly risen in recent years, which has helped to unlock new possibilities for performance improvement and even solving new problems [31]. As discussed earlier, the vertically mounted and East/West oriented bifacial PV systems perform well in Nordic countries. However, the selection of vertical bifacial PV systems oriented East/West for agrivoltaic concept against fixed tilted or tracking agrivoltaic systems must be justified reasonably. An attempt is made in the following sections to demonstrate via a modelling approach that vertical East/West bifacial PV systems performs well in terms of PV energy for the selected location (Skjetlein VGS (N63°40.95′ E10°44.77′)) and are also suitable to cultivate the crop 'timothy grass' in an agrivoltaic setup.

The width of the tractor that is typically used for harvesting grass from the fields of Skjetlein videregående skole (N63°34.12′ E10°30.16′) is about 10 m (information provided by Skjetlein VGS administrators) and hence a row spacing(P) of 10 m was selected in all the simulations. Initially, all the simulation trials, parameterization, and optimisation was performed for just two rows of PV arrays as shown in Figure 25b. The mounting structure and metal frames around panels were glossed over to reduce computational time and design space. These objects typically have little-to-no effect on the crops.

The variables that were changed to optimise the geometry of the set up is described in Figure 25d. The ground clearance height(H) is the vertical distance between the ground and the PV panel array. The effect of 'H' on PV energy yield and light available to the grass is examined by considering three values of H: 0 m, 0.5 m and 1 m. The module height(M) refers to PV panel height when it is placed in landscape way. In the Figure 25a it can be seen that 'M' is 'one module height' which is taken as 1 m and if stacked with one more row of PV panels above it then it is 'two module height' with 2 m module height. Only these two values of 'M' were changed for above mentioned values of 'H'.

The row length (R) is the length of PV array. Higher the row length means more number of panels and more PV energy yield. To minimise the computational time, it is taken as 20 m in all the above changes of 'H' and 'M'. However, the 'R' values are changed while examining the shading caused due to edge effects.

The specification of PV panel (JAM72D09 370) considered in subsequent calculations can be found by clicking here.

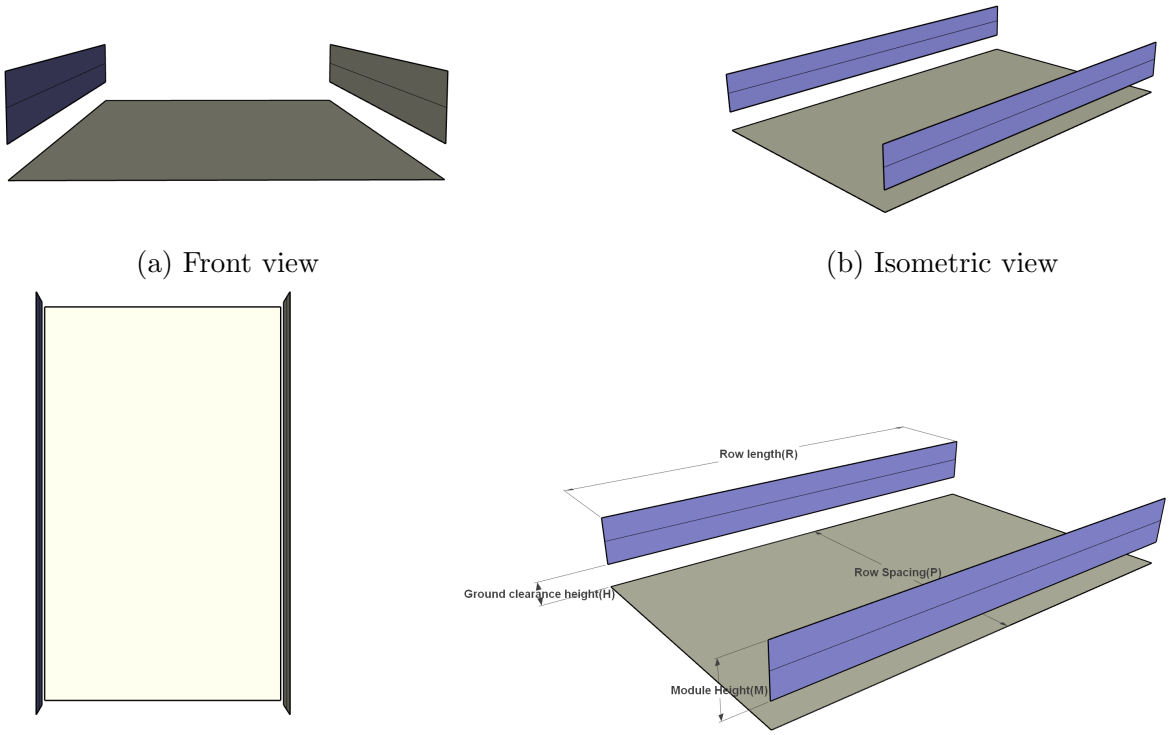

(a) Front view

(b) Isometric view

(c) Top view

(d) Isometric view with different geometric parameters

Figure 25: Graphical representation of different views of vertical bifacial PV system and different geometrical parameters. a) Front view of the system when observer is viewing from the South direction, b) Isometric view of the system, c) top view of the system, and d) Isometric view with all the geometrical parameters.

3.2.1 Land area occupancy

The prime goal of agrivoltaic system design is not to increase the demand for open land. One way of checking this criteria is by calculating land coverage ratio (LCR) and power-to-land ratio (PLR). The Skjetlein VGS has a 84 kWp rooftop PV system with a roof area of about 572 m^2, it is uses as a reference area. Using Equation 4 and Equation 5 [81] LCR and PLR values are obtained for these three configurations.

$$\text{Land coverage ratio} = \frac{\text{Land area occupied}}{\text{Total land area available}} \tag{4}$$

$$\text{Power-to-land ratio} = \frac{\text{Capacity of PV system}}{\text{Land area occupied}} \tag{5}$$

Where,
Land area occupied: Land area that is occupied by PV structure only out of the total land area used for PV power plant. This value varies for each type of PV system design i.e. rooftop, ground mounted either fixed or tilted, elevated, and vertical.

Capacity of PV system: This is the total PVPP capacity in kWp that has been planned for installation within the total land area.
The configurations considered are similar to the discussion in section 2.4.1 and as illustrated in Figure 26. These pictures are just graphical representation of geometry with sample dimensions and therefore actually size, number of PV panels, dimensions considered for estimating LCR and PLR might differ marginally.
Figures 26a, 26b and 26c clearly show the area occupied by PV structure (brown patch in the figures) and area available for farming activity (shown on only one part in each picture). The number of rows of panels and the capacity of the PV system was chosen based on the reference area mentioned above. The distance between rows has to be at least 8-10 m for the farm tractor to move while harvesting if not harvesting has to be done manually.
The dimensions used for calculating land area occupied by PV structures in vertical agrivoltaic system (VAPV) are based on the assumption that the PV structure occupies a width of 0.25 m and the length occupied by PV structure depends on panel dimensions. This assumptions is an engineering guess, can be varied according to design of VAPV.
There is no assumptions in land area occupied by PV structures in ground mounted agrivoltaic system (GMAPV). However, the area occupied by PV structure is the area where tractors cannot harvest. These are colored brown in the images below.
In an elevated agrivoltaic system (EAPV), it was assumed that a rectangular base structure of dimension 0.5 m x 1 m will be constructed using cement concrete to hold circular bars that take the load of PV panels. Again this is an engineering guess, more mechanical load and wind load calculations have to be performed to get exact dimensions.

3.2.2 Albedo

To know the effect of albedo on vertical bifacial panel performance, the ground reflection on the rear side (kWh/m^2) is estimated for East/West and North/South orientation. Similarly, it is possible to estimate ground energy reflected on front side (not computed in this thesis). Irradiance reflected by the ground (between rows) close to the PV arrays and reaching the front or rear side of the PV array is represented as the ground reflection on the front or rear side. They are weighted by the incidence angle modifier (IAM) loss. The ground reflected light on the front side is present in both monofacial and bifacial PV systems. However, the rear-side of bifacial PV systems is more dependent on ground reflected light as compared to monofacial PV systems [82]. Therefore, a parametric simulation was performed in PVsyst (version 7.2) to estimate ground energy reflected on rear side of bifacial PV panels as albedo percentage is was varied from 0 to 100%. The North/South and East/West results were compared.

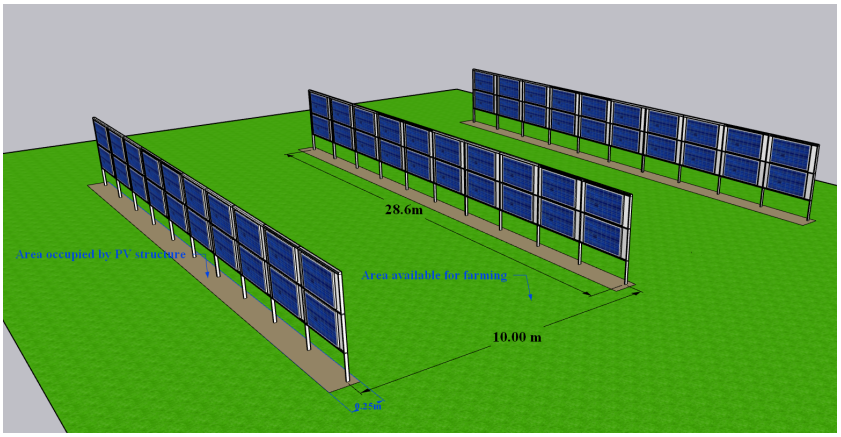

(a) Vertical agrivoltaic system (VAPV)

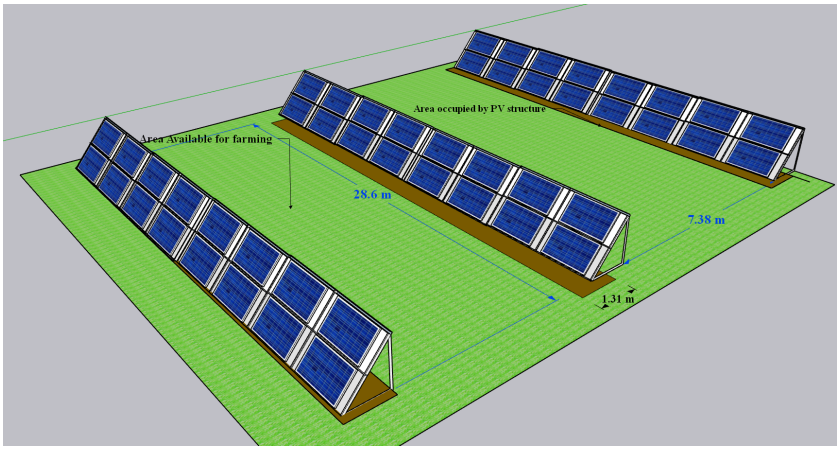

(b) Ground mounted agrivoltaic system (GMAPV)

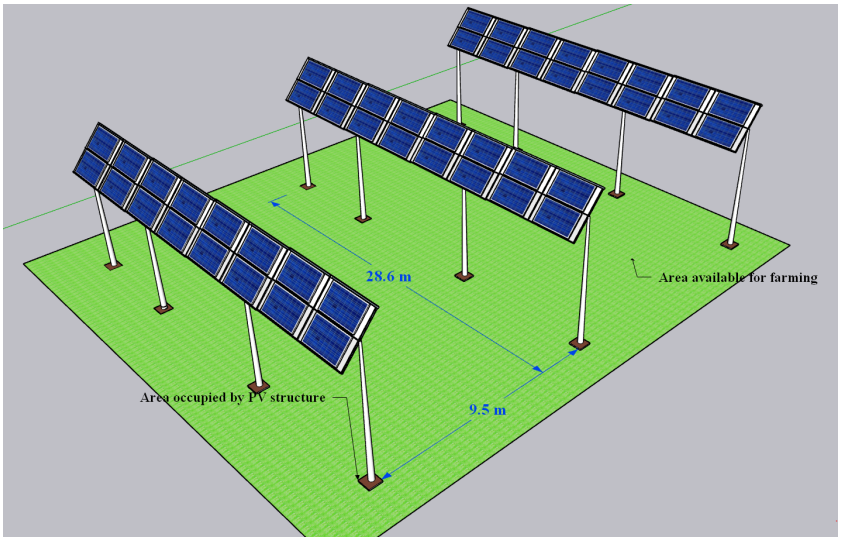

(c) Elevated agrivoltaic system (EAPV)

Figure 26: Graphical representation of agrivoltaic setup configurations with sample dimensions that help understand LCR and PLR calculations.

3.2.3 Latitude v/s bifacial gain

In this section, variation of energy yield of bifacial vertical East/West mounted PV system in terms of bifacial gain has been examined for two geographical locations. One location is Trondheim, Norway (N63°40.95′ E10°44.77′) because this is the intended study location. Another location selected is Phoenix, USA (N33°44.99′ E−112°6.74′) because this is the default location in the system advisor model (SAM) tool, and there are numerous agrivoltaic test sites around this part of the USA.
Using the SAM parametric analysis tool, plane of array (POA) rear-side bifacial gain is estimated for both locations by varying tilt and azimuth. The tilt (vertical angle) is changed from 0° to 90°. The azimuth (horizontal angle) is changed from 90°(East) to 270°(West) i.e., 180°(South) and 0°(North). The POA rear-side irradiance (weighted by bifaciality) adds to the front-side irradiance and thus contributes to the total energy yield. The bifacial panel used for this analysis is as mentioned above and bifaciality is set to 0.85.

3.2.4 Bifaciality

Bifaciality or bifaciality factor is crucial in terms of energy yield (kWh/kW) when designing a vertical PV system instead of conventional tilted South-oriented systems of same capacity. A simple parametric sweep was performed in SAM by changing the bifaciality of the PV panel with constant ground clearance height of 0.8 m and vertical mounting. This is done for three orientations and for two locations. The first location is Trondheim, Norway (N63°40.95′ E10°44.77′) where the agrivoltaic system is modelled. Second location is Fukushima Prefecture (N42°81.92′ E141°4.69′), where Japan's first vertical bifacial agrivoltaic system for growing pasture has been installed in a South-facing rather than East/West due to topographical restrictions [83].

3.2.5 Tregenza skydome

The sun's height (altitude angle) significantly affects the amount of energy available to the crops and PV panels in an vertical agrivoltaic systems (VAPV). This can be visualised using Tregenza sky domes. Ladybug uses the GenCumulativeSKy model developed by Robinson et al., (2004) to estimate the quantity of solar radiation that makes it to the earth's surface. This is usually represented as a Tregenza sky dome (artificial sky) which is a collection of radiation patches. The graphical representation of these patches provides an overall understanding of the radiation condition in the sky.
To understand seasonal variations of sky radiation and how that would impact the agrivoltaic setup, sky domes for all four seasons have been calculated for the Trondheim-Voll weather station data.
Figure 27 shows the flow chart that describes the step by step procedure followed to obtain sky dome using weather data for the selected location.
Step 1 & 2: Using built-in function of Labybug tool, the EPW file is searched in a local folder and feed it to the '*import EPW*' component. This component separates the data into various data fields. The required data fields for the 4th step are location, direct

normal radiation, and diffuse horizontal radiation.
Step 3: In this step, hours of the year (hoy) will be chosen. Four periods corresponding to four seasons that span an entire year (8760 hours) is chosen.
Step 4: The '*Ladybug(LB) skymatrix*' uses the gendaymtx model [84] to generate an annual Perez sky matrix for a selected location using the weather data provided in step 2.
Step 5: This step graphically visualises the results obtained in previous steps. This uses Python code that converts the given data into sky dome.

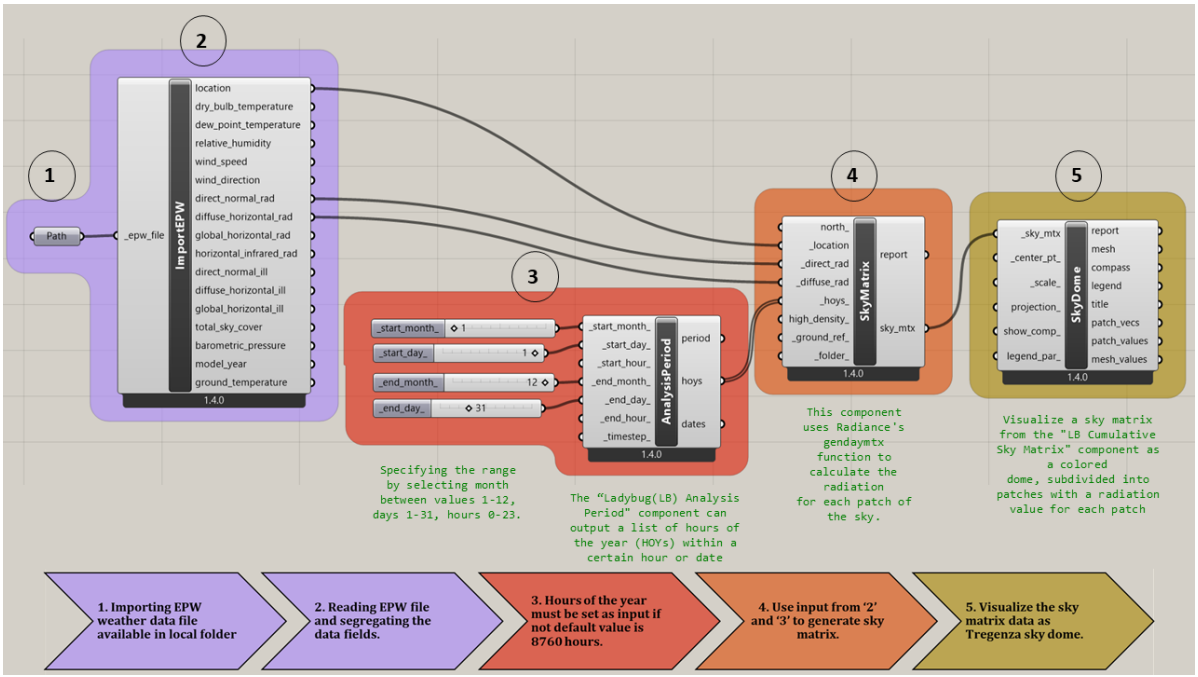

Figure 27: Steps followed in ladybug to obtain Tregenza skydome

3.2.6 Bifacial model in PVsyst

The following section describes the detailed optimization procedure used in the PVsyst software tool to determine energy yield (kWh/kW) and performance for bifacial PV systems. To determine the performance characteristics of a bifacial PV system, PVsyst uses a 2D bifacial model consisting of unlimited sheds or unlimited trackers. This means edge effects are neglected while calculating shade factors. The diffuse radiation and reflected radiation from ground(for set albedo) is assumed to be isotropic (Lambertian distribution). PVsyst still uses 1-diode model i.e., the extra radiation received on rear-side is added to the front-side radiation.
Figure 28 shows the parametric analysis window in PVsyst, that can be used to vary certain geometrical parameters of PV system to observe variation in irradiance on ground and daily irradiations. A few geometrical parameters that of relevance to agrivoltaic setup has been analysed in further sections.

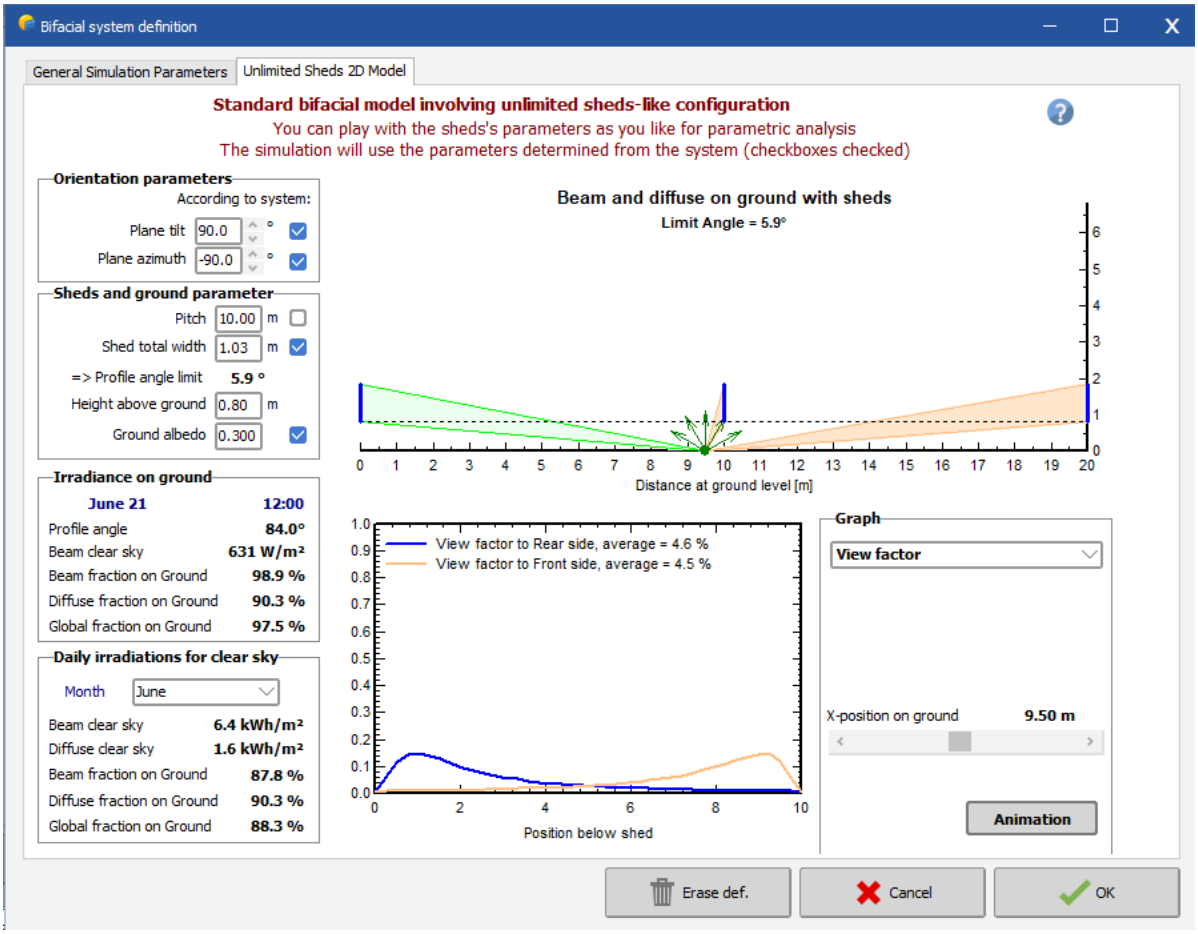

Figure 28: Parametric analysis window for bifacial systems in PVsyst (Version 7.2).

In PVsyst, the diffuse light available at every point on the ground is estimated by integrating the diffuse rays falling from all directions, which are not intercepted by the PV panels. This diffuse component is then expressed as diffuse acceptance percentage, representing a distribution function that shows how well light is distributed over the ground points. This function is not dependent on the position of the sun but dependent on the geometry of the system.
The irradiance value (illuminance) of each point on the ground is determined by its location on the ground and by sun's position. This radiation is reflected with same intensity in all directions, based on the albedo of the ground. A part of these re-emitted rays will be intercepted by PV panels and the rest is dismissed into the sky. The fraction of reflected light intercepted by PV panels is referred to as the view factor. Each ground point contributes a certain amount of irradiance to the rear side.
These two factors determine homogeneity of light distribution between PV panels, which is useful for the crop yield. An attempt is made in following sections to understand the relation between these two factors and geometry of PV system. Since PVsyst assumes isotropic hypothesis, there is no change in these factors with respect to azimuth.

a) Diffuse acceptance percentage versus ground clearance height (H)

In PVsyst bifacial model window (Figure 28), the Panel orientation is set to East/West, Row spacing(P)=10 m, Module height(M)=1 m, Row length(R)= unlimited sheds. Four ground clearance heights (H) were taken: 0 m, 0.5 m, 1 m, and 2 m. The plots and view factor figures are generated using built-in functions of PVsyst. The diffuse fraction on the ground stays constant for all the months of the year. However, the beam fraction on the ground was smaller during winter and larger during summer. Since the crop 'timothy' grows during the summer months (June-August), all the figures show the results for 21^{st} of June.

b) Diffuse acceptance percentage versus module height (M)

In PVsyst bifacial model window (Figure 28), the Panel orientation is set to East/West, Row spacing(P)=10 m, ground clearance height(M)=0 m, Row length(R)= unlimited sheds. Module height (H) were taken: 1 m and 2 m. Plots similar to the above section are presented.

3.2.7 Annual energy production in PVsyst

In this section, a 5 kWp vertical bifacial East/West oriented PV system has been designed in PVsyst for the location of Trondheim, Norway. The weather data source used is Meteonorm 8.0(1991-2013). The system consists of two strings with seven bifacial panels in each. A Gefran inverter of 4.5 kW is matched according to operating conditions. This step is carried out to understand system performance for different azimuths. More detailed analysis will be carried for actual agrivoltaic test system that will be installed at Skjetlein VGS, Trondheim.
Figure 29 shows 3D scene of PV system. A 4 m row spacing(P), 0.8 m ground clearance height(H), 1 m module height(M), average albedo for all months = 0.3 and bifaciality = 0.85 is chosen for this analysis. Bifacial modelling in PVsyst assumes unlimited sheds for row length(R) i.e. infinite length. The system production (annual energy to the grid) in kWh/yr and specific production in kWh/kW/yr results are presented for different orientations (Azimuths).
For the same system, parametric analysis was carried out for various values of row spacing(P), ground clearance height (H), and module height (M). The annual energy to grid has been plotted against tilt of the system. The P value is varied from 2 m to 8 m, H value from 0 m to 1.5 m, and M value from 1 m to 2 m. Even though this analysis could tell us which combination provide maximum energy production in a given area, same combination might not give enough light energy to the crops. An example is having too many close rows of PV system i.e. lower P values could give more energy but it is not possible to drive the tractors and there will be more shadow on the crops. This analysis helps to clarify how the system would perform given a variety of geometrical parameters.

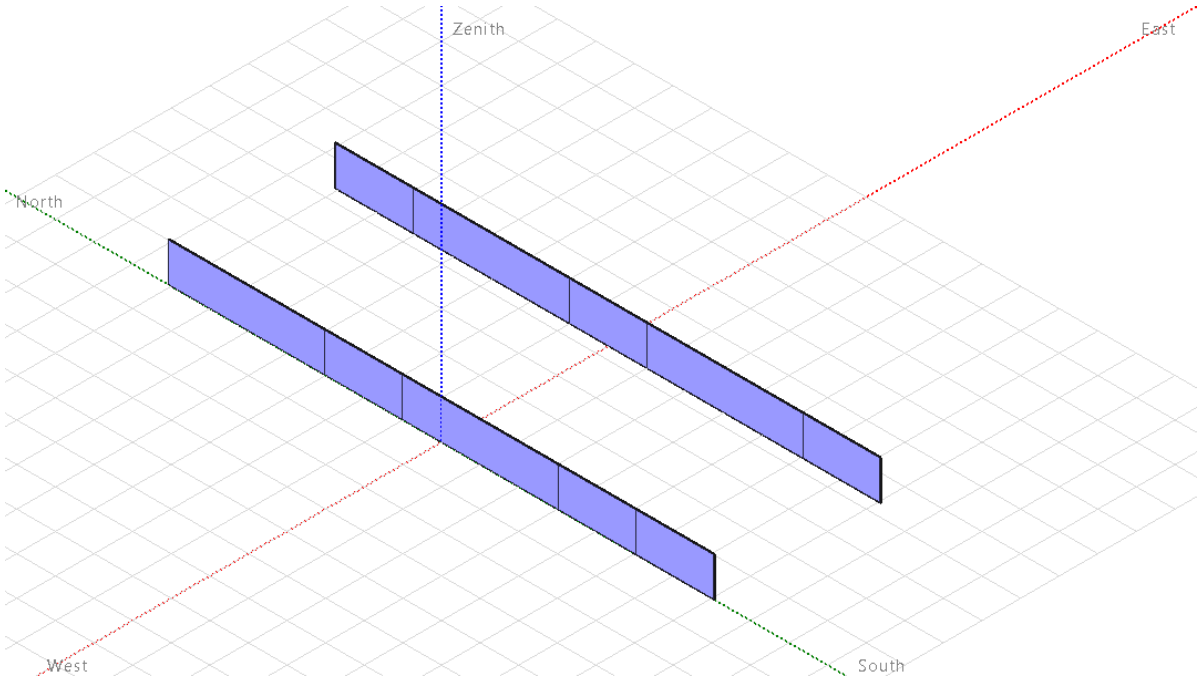

Figure 29: A 3D scene of vertical East/West oriented bifacial PV systems. There are seven bifacial PV modules in each string.

3.3 Light Management

The optimal light energy sharing between PV system and crops is a core challenge in the design of an agrivoltaic system. Ensuring required and homogeneous light to the crops can be achieved by various methods. These methods include a deviation from conventional South oriented PV system to East or West oriented systems, vertical or tracking systems instead of tilted, elevated systems instead of ground mounted. As described in previous sections, in this thesis a vertical East/West oriented bifacial PV system to be adapted as an agrivoltaic system is chosen. Subsequent sections will help understand how light is managed in this kind of system for the crops.

3.3.1 Sun Hour Analysis

Figure 30 illustrates the general steps followed when estimating sun hours from weather data..
Step 1: The number of sun hours is location specific and hence the climate data related to the location has to be downloaded. The '*ladybug(LB) download EPW*' component is the first option for downloading weather data. This component needs link(URL:Uniform Resource Locators) of location from the EPW map website as input and internet connectivity for downloading it. For offline (no internet connectivity) mode, EPW file is downloaded into the local disk and import the file location using *'LB file path'*. Either of these options can be used and fed as input.
Step 2: '*LB download EPW*' separates the data into various data fields like dry bulb

temperature, direct normal irradiance, wind speed etc.
Step 3: *'LB Sunpath'* uses location from previous step and provides output as sun vectors for a specified time range. *Hours of the year (hoys)* can be set using *'LB analysis period'*. Other input arguments here are optional. However, the 'center point' and 'scaling ratio' of sun path diagrams is set for good visualisation in the rhino scene. The optional input arguments will be set to their defaults if nothing is specified. For example, scale is set to 1:1 if not explicitly specified. The rhino scene here refers to a visualisation window that is available in the rhino3D software tool. GrassHopper (GH) is a plugin that can be used in rhino3D software tool. Ladybug is a plugin to GrassHopper. In simple words, Ladybug is a tool inside another tool (GrassHopper) and GH is inside rhino3D.
Step 4a: Setting up the analysis surface, context (shade from surrounding objects), grid size, grid offset distance and boolean toggle for running the python script. The analysis surface here refers to the region where sun hour distribution is estimated. *Context* in this case refers to vertical bifacial PV rows. The offset distance is provided such that the grid points are moved away from the analysis surface. Typically, this should be a small positive number to ensure points are not blocked by the analysis surface mesh. Grid size is specified in order to subdivide the analysis surface into several nodes and calculate direct sun hours at these nodes. Smaller grid size leads to high resolution outcome and high computational time. In order to get meaningful results, the recommended grid size is smaller than the dimensions of the smallest piece of the analysis surface and the context.
Step 4: Once all the input parameters are set, *'LB DirectSunHours'* calculates hours of sun at each grid points using a python script (More details is in Section 8.1).
The above procedure is used to estimate sun hour distribution between vertical bifacial agrivoltaic system. Further, this procedure is applied for various conditions as explained below.

a) Relation between geographical location (sun path) and sun hours distributions

To investigate if sun hour distribution changes with respect to location, four different locations in Norway have been chosen: Bergen (N60°39.46′ E5°30.21′), Oslo (N59°91.63′ E10°73.43′), Trondheim (N63°40.95′ E10°44.77′), and Tromsø (N69°64.98′ E18°95.27′). To compare, Enköping (N59°63.65′ E17°7.78′), Sweden (location near to vertical bifacial East/West agrivoltaic test site of Mälardalen University, Västerås, Sweden) and Seville (N37°39.57′ E−5°98.63′), Spain. The location in Spain was selected because it has more PV potential than Norway and it will be interesting to understand the differences (if any). The Enköping, Sweden location was selected instead of Västerås, Sweden mainly because weather data is available in EPW map. For this analysis, P=10 m, H=0 m, M=1 m, R=20 m and date: 21^{st} June (Summer solstice) is selected. Two orientations, East/West (E/W) and North/South (N/S) were selected for all these locations. This lets us examine whether the same agrivoltaic system design and orientation can be used within the country and elsewhere in the world. Sun hour analysis can be one way of examining this criteria. Summer solstice day is selected since this is the season during

which timothy grass is grown across Norway.

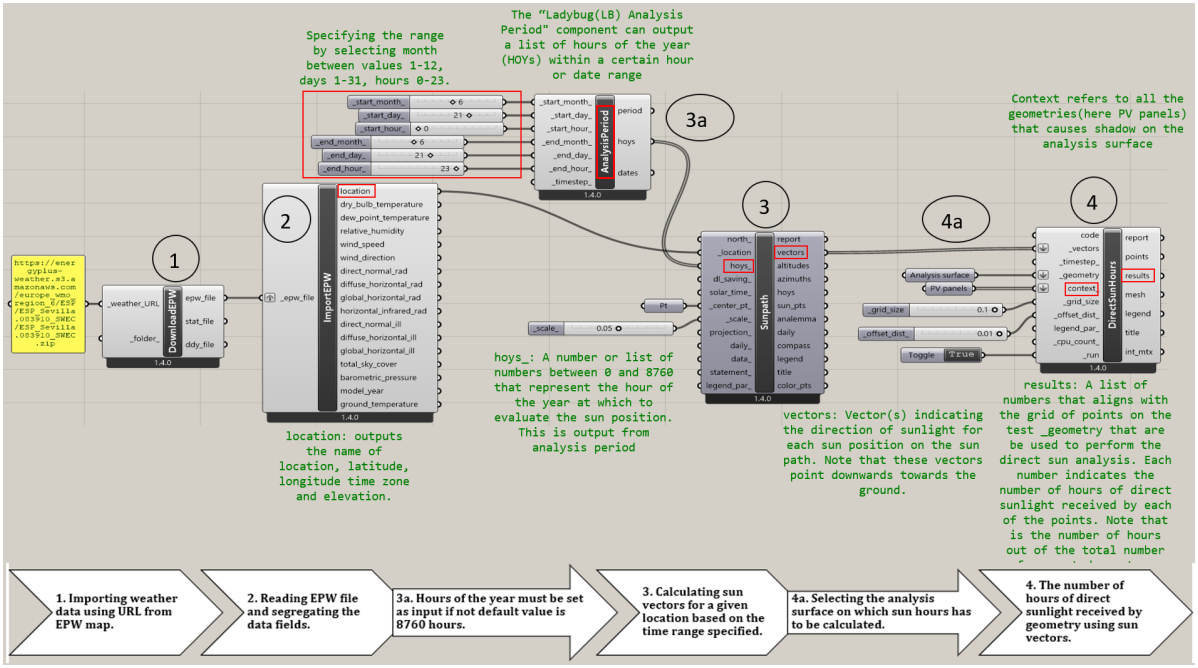

Figure 30: Steps followed in the Ladybug tool for calculating hours of sun on a given surface

b) Relation between orientation and sun hours distribution

In the above condition, only two orientations will be examined for vertical agrivoltaic setup. In this part, the geometry will be oriented at 45° azimuth to check if there is an better distribution of sun hours between the rows of PV panels. This condition is simulated for the Trondheim (N63°40.95′ E10°44.77′), Norway location with same geometry as before.

c) Relation between ground clearance height (H) and sun hours distribution

As described in Section 3.2.6, the ground clearance height 'H' has clear impact on diffuse acceptance percentage. It is possible to validate those results using sun hour analysis. In this part, the values of 'H' is varied to observe distribution of sun hours. For this analysis, P=10 m, M=1 m, R=20 m and date: 21^{st} June (Summer solstice) is selected. Vertical agrivoltaic system with East/West orientation is analysed for the Trondheim (N63°40.95′ E10°44.77′), Norway location. Initially H = 0 m is considered and stopped at H = 5 m where more homogeneous sun hour distribution is found. Results of selected values of 'H' are presented.

d) Relation between seasons and sun hours distribution

In a real agrivoltaic system, the performance in terms of crop yield and energy yield in mostly analysed during growth season of the crop. The growth season for timothy grass is summer in Norway. As explained in Section 3.2.5, the solar irradiance received from each sky patch is different during each season. How much of this irradiance from these patches reaches the ground during each season is examined in this part. Here sun hours available on the ground is obtained instead of solar irradiance. For this analysis, P=10 m, M=1 m, H=1 m, and R=20 m is selected. Vertical agrivoltaic system with East/West orientation is analysed for the Trondheim (N63°40.95′ E10°44.77′), Norway location. The value of 'H' is selected as 1 m because previous sections' results showed a uniform sun hours distribution.

e) Relation between module height (M) and sun hours distribution

A change in module height has shown significant impact on diffuse acceptance percentage in Section 3.2.6. It will be verified in this part using sun hour analysis. For this analysis, P=10 m, M=1 m & 2 m, R=20 m, H=0 m & 1 m and date: 21^{st} June (Summer solstice) is selected. Vertical agrivoltaic system with East/West orientation is analysed for the Trondheim (N63°40.95′ E10°44.77′), Norway location.

3.3.2 Radiation map

Sun hour analysis estimates the number of hours of direct sunlight a given surface receives. This is sufficient to understand the spatial distribution of light visually. However, the more exciting thing is to estimate the point-wise distribution of light energy available to crops. These results can be used as energy input in the timothy crop model to estimate the corresponding crop yield. To estimate the energy available to the crops, the ClimateStudio simulation program is used. One of the models of ClimateStudio generates radiation maps. Radiation maps are visual representations of yearly total solar radiation on a given surface. ClimateStudio uses EnergyPlus and Radiance based ray tracing algorithms for estimating total, direct, or indirect solar exposure on a selected surface for a period of one year. These exposure values are estimated after considering the shades(shadow) from the nearby objects.
In order to understand how diffuse solar radiation changes with row spacing and ground clearance height, the normalised diffuse acceptance is calculated using Equation 6.

$$\text{Normalised diffuse acceptance } \% = \frac{[\text{Total Exposure - Direct Exposure}]_{\text{with shade}}}{[\text{Total Exposure - Direct Exposure}]_{\text{without shade}}} \text{x}100 \tag{6}$$

The procedure for obtaining radiation maps using the ClimateStudio simulation program is explained in Figure 31. Before the first step, required geometry has to be drawn in the rhino3D scene area. According to Figure 25d, the dimensions selected are P=10 m, R=20 m, M=1 m and 2 m, and H=0, 0.5, and 1 m.
Step 1: The weather data is imported into ClimateStudio's location tab from the climate

one building website. Here either the location name or coordinates has to be entered. The data from the weather file will be used in ClimateStudio's simulation workflows. The components of solar radiation and sun angles are used in further computation procedures. The y-axis of rhino3D environment is taken as North arrow in ClimateStudio.
Step 2: Here material properties are assigned to the geometrical objects drawn in rhino. For this analysis sunpower solar panel material properties are assigned to vertical walls that represent PV panels. One thing to be noted here is that, ClimateStudio uses only reflectivity properties from materials window in its analysis. Hence there is no need to worry about assigning the exact panel material properties. However, assigning the closest possible PV panel's glass sheet property is most important. Similarly the horizontal surface between the panels is assigned as grass. Available material from the ClimateStudio library is used. There is a possibility of adding newer materials either from rhino3D library or ClimateStudio library.

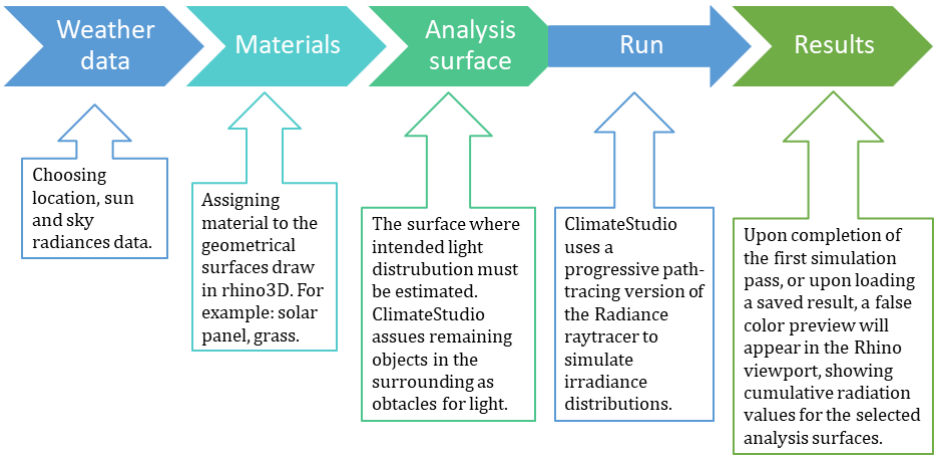

Figure 31: Steps followed to plot a radiation map using ClimateStudio.

Step 3: Here the analysis surface for which the radiation map has to be estimated is specified. The analysis surface in an agrivoltaic setting is the place where crops will be grown. This place is usually shaded from the PV panels. In fact the radiation map shows shade distribution or light available to the crops after considering quantity of shade. The radiation workflow function in ClimateStudio will work only if the analysis surface is divided into discrete set of sensor points. These points are separate by sensor spacing based on user defined values. Finer spacing increases the number of sensor points, which in turn increases computation duration. The UV mapping drop-down menu can be used to adjust sensor positioning and false color display. Here default surface mapping setting are used, which is usually used for flat and curved surfaces.
Step 4: Here the ClimateStudio ray-tracer algorithm generates rays that is bounced onto the analysis surface to raster a image consisting of total solar exposure on a surface for a duration of one year. The analysis also provides Direct (Beam) and Indirect (Diffuse) solar exposure results to be displayed as radiation map. These data is exported into a

CSV file. These CSV files contain solar exposure results for each month and whole year. This is interesting and useful for analysing crop (grass) energy during growth season (June-August).
Step 5: Here the radiation map is visualized by adjusting false color according to the requirement. The radiation maps gives first hand information about shade distribution on analysis surface. By changing different geometrical parameters of PV system, shade distribution are observed. It is also possible to compare the images by changing the azimuth using compass option available in ClimateStudio.
A more detailed procedure and background codes on which above procedure works can be found in climatestudiodocs.com.

3.3.3 Edge effects on crops

The performance of conventional bifacial PV systems i.e. bifacial gain is significantly influenced by edge effects especially at finite system size and higher ground clearance height. In simple words, higher the ground clearance, higher number of modules per row is suggested for higher energy yields of bifacial PV systems [85]. This means, there are effects of edges on inter row shading in an PV system. However, the focus of this section is to examine the influence of edge effect on crops i.e. different shading pattern caused at edges and internal rows of the panel. The light management for crops was analysed using sun hour distribution and radiation map. Therefore, the effect of edges is studied using both methods. For this analysis P=10 m, H=0.8 m, M=2 m, orientation: East/West (E/W) and simulated for entire year at Trondheim, Norway. Results for four row lengths are obtained: R=5 m, R=10 m, R=15 m, and R=20 m. The influence of ground clearance height has been presented in above sections and therefore a constant value of H = 0.8 m is chosen for this analysis. This value is between 0.5-1 m, which is recommended (outcome of this thesis) range for uniform shade distribution in an vertical bifacial East/West oriented agrivoltaic system. (Note: There is a possibility to check every combination between all these geometrical dimensions using parametric modelling. This has been presented in Erlend's master thesis.)

3.4 Case study

In this section, a 53.3 kWp agrivoltaic system will be designed. Energy modelling is carried out in PVsyst(Version 7.2). The energy for the crops is estimated using ClimateStudio. The results from ClimateStudio is used as solar energy input to the CATIMO crop model. A detailed PV system sizing, default values, and other relevant design information from PVsyst can be found in Appendix- 8.2. Relevant methods and results are presented in connection with this thesis.

3.4.1 Location and site selection

Skjetlein videregående skole (Skjetlein VGS) (N63°34.12′ E10°30.16′) is an upper secondary school located at a distance of 17 km from the city of Trondheim (N63°49.24′

E10°39.45′), Norway. The students are educated in organic farming, conventional farming, and renewable energy systems. Figure 32 shows an aerial view of the school premises. The school has two rooftop PV systems, a biomass plant, greenhouses, large fields for growing grass and other crops, and other facilities (not marked in the figure 32) like organic composting site, horse training sheds, cow sheds, grass storage sheds, laboratories, classrooms. The plan is to have this modelled system to be installed at the school area and collect data from the real system. The school will be a potential location for this project.

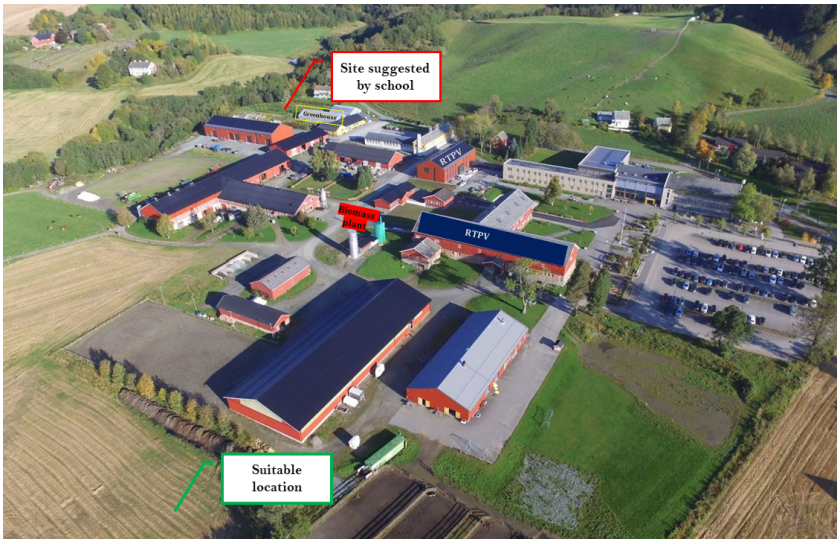

Figure 32: Aerial view of Skjetlein videregående skole showing selected site for the case study, greenhouse, and renewable energy systems [86].

The school authorities initially suggested a area near the greenhouse where some apple and berries are grown. However, initial shadow analysis using SketchUp reveal that having an vertical agrivoltaic setup at this site is not ideal. The reason for this is long duration shadows from nearby building as shown in Figure 33. The aim is to study the effect of shadow only from the vertical PV panels on the crop not by any other surrounding objects. Therefore, a area further down South-East as marked in Figure 32 is selected. This is presently a grass field and ideally suitable for this case study.

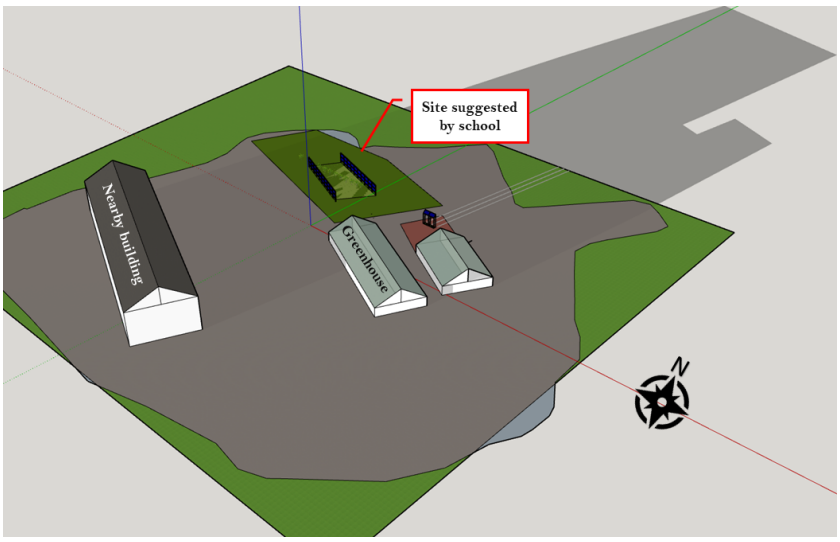

Figure 33: Shadow on summer solstice from surrounding buildings on suggested site at Skjetlein school.

PVsyst has four data sources from which weather data can be imported: PVGIS, NASA, Meteonorm and Solcast. In order to verify which database is most suitable for the location, an existing 84 kWp rooftop PV system at Skjetlein VGS is designed using PVsyst. Complete details of rooftop PV system design is available by clicking here. Note: The obtained report is in good agreement with the preliminary PVsyst report by Solbes company that had installed rooftop PV system at Skjetlein VGS.
The energy modelling results from these four data sources are compared with actual system production values for the month of June in 2020 and 2021. The reason for selecting only one month's worth of data is that, no data exists for winter months in 2020 and 2021. The real-time production data is collected and made available in solar edge link.
From the data in Figure 34 the average of actual system production for the month of June in 2020 and 2021 will be 12.8 MWh. This is quite high as compared with estimated values from four database. From Figure 34 it is clear that the closest possible estimate is from Meteonorm database. Even though the estimated value and real-time data has a lot of ambiguities, Ulrik Vieth Rør's thesis report [87] compared weather station data with PVsyst data sets and recommended Meteonorm data source is good for locations in Norway. However, these are numerically estimated dataset. Meteonorm dataset is assumed to be good data source for the Skjetlein and proceed further.

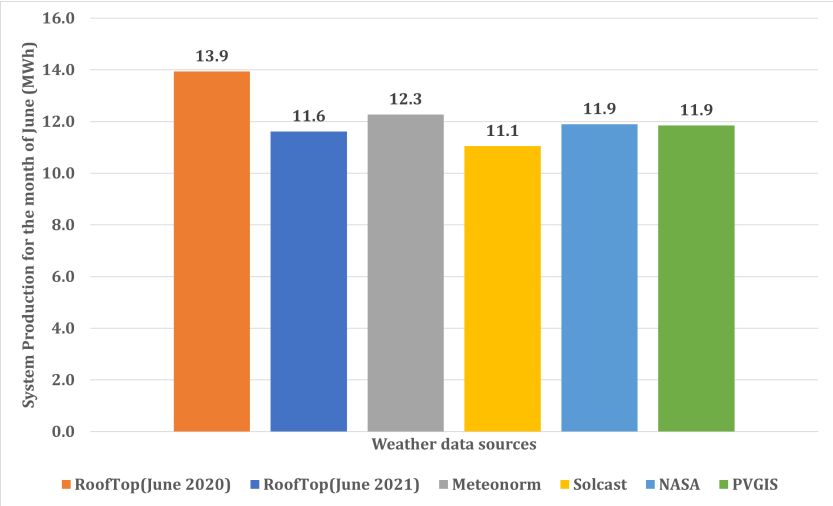

Figure 34: Comparing different weather source with actual data measurements from rooftop PV system by plotting system production (MWh) for the month of June

3.4.2 System sizing in PVsyst

The operating temperatures are kept at default values mentioned in PVsyst. The panel orientation is East/West (front face of the panel faces East), Row length (R) = Unlimited sheds (edge effects are neglected), Row Spacing(P)=10 m, Ground clearance height(H)=0.8 m, and albedo of 0.3 is selected for entire year. Table 6 show default losses values recommended in PVsyst. If the system is tilted ground or roof mounted, then different soiling percentages are recommended for the location of Norway due snow in winter. Since the system is mounted vertically, there is less chance of soiling loss due to snow and assuming that the dust collected during grass harvesting is washed by rain.

Table 6: Losses in percentage

Soiling	Mismatch	Ohmic losses	DC Wiring	Module efficiency loss	AC Wiring	Tracking	LID
3	2	1.5	2	-0.8	1	0	2

Table 7 shows a data sheet of bifacial modules used in this analysis as well as the total number of PV modules used. A Fronius inverter 'Tauro 50-3P' of 50 kW was selected from PVsyst database.

Table 7: PV Module datasheet & string details

JA Solar Bifacial panel 'JAM72-D09-370-BP' datasheet	
Parameter	Data
Rated Maximum Power (Pmax)[W]	370
Open Circuit Voltage(Voc)[V]	48.2
Maximum Power Voltage(Vmp)[V]	39.41
Short circuit current(Isc)[A]	9.91
Maximum power current(Imp)[A]	9.39
Module Efficiency(%)	18.64
Temperature Coefficient of Isc(α_Isc)	+0.060%/°C
Temperature Coefficient of Voc(β_Voc)	-0.36%/°C
Temperature Coefficient of Pmax(γ_Pmp)	-0.37%/°C
Maximum System Voltage	1500V DC(IEC)
Operating Temperature	-40°C∼+85°C
NOCT	45±2°C
Bifaciality	70%±5%
Weight	28.5kg±3%
Dimensions	1998mm×994mm×25mm
No. of cells	72(6x12)
Bifaciality factor	0.85
Number of modules per row	8
Number of modules stacked	2
Number of rows (Strings)	9
Total number of modules	144

Modules in series are 16 i.e 8 modules in row stacked at 2 modules in height, and the number of strings is 9. This arrangement was graphically created in PVsyst for shade analysis as shown in Figure 35. The total land area occupied by this system between the first row and the last row is around 1280 m^2 i.e. multiply the row length (16 m) by the total row spacing (80 m). The PV system area is 291 m^2. To make things simpler it is assumed that there are no nearby objects or buildings exist. Through PVsyst's inverter sizing function, inverter sizing was done and a DC-to-AC ratio of 1.066 was estimated.

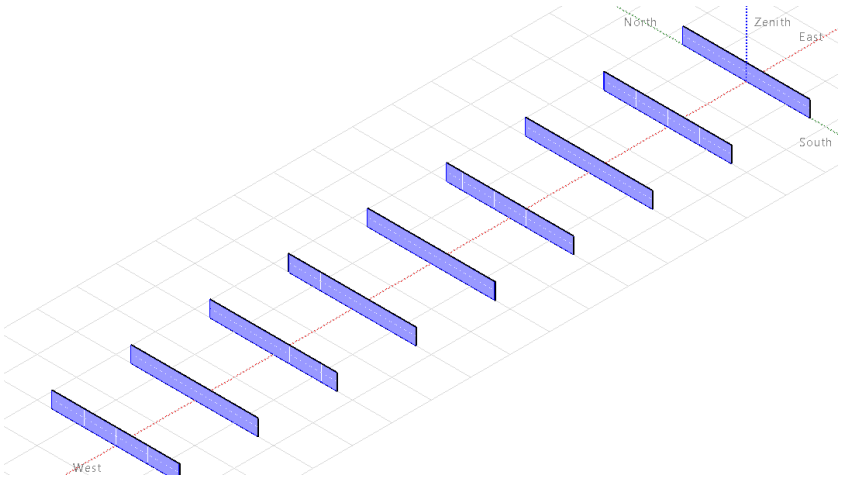

Figure 35: Shading scene construction in PVsyst showing 9 rows of PV array oriented in the East/West direction, separated by a row spacing of 10 m, ground clearance height of 0.8 m.

Figure 36 shows the horizon profile imported from Meteonorm data source for the location of Skjetlein.

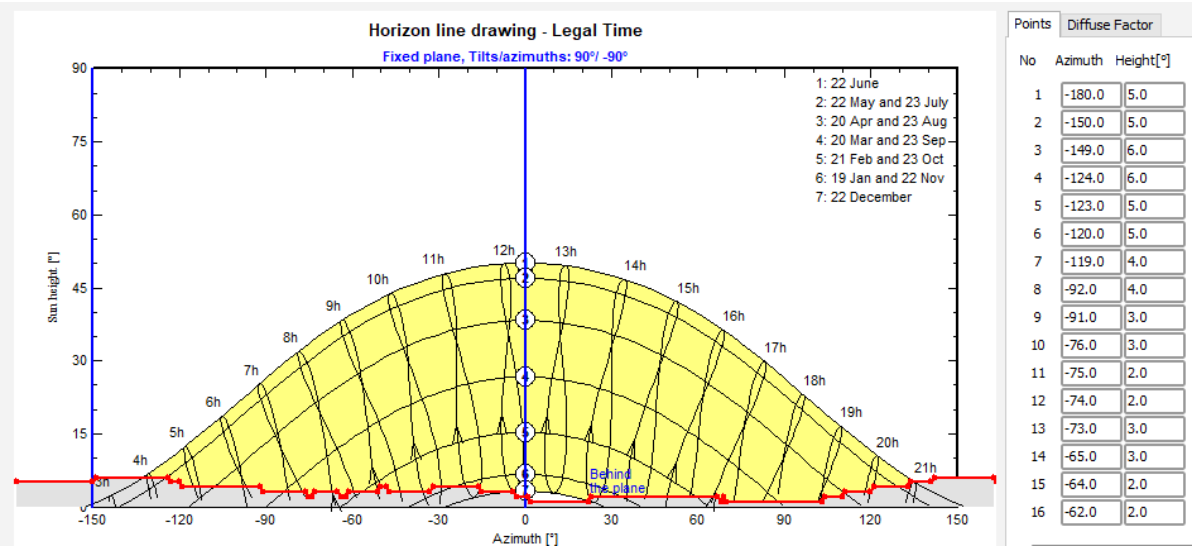

Figure 36: Horizon line drawing for the location of Skjetlein.

3.4.3 Crop yield

The geometry shown in Figure 37a was drawn in rhino3D and the radiation map procedure described earlier was applied to it. Figure 37b shows the grid point selected for this analysis. The results from ClimateStudio were exported and used in the timothy crop model (the CATIMO crop model). The crop 'timothy' chosen in this study is unique and grown in cold countries like Norway, Canada, and parts of Russia.

Helge et al. (2002) [88] originally developed the CATIMO (Canadian Timothy Model) for estimating growth of timothy grass by considering solar radiation, Nitrogen content, soil moisture and temperature. This model has been validated with three other crop model in [89]. The equations mentioned in original paper has been used to develop a Python based crop model exclusively for timothy grass. This has been developed and written by Erlend Hustad Honningdalsnes, Master student at NTNU in consultation with the author(for the [88]) Helge Bonesmo, a researcher at The Norwegian Institute for Bioeconomics (NIBIO). The crop model is part of his thesis and both of us have spent long hours discussing the processes mentioned above as well.

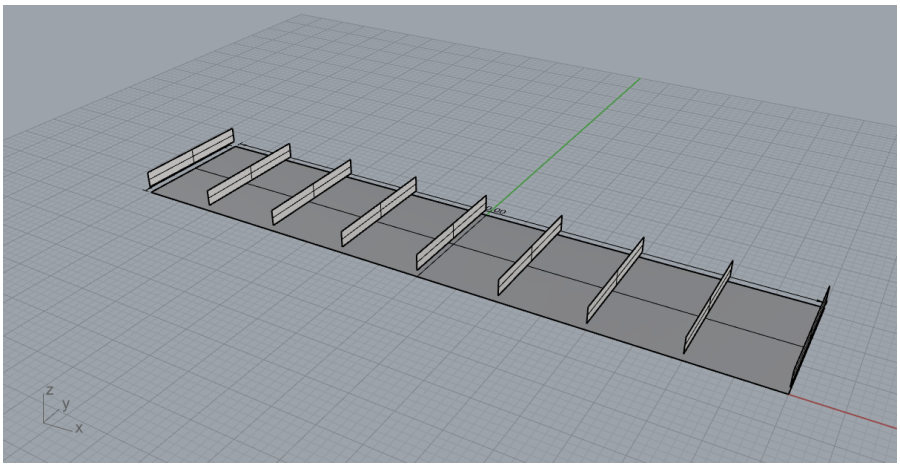

(a) Isometric view of 53.3 kWp agrivoltaic system drawn in rhino3D software

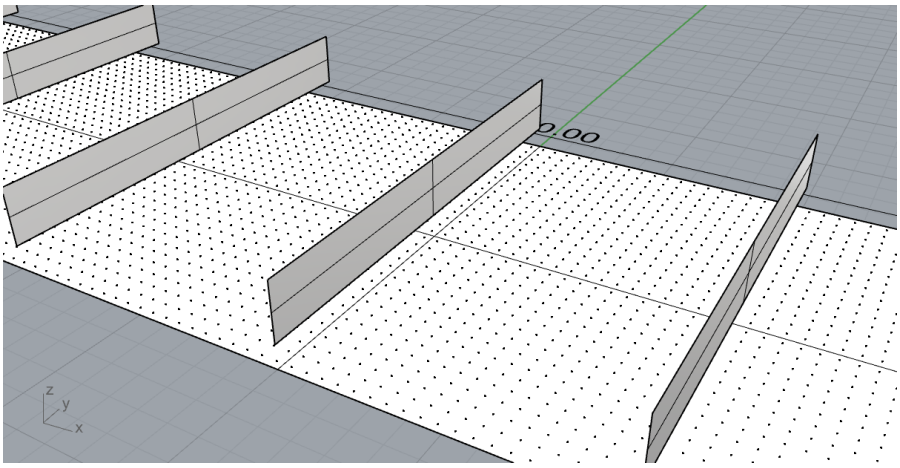

(b) Section of 53.3 kWp agrivoltaic system showing grid points

Figure 37: Geometry of 53.3 kWp vertical bifacial agrivoltaic system.

The output from ClimateStudio is used to calculate how much sun light energy is reduced due to shade from the vertical bifacial panels. This reduction percentage (annual average of shadow percentage) is multiplied by the daily global horizontal radiation TMY data available for the location of Skjetlein (N63°34.12′ E10°30.16′). Then the crop model

is used to estimate the available daily global horizontal radiation to the crops for the entire year. However, the grass growth begins only after early June and ends in late September.
Part of this radiation energy is used by crops for photosynthesis and it is called PAR. According to [88] for timothy grass, 48% of available daily global horizontal radiation is equal to PAR. This radiation energy i.e PAR is then converted into crop biomass (kg/decare). The crop model assumes sufficient water, nitrogen & other nutrients, soil temperature levels are available for the required crop yield. These values are assumed based on the real data that are calibrated by Helge Bonesmo.
There are three ways crop yield is estimated in this vertical agrivoltaic system. The first way is to add all the yields from the agrivoltaic area, assuming the exact crop yield at every region and also counting crops' yield from the area below PV rows. However, assuming the exact crop yield at every region is not an accurate method because most shaded and less shaded areas exist between the vertical PV rows. Also, the tractor equipment cannot harvest crops grown below the PV panel rows, so even this cannot be considered.
The land equivalent ratio is calculated using obtained crop yield and energy yields. LER is represented by a simple equation below

$$LER = \frac{Y_{cropAVS}}{Y_{monocrop}} + \frac{Y_{electricityAVS}}{Y_{electricityPV}} \tag{7}$$

where the monocropping system refers to growing crops in open field; PV refers to a conventional ground mounted PV plant, and AVS refers to the dual-use agrivoltaic system.

4 Results

The results obtained in the previous chapter are presented here. The flow of results is in line with the methodology sections 3.2, 3.3, and 3.4.

4.1 Vertical bifacial system

The results obtained from the methodology section 3.2 are explained below.

4.1.1 Land area occupancy

Table 8 shows step-by-step calculations of land coverage ratio (LCR) and power-to-land ratio (PLR) for three different agrivoltaic system configurations and rooftop PV. The rooftop PV is for the reference area and is not used for comparison with the agrivoltaic system.

Table 8: Comparison of LCR & PLR calculations for three different agrivoltaic configurations.

	RoofTop PV	VAPV	GMAPV	EAPV
Total land or roof area available (m^2)	572	572	572	572
Tilt	25	90	49	49
Wp of PV panels	300	375	375	375
Total number of PV panels	280	102	102	102
Installation Capacity (kWp)	84	38.25	38.25	38.25
Panel placing type	Portrait	Landscape	Landscape	Landscape
Panel length (m)	1.62	1.7	1.7	1.7
Panel height (m)	1	1	1	1
Number of Rows	5	3	3	3
Number of stack	NA	2	2	2
Panels per row	56	17	17	17
Row length (m)	56	28.6	28.6	28.6
Length occupied by PV panel mounting structure(m)	NA	28.6	28.6	0.5
Width occupied by PV structure (m)	NA	0.25	1.31	1
Number of base structure required per row in EAPV	NA	NA	NA	5-6
Land or roof area occupied by PV structure (m^2)	572	21.45	107.068	8.58
Area that is available for farming (m^2)	NA	550.6	459.4	563.4
Land coverage ratio (LCR)	1:1	0.04:1	0.2:1	0.02:1
Power to land ratio (PLR)	0.15:1	1.78:1	0.34:1	4.46:1

Figure 38 shows PLR and LCR values for three agrivoltaic system configurations and a rooftop PV system. The rooftop PV system results mentioned in the Figure 38 is for the reference alone and has not been used in comparison with agrivoltaic configurations. This information, of course, is helpful if the economy and energy yields of all these systems are estimated in future studies.

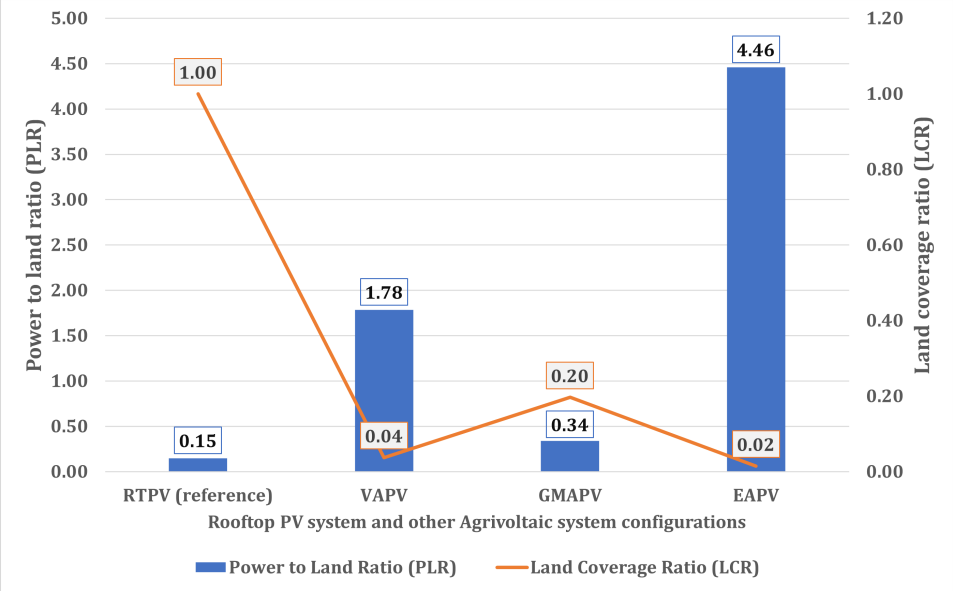

Figure 38: Power to land ratio and Land coverage ratio for rooftop PV system and agrivoltaic configuration: vertical agrivoltaic system (VAPV), elevated agrivoltaic system (EAPV), ground mounted agrivoltaic system (GMAPV)

In EAPV, the PV panels and structure is mounted on the poles, as shown in Figure 26c. These poles are supported by a base concrete structure, i.e., a footing. Hence, this concrete base area is occupied by PV structure in EAPV. Each of these footings and structures is highly specific on a case-by-case basis. The design is influenced, among other things, by the crops, the solar radiation, wind speed, farming machinery and practices followed. Furthermore, as shown in Figure 26c, the structures have to be sturdy and massive, which also elevates the CAPEX. In general, the land area occupied in EAPV is by footings alone.
In the case of VAPV, the land right below rows of PV panels cannot be used for any other purpose; hence, this is considered an area occupied by a PV structure. The LCR of both of these systems is almost equal, but PLR for EAPV is larger than for VAPV. This is because EAPV occupies less ground area for the exact PV capacity than VAPV. Ground mounted agrivoltaic system (GMAPV) has very small PLR and large LCR. So these kind of systems are not suitable for driving tractors with width 8-10 m and as grass grows taller, this might shade the PV arrays. However, these systems can be suitable where obtaining large land area not an issue. Whereas VAPV and EAPV suits best in places with shortage of land area. Depending on the type of crop and selected location, either of these configurations can be implemented. All of these agrivoltaic settings aims

to ensure required quantity of light to the crops and on the one hand, reduce dependency on new land for setting up new PV power plants on the other hand.
The capital expenditure (CAPEX) for all these systems would change depending on the PV system design and capacity. The factors that influence the design of these systems are tractor dimensions, crop type, and land terrain. In the case of EAPV systems, there is a possibility of having shade on the neighbouring land due to elevated PV structures. Considering all these factors, a vertical agrivoltaic system (VAPV) is good for the location of Norway due to its low LCR and avoiding conflicts with neighbouring land.

4.1.2 Albedo

Figure 39 shows the variation of ground reflected energy on the rear-side as albedo values are varied. The ground energy reflected on the rear-side increases with albedo percentage, and it is received higher when PV surfaces are oriented East/West than South/North. East/West oriented systems are less susceptible to self-shading than North/South systems, and therefore they receive high ground reflected radiation at higher albedo, especially after 0.5 albedo. Similar observations was made by Sun X et al.[90]. The Trondheim region receives frequent snowfall during winter; hence, vertical systems provide additional protection from soiling, less cleaning, and extra energy from ground reflections during fresh snow.

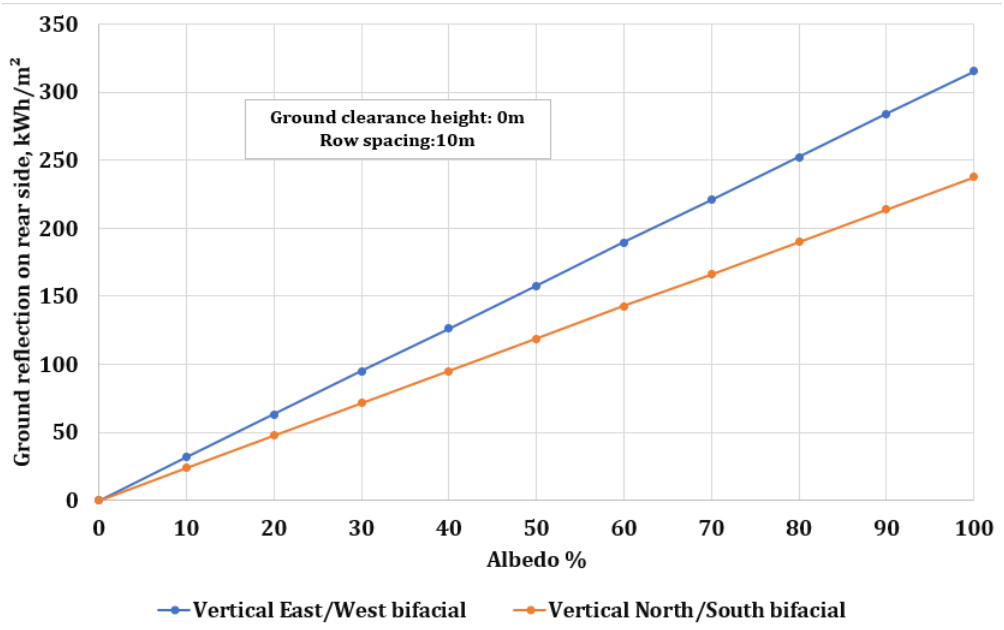

Figure 39: Ground reflection on rear side of bifacial PV panels v/s albedo % for East/West and North/South oriented vertical PV systems.

4.1.3 Latitude v/s bifacial gain

Figure 40 and Figure 41 are the direct result obtained when a parametric sweep is performed in SAM. The colorful plot is beautiful yet complex to read and understand the results. Figure 40 show POA rear-side bifacial gain percentage against tilt angle and azimuth for the Trondheim location. As it can be observed, the colors are spread over the range of axes values and it is difficult to obtain specific results. Therefore, a simple graph has been prepared using these results and is presented in Figure 42 and Figure 43.
Figure 40, 41, 42 and 43 show POA rear-side bifacial gain percentage for two locations as the angle of tilt and azimuth is varied. It is very much evident from Figures 41 and 43, the azimuth does not have much impact on bifacial gain at Phoenix (N33°44.99′ E−112°6.74′), USA and has symmetric profiles. Whereas azimuth has much impact on bifacial gains at Trondheim (N63°40.95′ E10°44.77′), Norway and Figure 42 show asymmetric profiles. In both locations, bifacial gain increases with the angle of tilt. At 90° tilt angle with East facing front-side, the bifacial gain at Trondheim is around 100% whereas at Phoenix it is 80% in comparison with around 10% bifacial gain at 10° tilt for both locations.

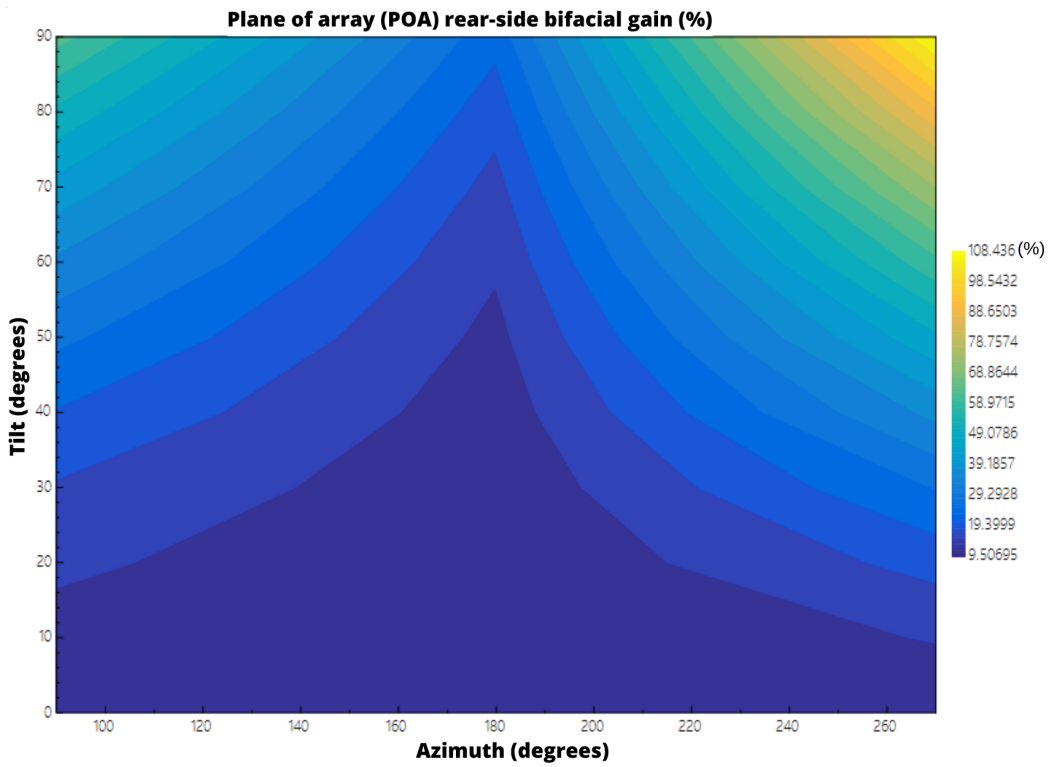

Figure 40: System Advisor Model (SAM) result showing POA rear-side bifacial gain percentage v/s azimuth and tilt for Trondheim, Norway.

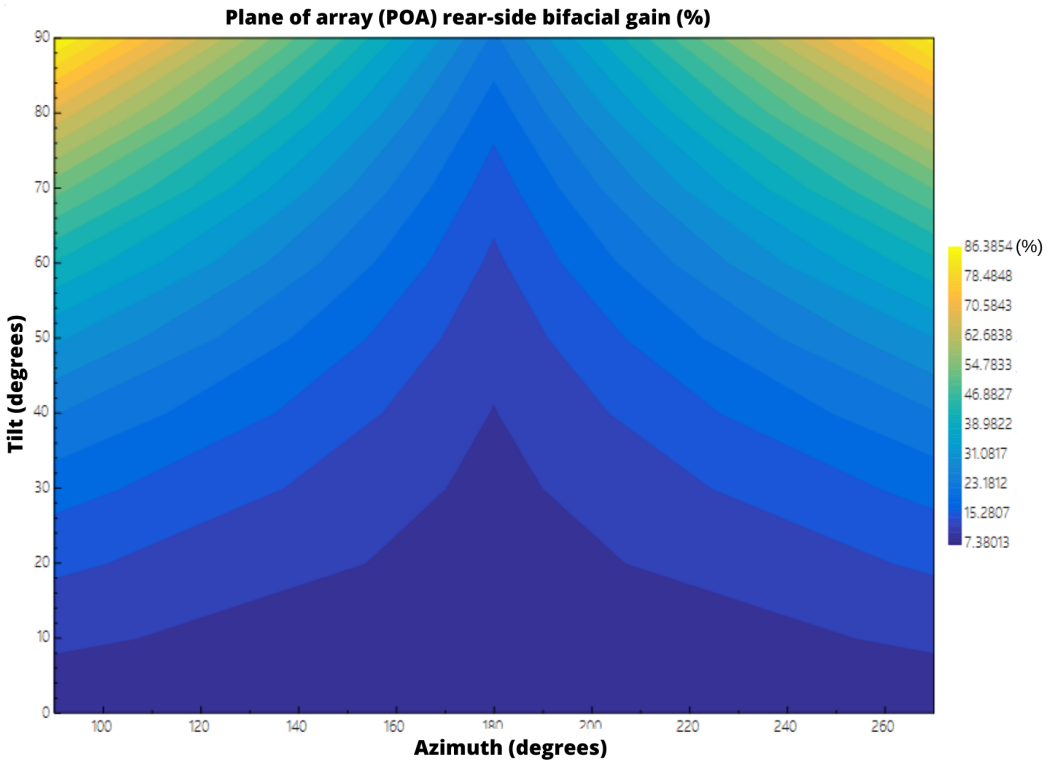

Figure 41: System Advisor Model (SAM) result showing POA rear-side bifacial gain percentage v/s azimuth and tilt for Phoenix, USA.

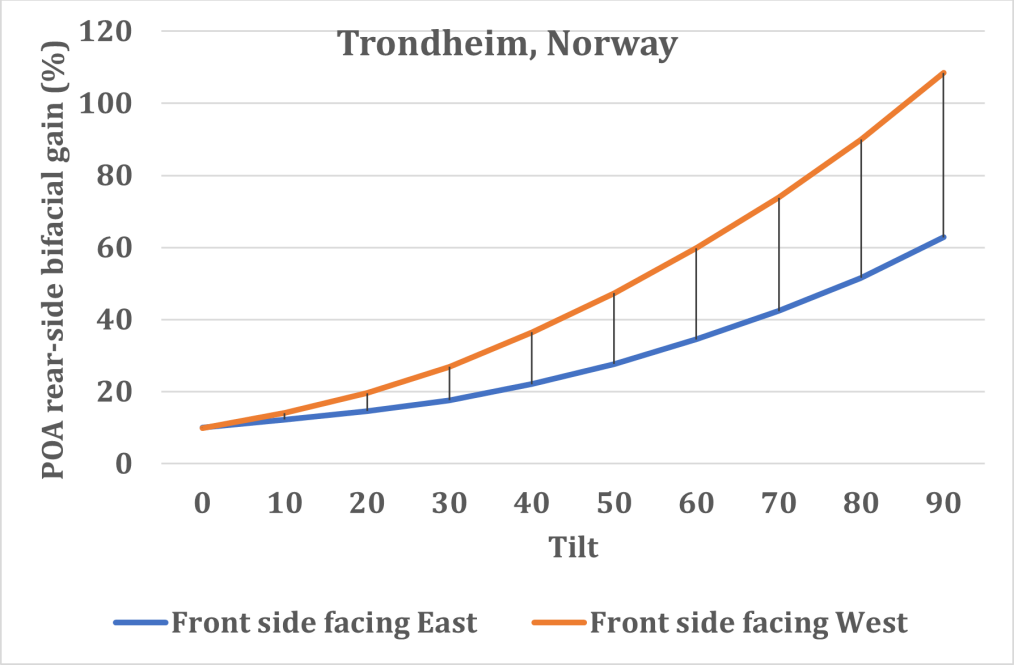

Figure 42: POA rear-side bifacial gain percentage v/s tilt results for Trondheim, Norway

A higher bifacial gains observed in Figure 42 for West facing system than East facing system. One reason could be relative humidity, i.e. the amount of water particles in the air is lower in the afternoon than in the morning due to higher air temperatures. Also, the mountains (horizon) and wind directions might be additional reasons.

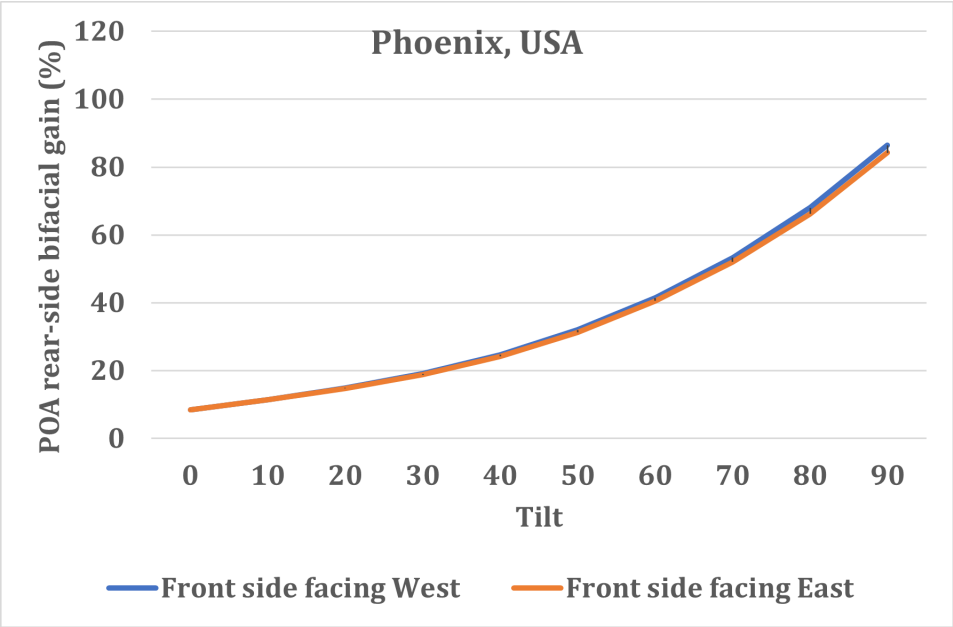

Figure 43: POA rear-side bifacial gain percentage v/s tilt results for Phoenix, USA

The above mentioned reason is validated by obtaining POA rear side total radiation for each season and hourly resolution. Figure 44 shows rear-side total radiation for all four seasons at summer & winter solstice and spring & fall equinox.

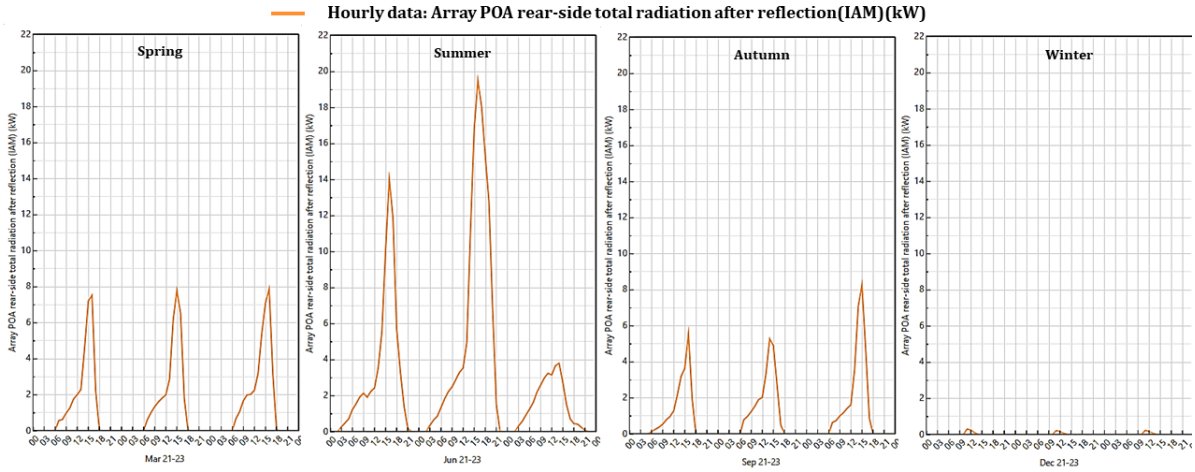

Figure 44: POA rear-side total radiation after reflection(IAM)(kW) for various periods during four seasons at Trondheim, Norway.

There is clear evidence that the rear side receives more radiation post noon in all seasons. Based on this, it can concluded that bifacial PV panel with the front-side facing West have better rear-side bifacial gain than its counterpart. Note: Figure 44 shows results with an hourly offset.
Figure 45 and Figure 46 further investigate the asymmetric profile of bifacial gains observed for the location of Trondheim in Figure 42. Even though there is a high rear-side bifacial gain when the PV panel faces West, it still has a lower energy yield than an East facing panel for the same tilt as shown in the Figure 45. This is evident in Figure 46 where the East facing front side receives more irradiance than West facing.

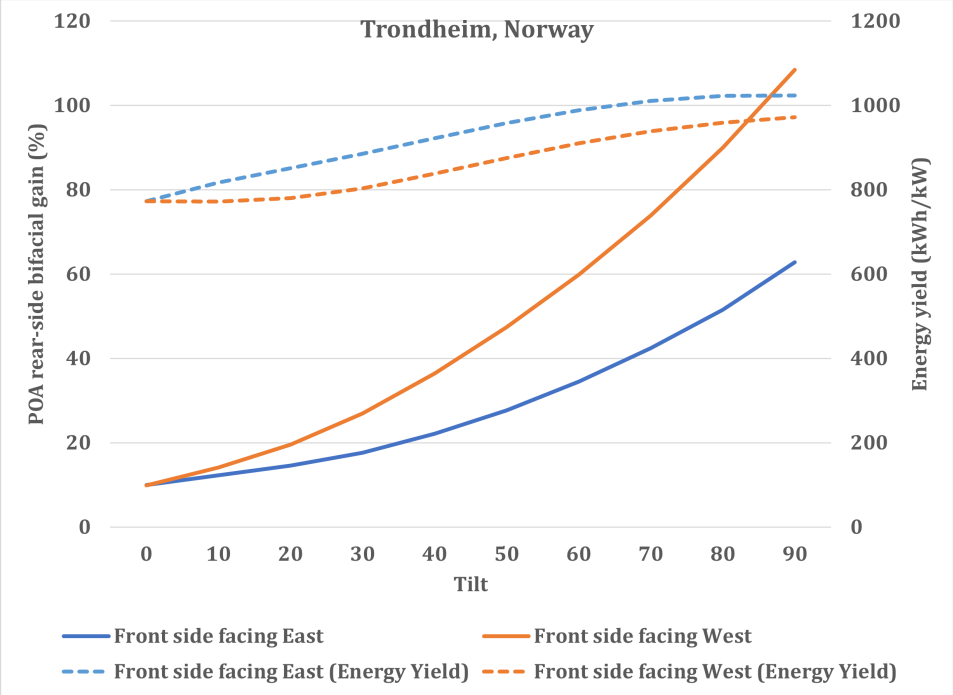

Figure 45: POA rear-side bifacial gain percentage (left axis) & energy yield (right axis) v/s tilt

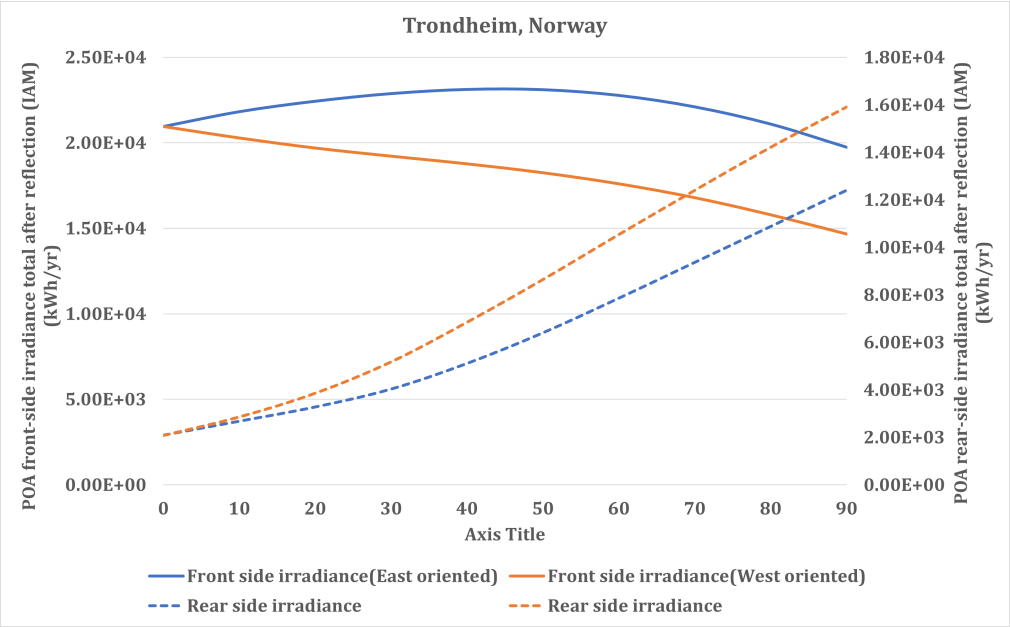

Figure 46: POA front-side irradiance total after reflection (IAM) (kWh/yr) (left axis) & POA rear-side irradiance total after reflection (IAM) (kWh/yr) (right axis) v/s tilt

Figure 47 shows the variation of energy yields with the tilt of a PV system plotted for monofacial and bifacial PV module technology. The module rating and specification used are the same for monofacial and bifacial PV modules, except for bifaciality for bifacial modules. In both latitudes i.e. Phoenix (N33°44.99′ E−112°6.74′) (Figure 47b) and Trondheim (N63°40.95′ E10°44.77′) (Figure 47a) the vertically mounted East-facing bifacial modules outperform vertically mounted South facing monofacial modules.
In most cases, the optimal tilt angle for a location to produce maximum PV energy in a monofacial system is the same as its latitude. So at Phoenix, the optimal tilt would be around 33°, and South oriented monofacial system performs well. That means this logic would work. Similarly, at Trondheim, the optimal tilt would be 63°, but the South monofacial system performs at around 49°. So this logic does not work at higher latitude locations.
If East facing bifacial system is consider at both locations, the optimal tilt is 90°. After 55° tilt, the bifacial modules outperform monofacial modules at both locations.

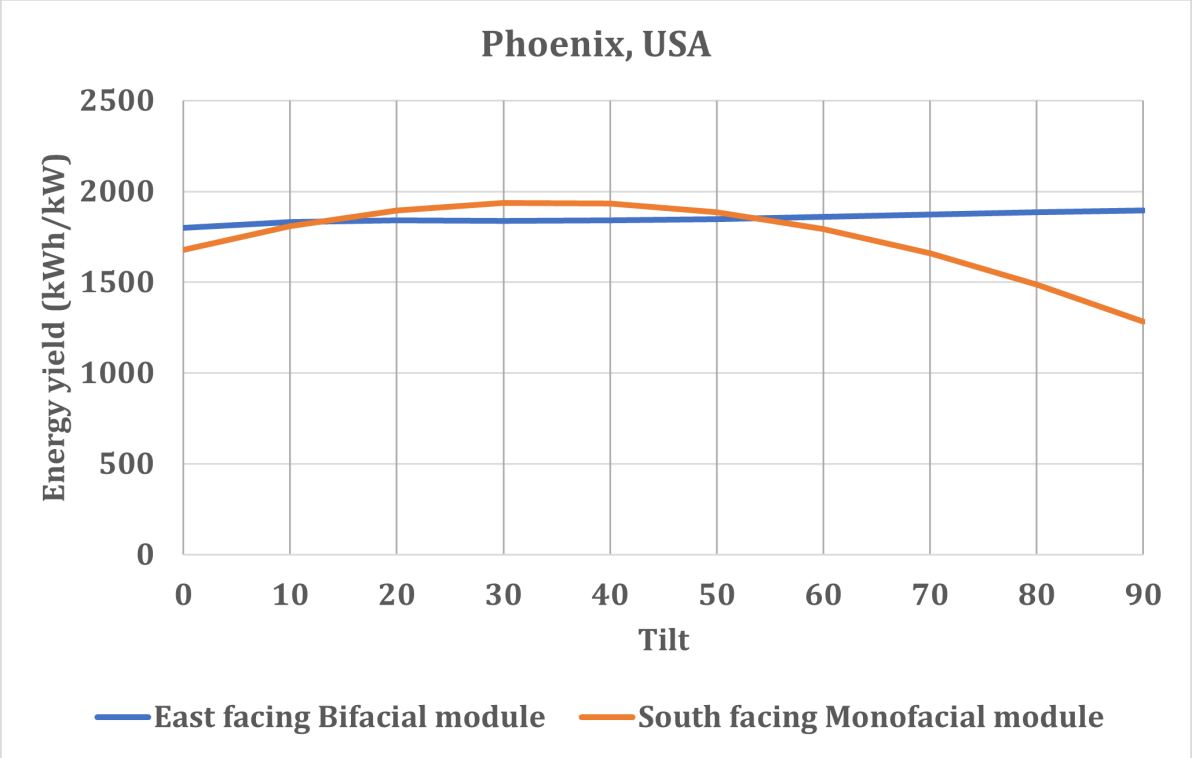

(a) Energy yield versus tilt at Phoenix, USA

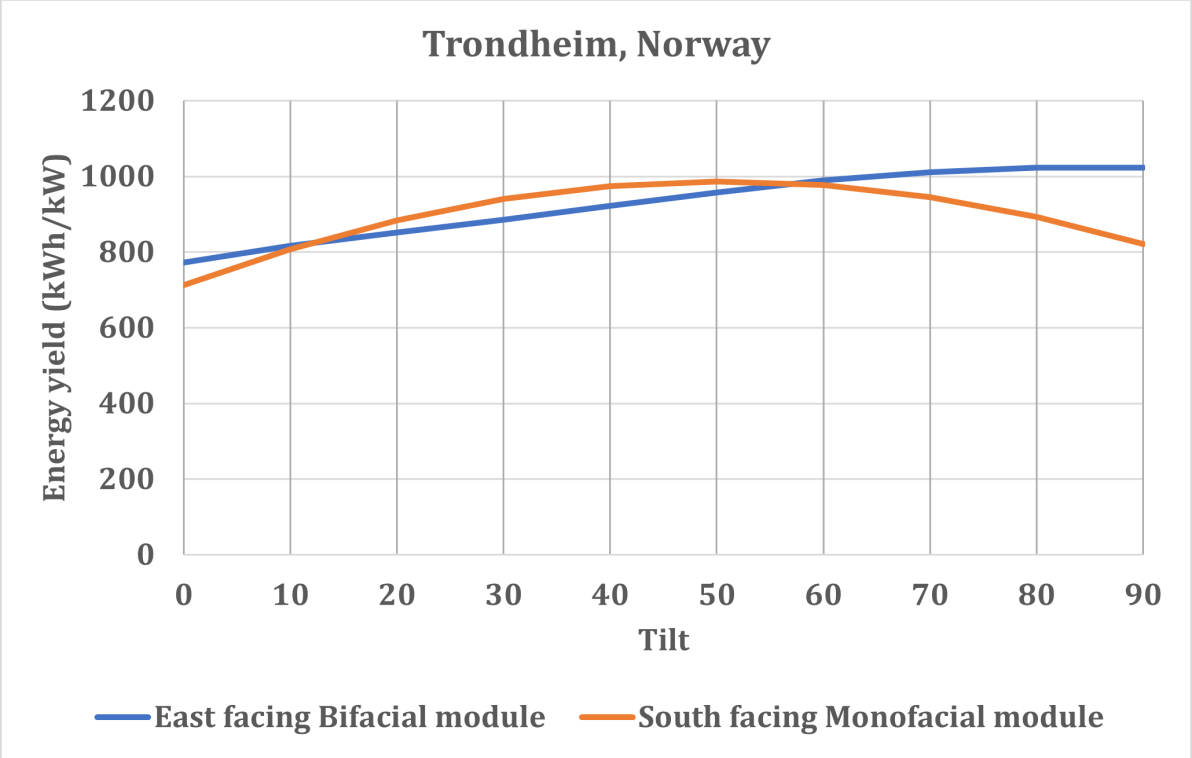

(b) Energy yield versus tilt at Trondheim, Norway

Figure 47: Energy yields for different type of PV modules at two different latitudes.

4.1.4 Bifaciality

Figure 48 shows increase in energy yield(kWh/kW) as bifaciality increases. This is a well-predicted outcome; however, the interesting fact is how the orientation of PV systems behave with different bifaciality. Figure 48 indicates that it is recommended to have bifacial panels with a higher bifaciality of at least 0.85 for East/West systems to outperform the South/North system in high latitude places like Trondheim, Norway. In the South-oriented systems case, the energy yield increase is 23.97% from bifaciality 0 to 1. The same in West and East oriented systems are 111.03% and 65.92% respectively. Therefore, choosing bifacial panels with higher bifaciality could yield higher energy in East/West vertical systems than South-oriented systems.
Further, to show aforementioned criteria could be different for lower latitude place like Japan, Figure 49 has been obtained through similar calculations. It shows that even as low as 0.65 bifaciality could have slightly better yields in the East/West system than in South-oriented systems. The higher the bifaciality higher is the cost of the PV panels.

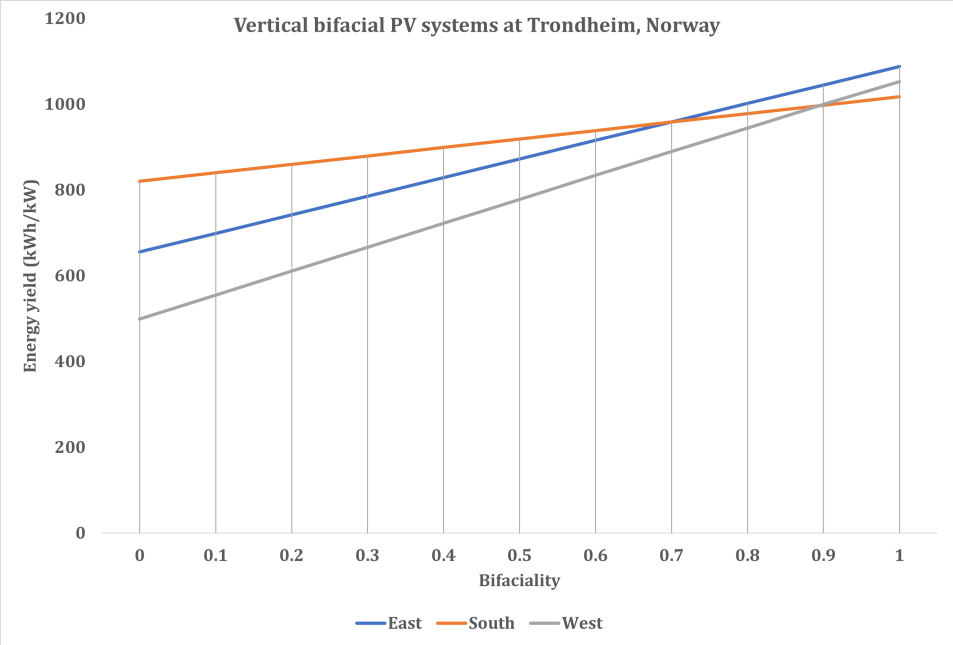

Figure 48: Bifaciality v/s energy yield(kWh/kW) at Trondheim, Norway for three orientation: South, East and West.

Figure 49 shows energy yield versus bifaciality for the location of Fukushima prefecture, Japan.

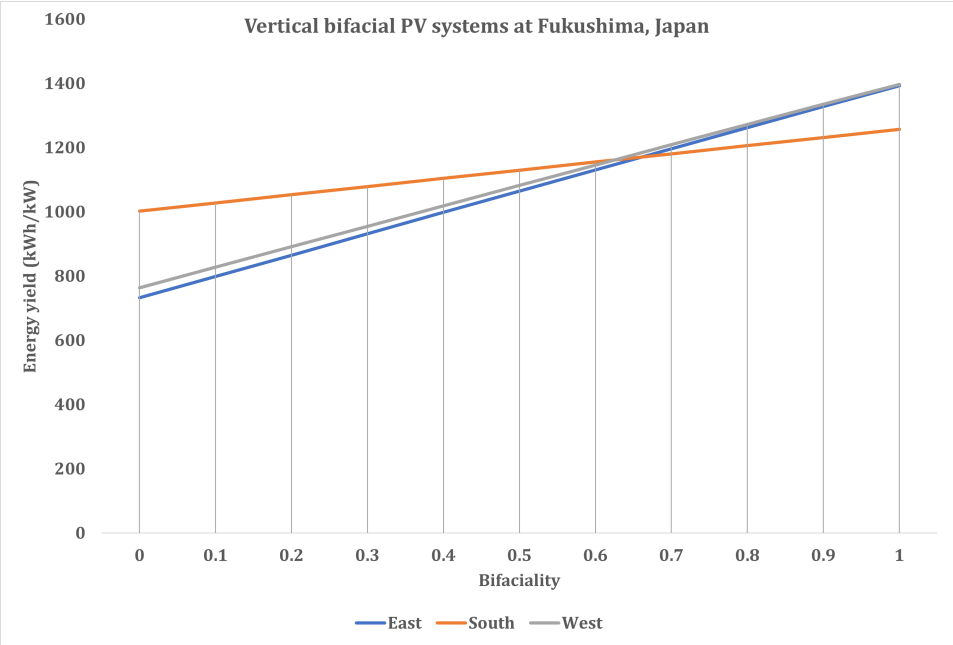

Figure 49: Bifaciality v/s energy yield(kWh/kW) at Fukushima prefecture for three orientation: South, East and West.

4.1.5 Tregenza skydome

Figure 50 shows a colored Tregenza sky dome representing sky radiation conditions for each season. The Tregenza sky dome is subdivided into patches with a total solar radiation value for each patch. The solar radiation patches are horizontal during winter and autumn, as shown in Figure 50d and Figure 50c. Furthermore, the sun's azimuth (horizontal angle) coverage is also less, i.e., East to West in Autumn, ESE to WSW in Winter. Figure 50b shows the sky dome of the summer months. It shows the highest radiation values(long daylight hours), higher sun's azimuth coverage (from NE to NW), and more radiation coming from ESE and WSW directions. This helps for higher electricity generation in a vertical bifacial PV system and protects crops from the sun's heat stress, thus allowing required radiation for crop photosynthesis. During the Spring months, as shown in Figure 50a, the radiation is more concentrated between SSE and SSW, thus helping to melt the snow from winter and prepare the land for farming activities in summer.

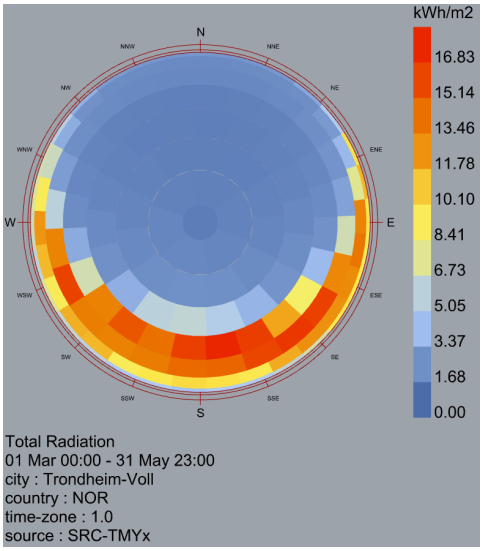

(a) Spring (March-May)

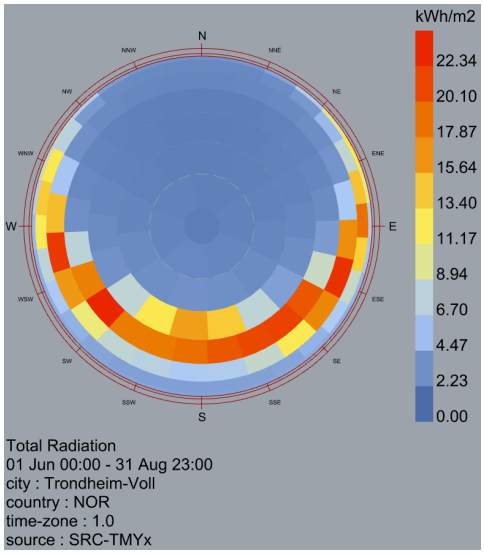

(b) Summer (June-August)

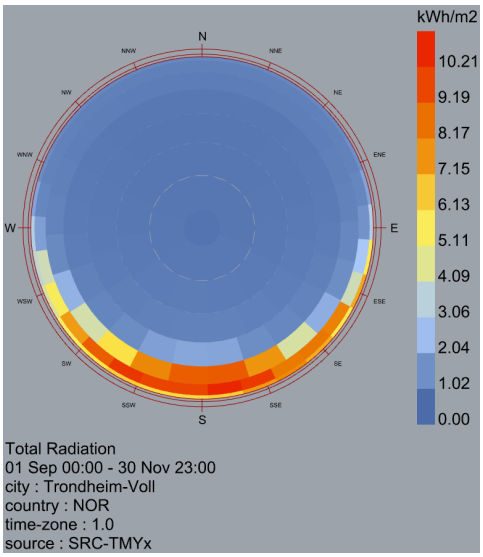

(c) Autumn (September-November)

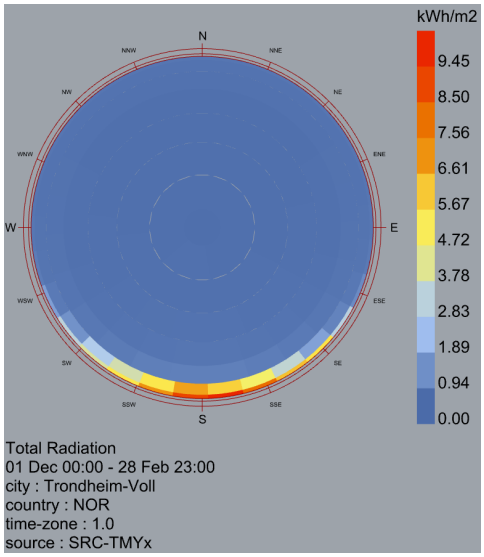

(d) Winter (December-February)

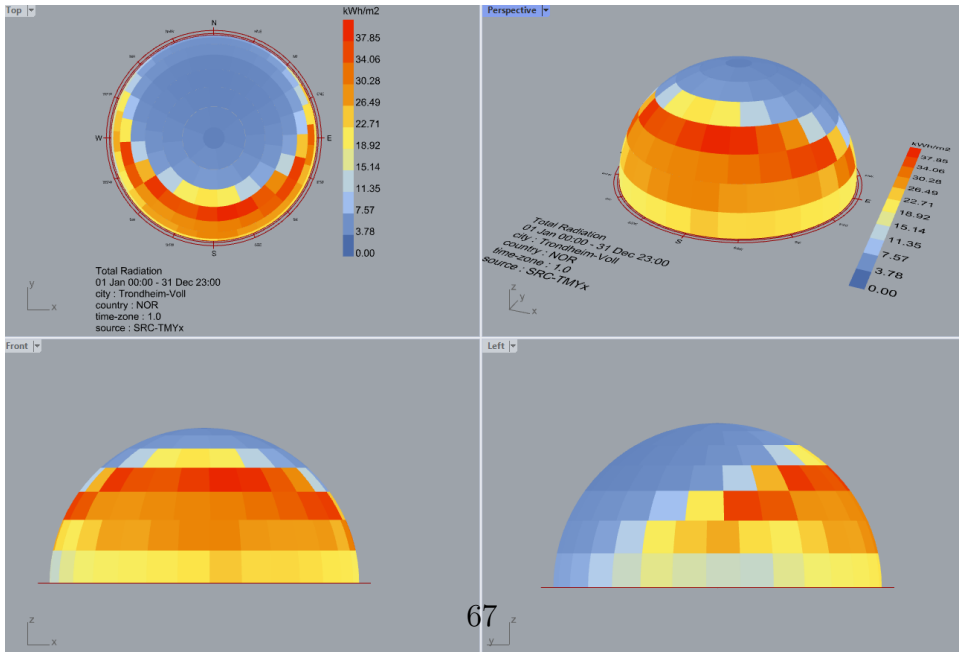

(e) Entire year solar radiation sky dome

Figure 50: The sky condition for Voll,Trondheim during all seasons of the year. a)Spring Fig. 50a, b) Summer Fig. 50b, c)Autumn Fig. 50c and Fig. 50d. Sky condition for whole year is shown in Fig. 50e.

4.1.6 Bifacial model in PVsyst

a) Diffuse acceptance percentage v/s ground clearance height (H)

Figure 51 shows changes in diffuse acceptance values as 'H' is increased from 0 m to 2 m. In Figure 51a, 51b, 51c, and 51d the view factor on the rear-side of the panels and reflected diffuse percentage is also shown. In each of these figures, the top part shows how ground reflected irradiance is intercepted by PV panels. The reflected ground radiation intercepted by PV panel rows decreases as 'H' is increased, depicted by a decrease in view factors in Figure 51a to 51d. However, at H = 2 m, the view factor is increased to 4.5% from 4.4% at H = 1 m. This is due to additional ground radiation that is reaching the bottom edges of PV panel rows as it can be observed in top pictures of Figure 51c and 51d.
There is an increase in average diffuse acceptance percentage values as 'H' increases, and it tends to become more uniform distributions between PV panel rows. There is a clear indication of a drop in these values at the edges. Further increase in 'H' is advantageous in terms of light to the crops, but the CAPEX for mounting structure would increase, and sturdy footings are needed to withstand wind loads. An optimal 'H' value between 0.5 - 1 m is recommended for a vertical East/West bifacial system because of a more uniform distribution of diffuse light. This is in good agreement with values mentioned by Elin Molin et al., [91] i.e. 0.5 m for Oslo, Norway.

b) Diffuse acceptance percentage v/s module height (M)

Figure 52 shows diffuse acceptance percentage values at module height 1 m and 2 m respectively. The average diffuse acceptance dropped to 81.6% from 90%. For the same ground clearance height, the diffuse light at the ground level decreases with an increase in module height. This is very much evident in Figure 52a and 52b for 'M' values 1 m and 2 m respectively. A 10% decrease in diffuse acceptance results in the gain of average view factor on the rear-side, around 67%. This gain is beneficial for the PV energy yield and its performance. Therefore, increasing module height (stacking two modules) does not impact the light energy available to the crops as anticipated. Further increase in module height (> 2 m) would probably decrease the light available to the crops by imparting more shade. Even though more energy is produced from three-module stacking, this is not the purpose of agrivoltaics. Also, the row spacing have to be increases to reduce inter-row shading.
Hence upto two module heights and a ground clearance height between 0.5-1 m would suit crops in a vertical bifacial East/West agrivoltaic system for selected location.

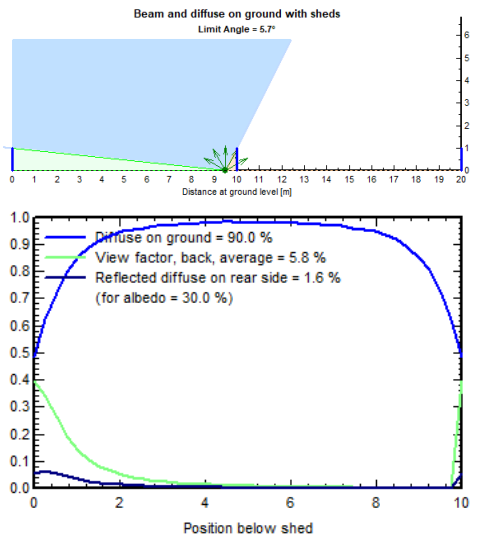

(a) H = 0 m

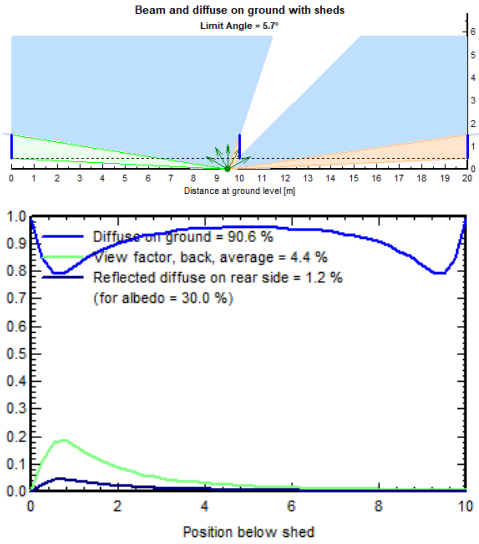

(b) H = 0.5 m

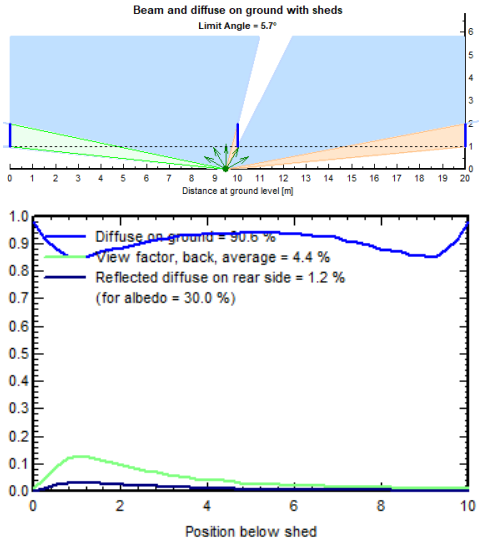

(c) H = 1 m

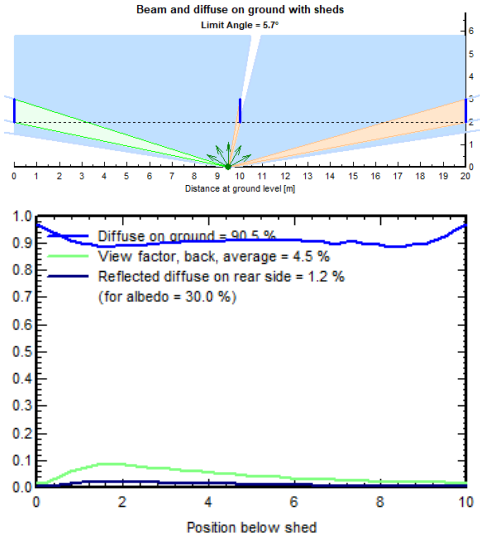

(d) H = 2 m

Figure 51: Variation of diffuse acceptance percentage with ground clearance height(H) in a vertical bifacial PV system. The PV panel is orientation in East/West with Row spacing(P)=10 m, Module height(M)=1 m, and Row length(R)= unlimited sheds. a) Fig. 51a for H=0 m, b) Fig. 51b for H=0.5 m, c) Fig. 51c for H=1 m, and d) Fig. 51d for H=2 m.

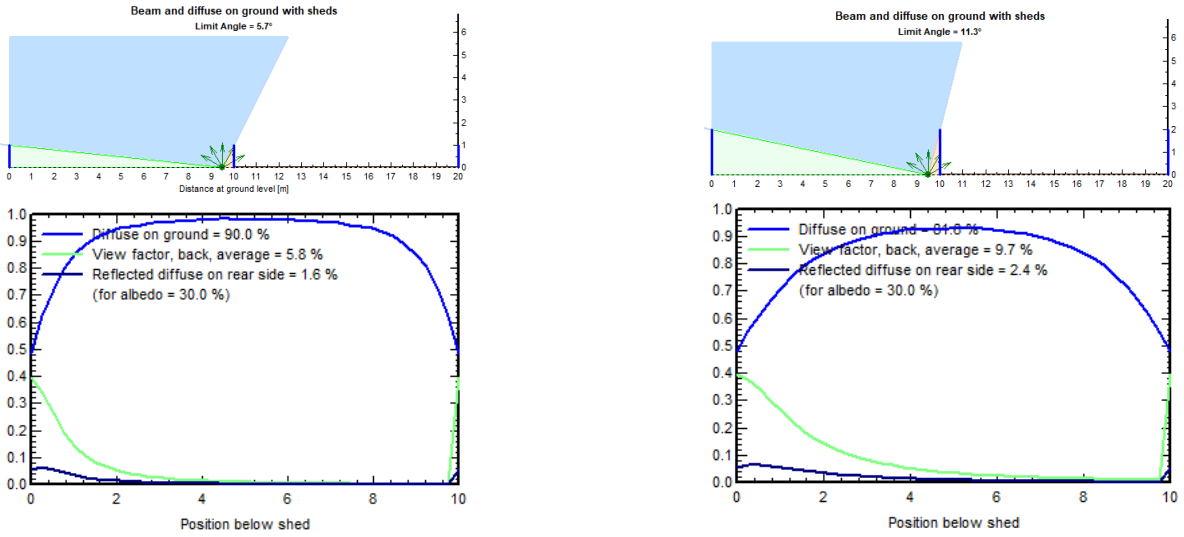

(a) H = 0 m, M = 1 m

(b) H = 0 m, M = 2 m

Figure 52: Variation of diffuse acceptance percentage with module height(M) in a vertical bifacial PV system. The PV panel orientation is East/West with Row spacing(P)=10 m, Ground clearance height(H)=0 m, and Row length(R)= unlimited sheds. a) Fig. 52a is for module height = 1 m and b) Fig. 52b is for 2 m.

4.1.7 Annual energy production in PVsyst

Figure 53 shows annual energy produced in a 5 kWp vertical bifacial PV system for different orientations at the location of Trondheim, Norway. Figure 53a, 53b, 53c, and 53d compares the total energy produced in each hour of the day over the year against hour number.

When comparing an South oriented system with South/East and South/West i.e., shown in Figure 53a and 53b, the South/East and South/West curves spread across the day with one large peak and one short peak. Whereas in South-oriented system there is only one peak at around noon. The difference in energy production curves indicates tapping of solar energy available during pre-noon and post-noon hours of the day. There is a significant difference in total system production (annual energy to the grid) and specific production values for these three orientations as shown in Figure 53e. The South/West oriented system have the highest output among these three orientations.

While comparing South oriented with East and West, two peaks and a wide spread energy generation across the day is observed in Figure 53c and 53d. Thus able to match the daily load (electricity demand) profiles with production profiles. Among these five orientations, an East facing vertical bifacial system has better energy output. Energy yield is more in East facing system than West facing system (Figure 53e) and this is in agreement with the results (Figure 46) obtained in SAM for the same location.

Note: 'East or West or South' facing means the front-side of the bifacial PV panel is facing that direction. In a South/West facing system, the front side covers all solar radiation from East to South and it is opposite in South/East system.

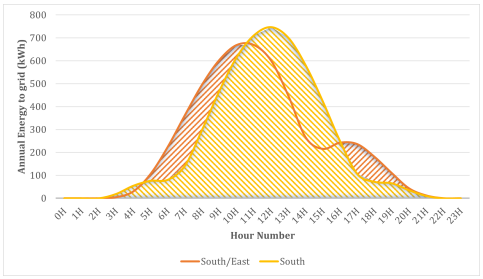

(a) Comparing South & South/East

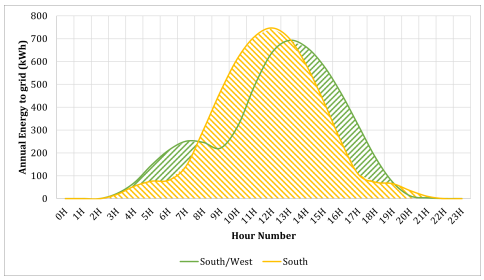

(b) Comparing South & South/West

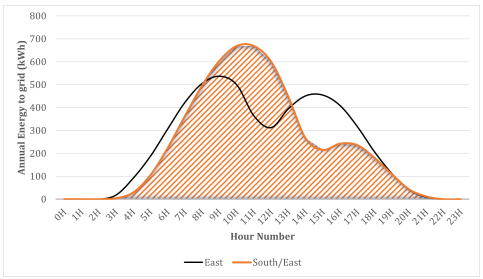

(c) Comparing South & East

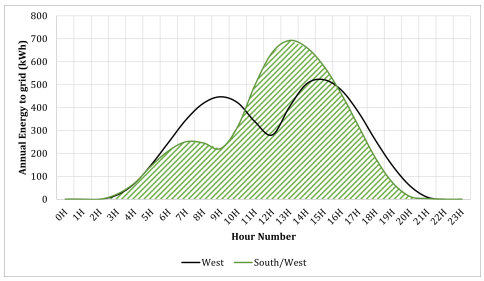

(d) Comparing South & West

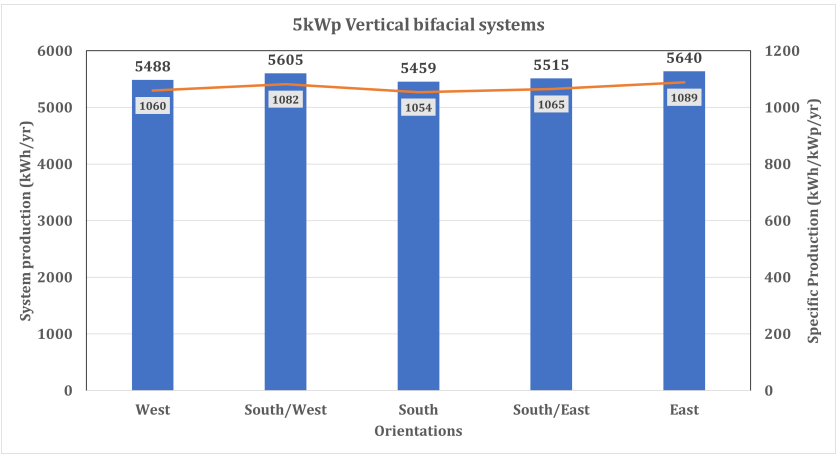

(e) System production (annual energy to the grid) in kWh/yr and specific production in kWh/kW/yr for different orientations

Figure 53: Comparison of annual energy produced in an 5 kWp vertical bifacial PV system for different orientations at the location of Trondheim, Norway. a) Comparison of South oriented system with South/East oriented system is shown in Fig. 53a, b) Comparison of South oriented system with South/West oriented system is shown in Fig. 53b, c) Comparison of South oriented system with East oriented system is shown in Fig. 53c, d) Comparison of South oriented system with West oriented system is shown in Fig. 53d, and e) Annual energy to the grid and specific production for these orientations is shown in Fig. 53e.

Figure 54 shows results from parametric analysis of 5 kWp vertical bifacial East/West oriented PV system. The overall best combination for maximum energy production would be P=8 m, M=1 m, H=1.5 m and tilt = 90°. This combination results in 5494kWh i.e around 1098kWh/kWp. For same combination except at M=2 m i.e. two PV modules are stacked one above the other, the energy production decreases by 5.71%. In all the cases, as H value increase from 0 m to 1 m, a considerable increase in energy values at every tilt is observed. However, there is no large difference in energy values between H=1.5 m and H=1 m. This is true for both M=1 m and 2 m.
At P=2 m and M=1 m as shown in Figure 54a, the energy produced increases with increase in tilt angle values upto the 80° and it is true for all values of H. For P=2 m and at M= 2 m, a different trend shown in Figure 54b and there is significant drop in energy yields for all values of H as compared with M=1 m. A same maximum energy is produced at tilt=0° for all values of H and then it decreases upto 30°, again increase till 80°, then decreases. Here the P/M ratio 1 and tilt 0° means placing modules flat on the ground. The sinusoidal variation is due to variation in inter-row shade values.
At P=4 m and for M=1 m & 2 m as shown in Figure 54c and 54d, the energy produced increases with increase in tilt values upto the 80° tilt and it is true for all values of H. Compared to energy values at M=1 m, the energy values at M=2 m drop considerably. At this P value for both M values, the highest energy is produced at a tilt of 80° and H =1 m, also almost same energy value is produced at H =1.5 m.
At P=8 m, for M=1 m the highest energy is produced at H=1.5 m and tilt=90°. At P=8 m, for M=2 m the highest energy is at tilt=80° and for both H=1 m & 1.5 m.
The general conclusion from this analysis is that increasing row spacing(P) and ground clearance height(H) values increase total energy production, and increasing module height(M) decreases total energy production. A higher tilt angle gives better energy production in an East/West orientation for a selected geographical location (Trondheim in this case). However, this is not true for the P/M ratio of 1. A P/M ratio greater than 1 gives good energy yields than other ratios in this kind of PV system setup.

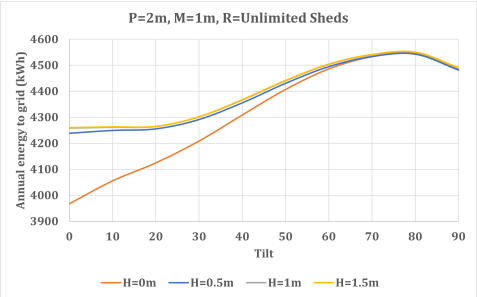

(a) P=2 m & M=1 m

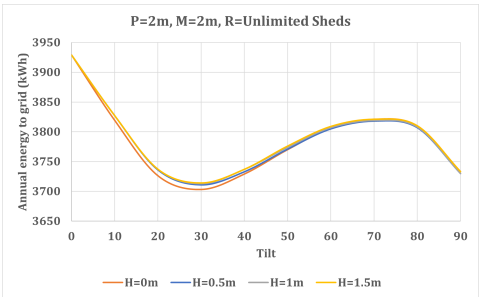

(b) P=2 m & M=2 m

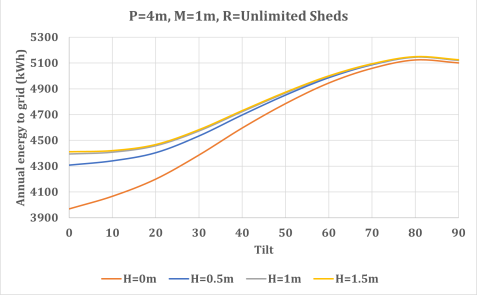

(c) P=4 m & M=1 m

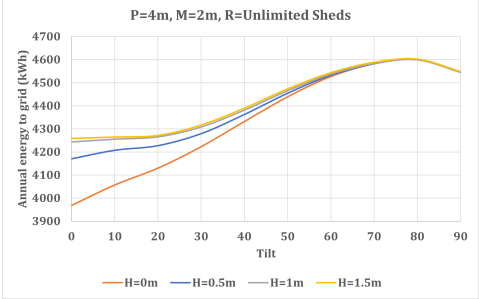

(d) P=4 m & M=2 m

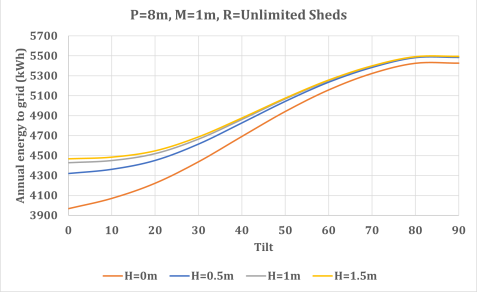

(e) P=8 m & M=1 m

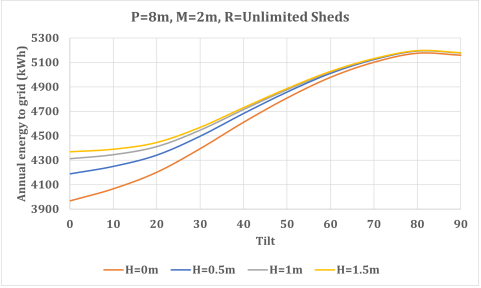

(f) P=8 m & M=2 m

Figure 54: Parametric analysis results showing annual energy to grid v/s tilt. The vertical bifacial East/West oriented system size is 5 kWp and designed for the location of Trondheim, Norway. a) Fig. 54a shows results for row spacing(P)=2 m and module height(M)=1 m, b) Fig. 54b shows results for P=2 m and M=2 m, c) Fig. 54c shows results for P=4 m and M=1 m, d) Fig. 54d shows results for shows results for P=4 m and M=2 m, e) Fig. 54e shows results for P=8 m and M=1 m, and f) Fig. 54f shows results for P=8 m and M=2 m

4.2 Light Management

4.2.1 Sun Hour Analysis

In the following subsections, different results of the sun hour analysis are presented. All the plots show a top view similar to Figure 25c.

a) Relation between geographical location (sun path) and sun hours distributions

Figure 55 and 57 show direct sun hours on summer solstice for four locations of Norway, Enkoping (N59°63.65′ E17°7.78′), Sweden and Seville (N37°39.57′ E−5°98.63′), Spain for East/West and North/South orientation respectively. Understanding the pattern of sun hour distribution with the help of corresponding sun path diagrams is possible.
From Figure 55a, 55b, 55c, and 55d it has been observed that the total sun hours in Bergen (N60°39.46′ E5°30.21′) and Oslo (N59°91.63′ E10°73.43′) is 19 hours whereas in Trondheim (N63°40.95′ E10°44.77′) it is one hour more and at Tromso (N69°64.98′ E18°95.27′) it is 24 hours. The interesting distribution is near the edges, where more sun hours are available than deep into the rows. The edge effect can be seen evidently. Except in Tromso, the distribution pattern is similar in all other locations deep into the rows. In Tromso, the middle area receives more sun hours, reducing towards PV panels row. The pattern variation is due to the difference in the sun's azimuth in all four locations.
The sun hour distribution for Sevilla in Figure 55e clearly shows more sunlight is available between rows compared to Norway's locations. The patterns of distribution in Enkoping (figure 55f) and Trondheim are more or less same. There is a vertical bifacial agrivoltaic test site close to Enkoping with grass as a crop [19] and East/West orientation has shown the homogeneous distribution of light in their studies too. That means the shade from PV panel rows is not affecting the distribution pattern in this orientation except at the Northern edges.
Figure 57 show sun hour distribution in North/South orientation for Bergen (N60°39.46′ E5°30.21′), Oslo (N59°91.63′ E10°73.43′), Trondheim (N63°40.95′ E10°44.77′), Tromsø (N69°64.98′ E18°95.27′) in Norway & for Enköping (N59°63.65′ E17°7.78′), Sweden AND Seville (N37°39.57′ E−5°98.63′), Spain. The edge effect (deeper shadows) is predominant on the Eastern and Western sides here than on just one side like in the East/West configurations. In all locations of Norway (Figure 57a, 57c, 57b & 57d) more light is available towards Southern edges and scattered distribution towards Northern edges. Even though the distribution is not homogeneous, the amount of sun hours available is more in all locations between the PV rows except at row length (down South). The shade from PV rows plays a major role in creating an uneven distribution pattern. In Sevilla (Figure 57e) homogeneous pattern is observed up to a certain length from the South towards the North. This means that in places with good sunlight and not much variation in sun's azimuth, the orientation does not influence the light available to the crops. However, the crops will not utilize all the light available for photosynthesis, and there is a potential to trap extra light in these locations. Therefore an agrivoltaic setup

with optimal light sharing between crops and PV would be a successful project here.

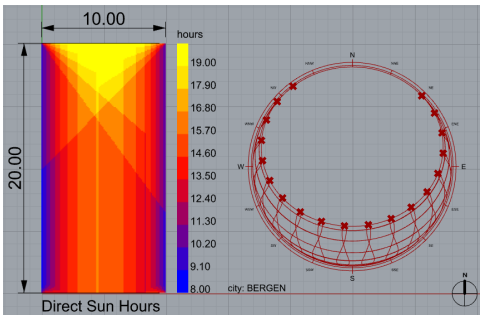

(a) Bergen, Norway

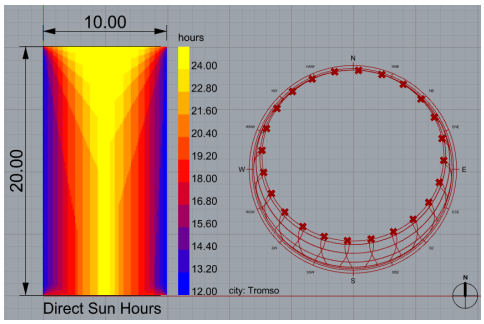

(b) Tromsø, Norway

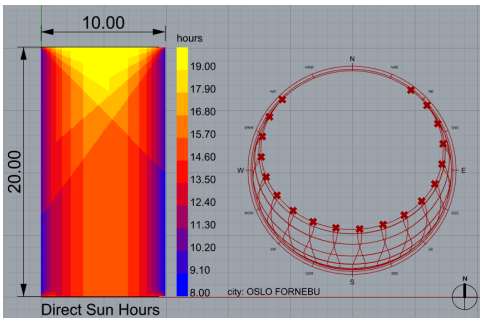

(c) Oslo, Norway

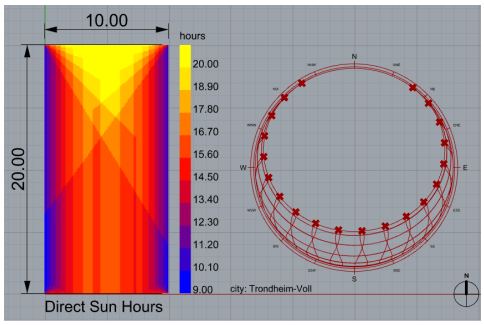

(d) Trondheim, Norway

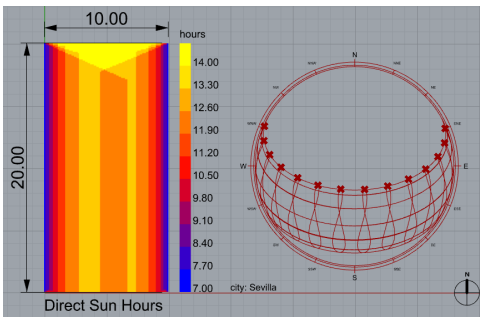

(e) Seville, Spain

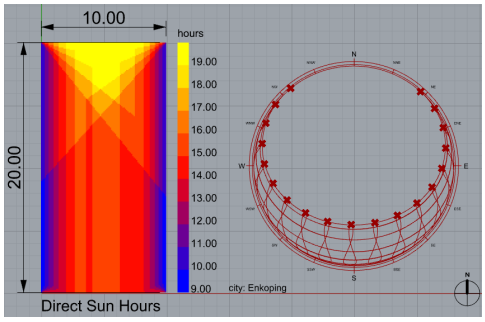

(f) Enköping, Sweden

Figure 55: Direct sun hours distribution and sun path for different locations on summer solstice (Top view). The PV panel orientation is East/West with Row spacing(P)=10 m, Ground clearance height(H)=0 m, Module height(M)=1 m, and Row length(R)=20 m. a) Sun hours distribution at Bergen is shown in Fig. 55a, b) Sun hours distribution at Tromsø is shown in Fig. 55b, c) Sun hours distribution at Oslo is shown in Fig. 55c, d) Sun hours distribution at Trondheim is shown in Fig. 55d, e) Sun hours distribution at Seville is shown in Fig. 55e, and f) Sun hours distribution at Enkoping is shown in Fig. 55f.

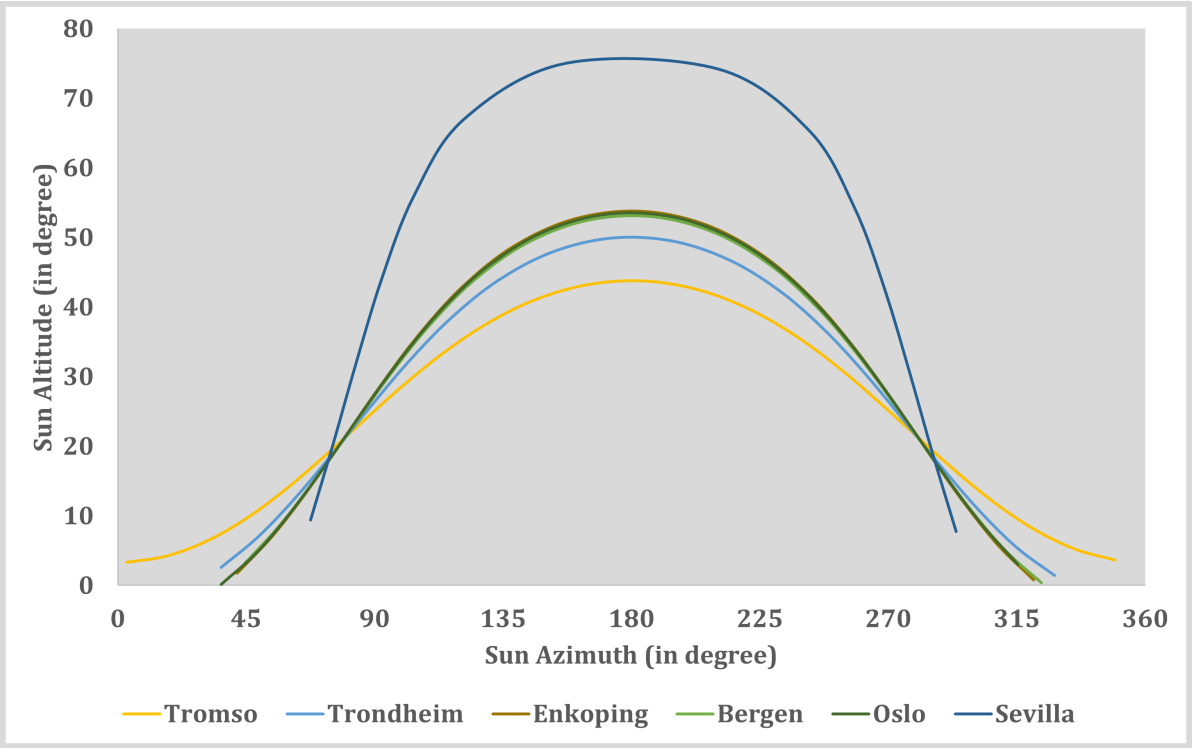

Figure 56: Sun azimuth versus Sun altitude on the summer solstice for different geographical locations

Comparing Figure 57d and 57f for Trondheim and Enkoping, the distribution pattern is not same as like East/West case. This might be due to the sun's altitude difference in both locations.
Figure 56 shows sun altitude on the summer solstice for these locations plotted against the sun's azimuth. It can be observed that the wider the azimuth, the shorter the sun's altitude and vice-a-versa. As said earlier, the sun's elevation plays a significant role in sun hour distribution at a given location.

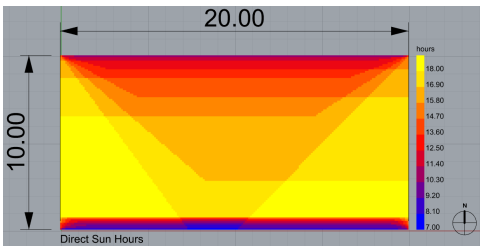

(a) Bergen, Norway

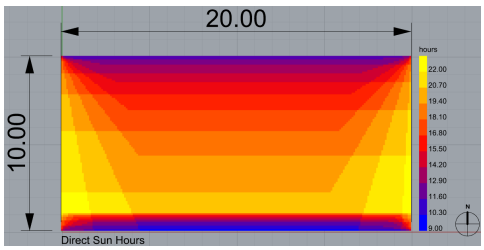

(b) Tromsø, Norway

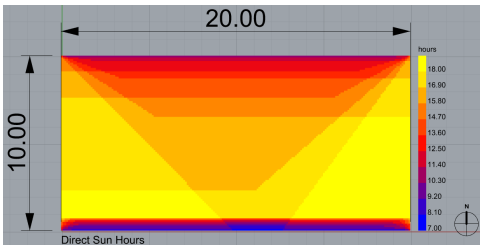

(c) Oslo, Norway

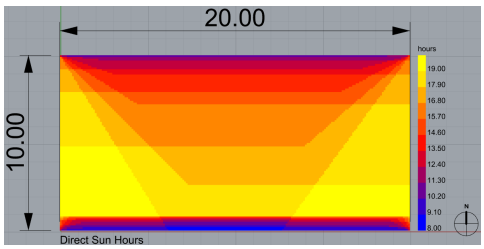

(d) Trondheim, Norway

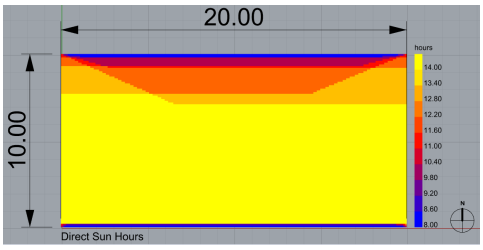

(e) Seville, Spain

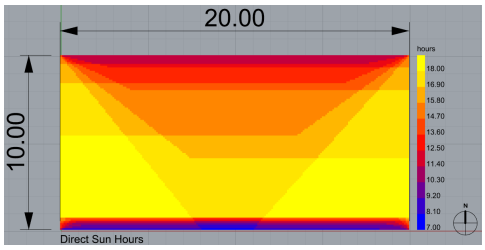

(f) Enköping, Sweden

Figure 57: Direct sun hours distribution for different locations on summer solstice (Top view). Panels orientation: North/South, Row Spacing(P)=10 m, Ground clearance height(H)=0 m, Module height(M)=1 m, Row length(R)=20 m.

b) Relation between orientation and sun hours distribution

Figure 58 shows sun hour distribution on summer solstice between rows of PV panels oriented East/West, North/South, and South/East at 45° azimuth for the location of Trondheim (N63°40.95′ E10°44.77′). In Figure 58a the Northern side has a mixed pattern of sun hours, and as azimuth changes, this pattern becomes clearer. Between Figure 58d and 58c, South/West looks more uniform distribution. Therefore, the optimal azimuth for homogeneous light availability to the crops exists between 45° South/West and East/West.

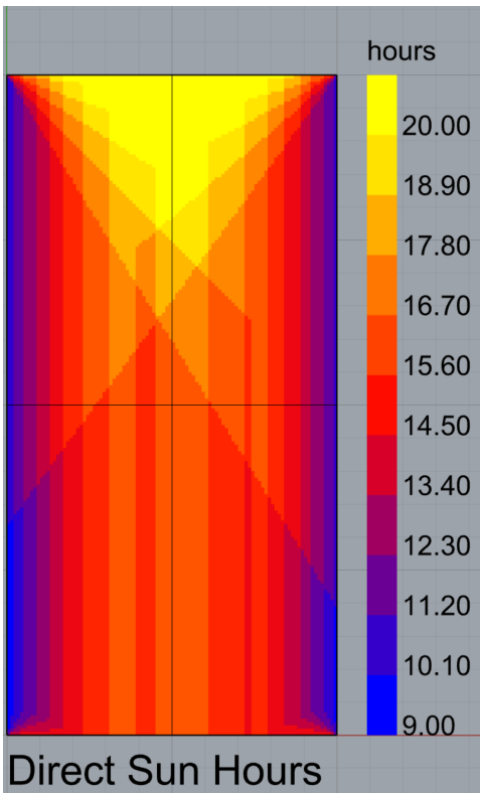

(a) East/West oriented

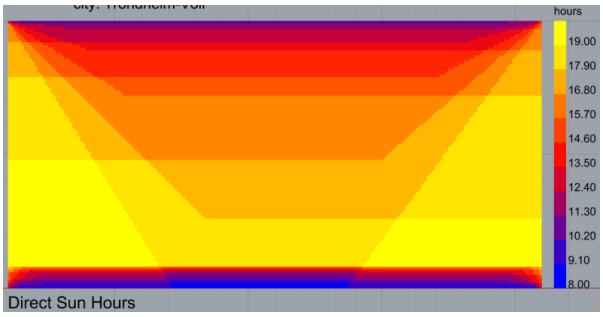

(b) North/South

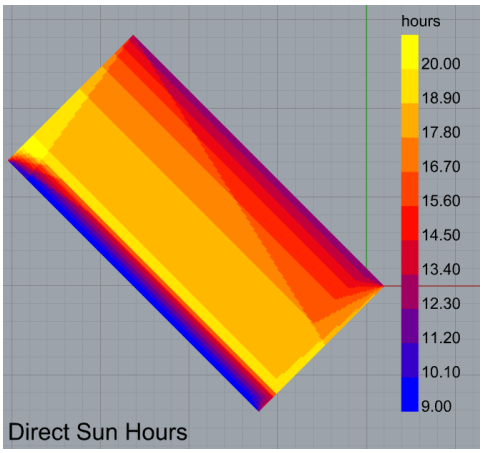

(c) South/West at 45° azimuth

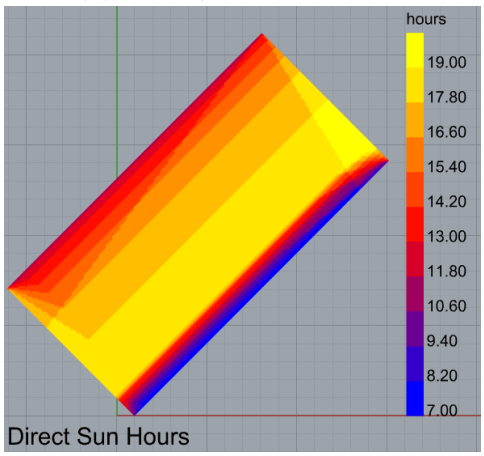

(d) South/East at 45° azimuth

Figure 58: Direct sun hours for three different orientation for Trondheim, Norway location on summer solstice. Row Spacing(P)=10 m, Ground clearance height(H)=0 m, Module height(M)=1 m, Row length(R)=20 m. a) Sun hour distribution in East/West orientation is shown in Fig. 58a, b) Sun hour distribution in North/South orientation is shown in Fig. 58b, c) Sun hour distribution in South/West orientation is shown in Fig. 58c, and d) Sun hour distribution in South/East orientation is shown in Fig. 58d.

c) Relation between ground clearance height (H) and sun hours distribution

Figure 59 shows sun hours distribution for different values of 'H' in a vertical bifacial East/West oriented agrivoltaic system. This is plotted for the Trondheim (N63°40.95′ E10°44.77′) location on summer solstice day. As ground clearance height 'H' increases, the shade from the PV panels onto the 'crop space (where the crop is grown)' decreases, thus allowing more light. In a vertical PV system, as the substructure height increases, the footing has to be sturdy to withstand wind loads, increasing capital expenditure (CAPEX). The footings must hold all the panels' weight against the wind load. In both vertical and tilted elevated PV systems, the CAPEX will increase as the substructure height increases.

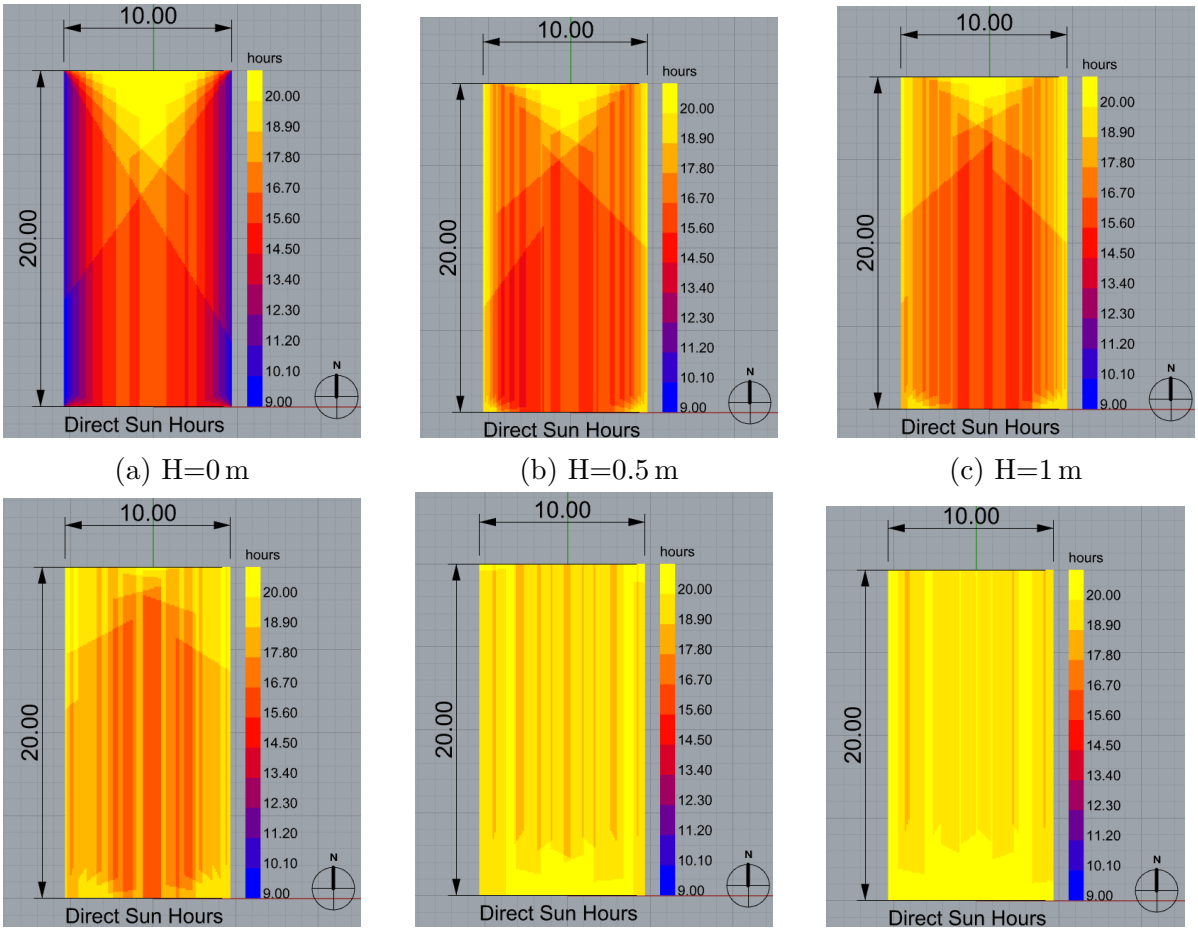

(a) H=0 m (b) H=0.5 m (c) H=1 m

(d) H=2 m (e) H=4 m (f) H=5 m

Figure 59: Distribution of sun hours on summer solstice at Trondheim when ground clearance height(H) is varied. Panels orientation: East/West, Row Spacing(P)=10 m, Module height(M)=1 m, Row length(R)=20 m.

However, at H = 1 m (Figure 59c) there are enough sun hours available between the PV panels. This must be enough for crops to grow (it will be validated with the crop

model later). Even though there is an increase in the number of sun hours after this height, as said earlier, it would lead to higher capital costs.

d) Relation between seasons and sun hours distribution

Figure 60 shows the total sun hours distribution between PV panels in a vertical agrivoltaic setup for each season. Trondheim (N63°40.95′ E10°44.77′) weather data is considered for this analysis. The edge effects are evident in similar figures in the previous section. This section, however, does not show edge effects since it shows cumulative sun hours between the rows of PV panels. Spring and summer are the most important seasons for vertical East/West oriented agrivoltaic systems. Spring and summer are active seasons for farming practice in Trondheim (N63°40.95′ E10°44.77′).
During spring (Figure 60b), deep into the row, the sun hours are uniformly distributed and scattered at edges towards the South. In summer (Figure 60c) the maximum number of sun hours are available compared to any other season. In summer, more sun hours are observed at the Northern edges due to the sun's azimuth (mentioned earlier). The Southern edge has comparatively fewer sun hours and drops deep into the rows. However, the minimum value in the summer (1328 sun hours) is marginally less than spring's maximum value (1342 sun hours). This is good for growing grass between the PV panel rows. During autumn, sun hour reduces, and a non-uniform distribution is noticed (Figure 60d). The sun hours distribution plot for winter (Figure 60a) looks less scattered than autumn, but there will be snowfall and fewer sun hours each day in winter. So, the autumn and winter seasons are not desirable for growing crops in this agrivoltaic setup.

e) Relation between module height (M) and sun hours distribution

Figure 61 shows the distribution of sun hours between PV panel rows when module height changed from 1 m to 2 m for two different ground clearance heights (H). The results for the summer solstice in Trondheim, Norway, are presented. For both module heights and at H=0 m, the sun hour distribution is non-uniform up to half of the row length from the North direction, and later it is moderately uniform. The edge effects are predominant here. The average drop in sun hours is 15% when the module height increases from 1 m to 2 m, and it drops more near the edges along the row length. At H=1 m more uniform sun hours distribution results are observed for both module heights. The overall availability of sun hours is 10-12% higher. At the edges along the row, it is much higher. Thus, elevating the PV panel rows is advantageous in an agrivoltaic setup.

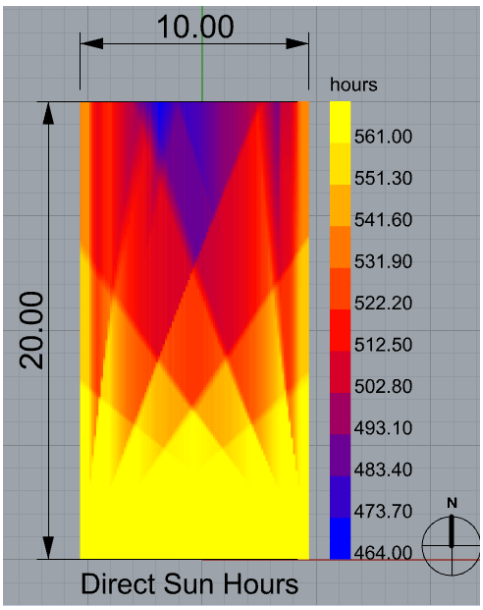

(a) Total Sun Hours during Winter months (December to February)

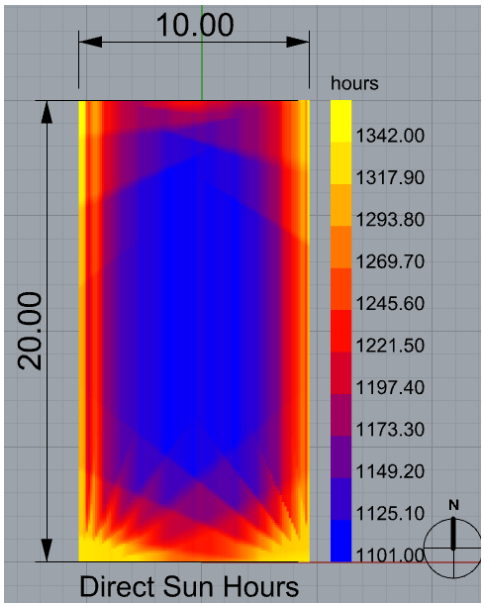

(b) Total Sun Hours during Spring months (March to May)

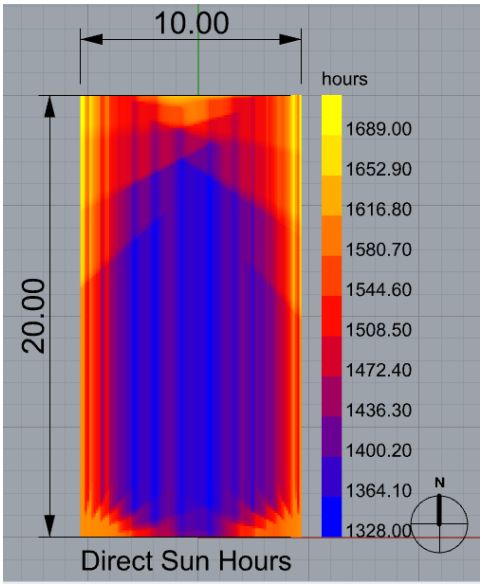

(c) Total Sun Hours during Summer months (June to August)

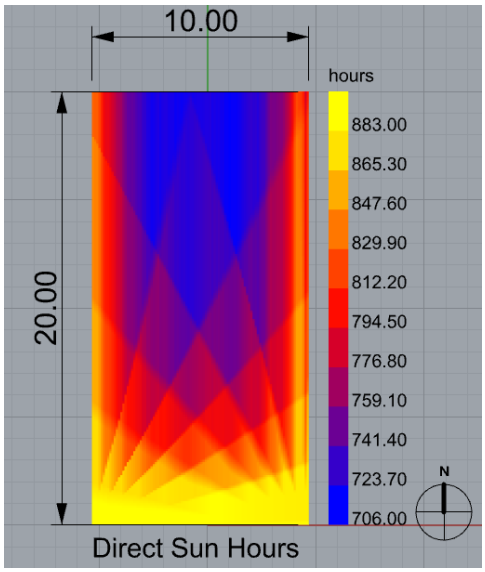

(d) Total Sun Hours during Autumn months (September to November

Figure 60: Distribution of sun hours during four seasons of the year at Trondheim. Panels orientation: East/West, Row Spacing(P)=10 m, Module height(M)=1 m, Ground clearance height = 1 m Row length(R)=20 m.

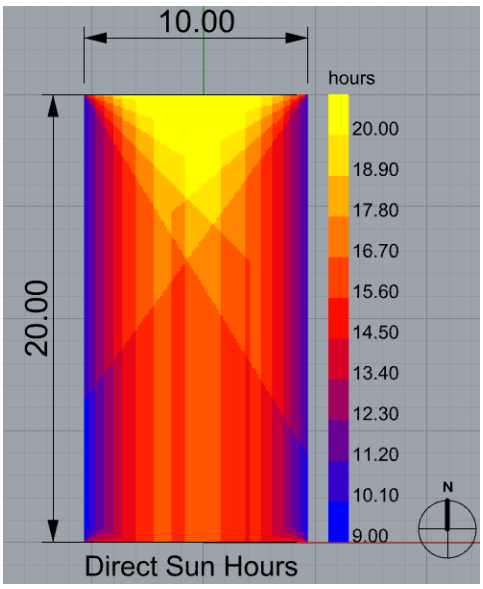

(a) H=0 m, M=1 m

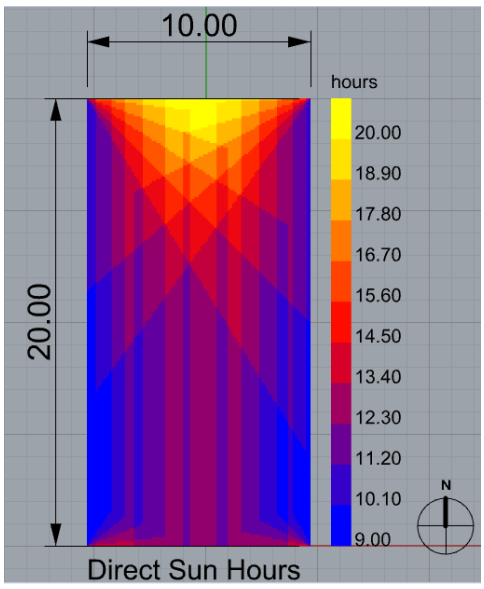

(b) H=0 m, M=2 m

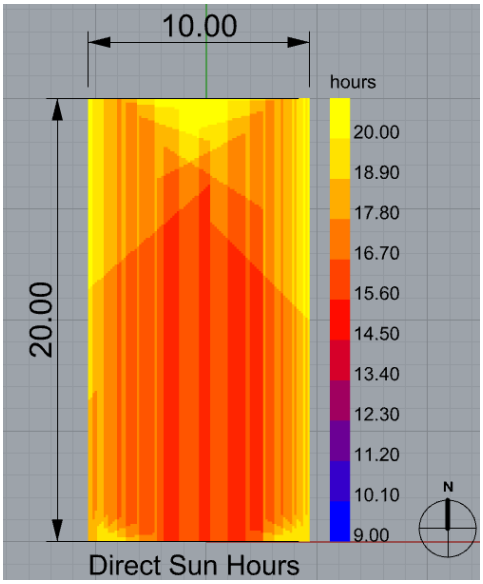

(c) H=1 m, M=1 m

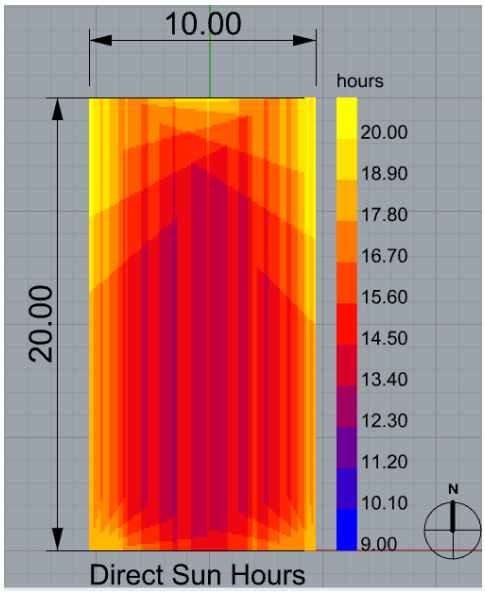

(d) H=1 m, M=2 m

Figure 61: Distribution of sun hours on summer solstice at Trondheim when Module height 'M' is varied. Panels orientation: East/West, Row Spacing(P)=10 m, Ground clearance height(H)=0 m & 1 m, Row length(R)=20 m.

4.2.2 Radiation map

Figure 62 shows radiation maps obtained using ClimateStudio. Each radiation map shows total solar exposure between two rows of vertical bifacial agrivoltaic systems. In Figure 62a, 62b and 62c radiation maps for three ground clearance height (H) at same module height (M) is presented. Four azimuth/orientation results are presented in each of these three figures.
At H = 0 m, there is low solar exposure near the edges long the row length, increasing towards the middle of the row spacing. The East/West orientation and 10° azimuth show more uniform solar exposure except at the edges. As 'H' values increases, more clear and homogeneous solar exposure is available in East/West and 10° azimuth. There is still low solar exposure in some areas of 20° azimuth and North/South orientation.
The radiation map gives us visual results of shading effects on crops. It clearly shows how shade (shadow) will affect the region between rows of vertical bifacial PV panels. However, it is essential to know the quantity of solar radiation available to the crops. This has been examined by estimating the diffuse acceptance percentage at every grid point between the rows. The averaged diffuse acceptance percentage is plotted in the following figures.
Figure 63 shows results extracted from above radiation map outcome. The Figures 63a, 63c, and 63e are graphs with average diffuse acceptance percentages at between rows of vertical bifacial agrivoltaic system. When H = 0 m, from the left edge up to 2.5 m and from right edge up to 2 m there is less diffuse acceptance percentage as compared to between 3 m to 8 m row spacing. Between this distance more than 90% diffuse acceptance is available.
When H = 0.5 m (Figure 63c), there is a different nature of curve as compared with earlier curves. This is similar to the results (Figure 51 and 52) obtained in the PVsyst bifacial model. East/West, 20° azimuth and South/North are asymmetric about mid-position of row spacing. Whereas 10° azimuth or even lesser azimuth (excluding East/West) show a symmetric curve about mid-position of row spacing (mid-position mean at tick '5' on the x-axis).
A similar and more uniform nature of curve is observed at H = 1 m as shown in Figure 63e. In this case, azimuth 10° also shows a symmetric curve. So the suggested azimuth from this analysis is between 10° $\leq$ azimuth $\geq$ 0°(East/West). Note: 10°azimuth is achieved by rotating the entire system from East/West in the anti-clockwise direction.
The symmetric and asymmetric nature of the above-said curves can be observed more clearly in the zoomed graphs: Figure 63b, 63d, and 63f.

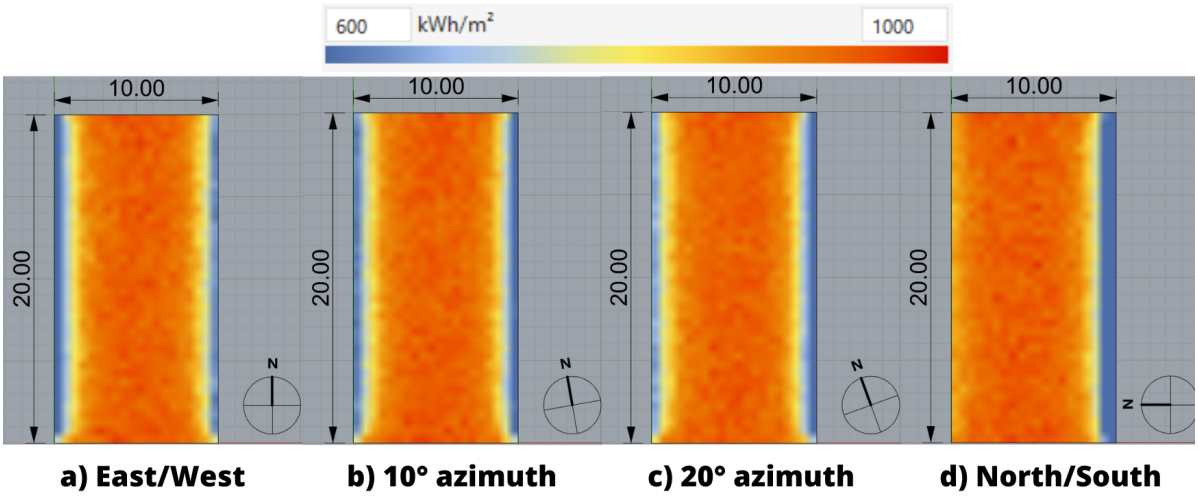

(a) H = 0 m, M=1 m

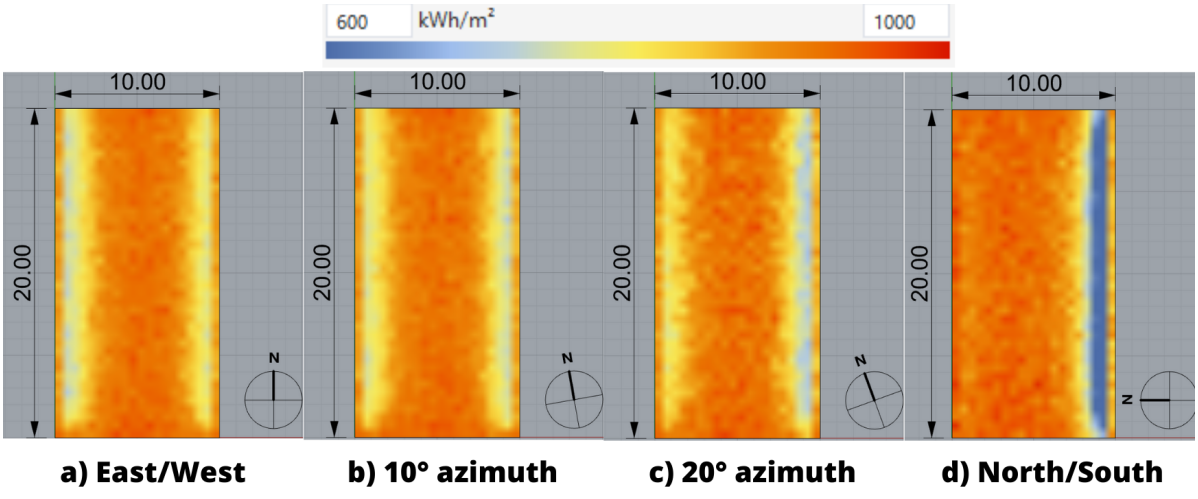

(b) H = 0.5 m, M=1 m

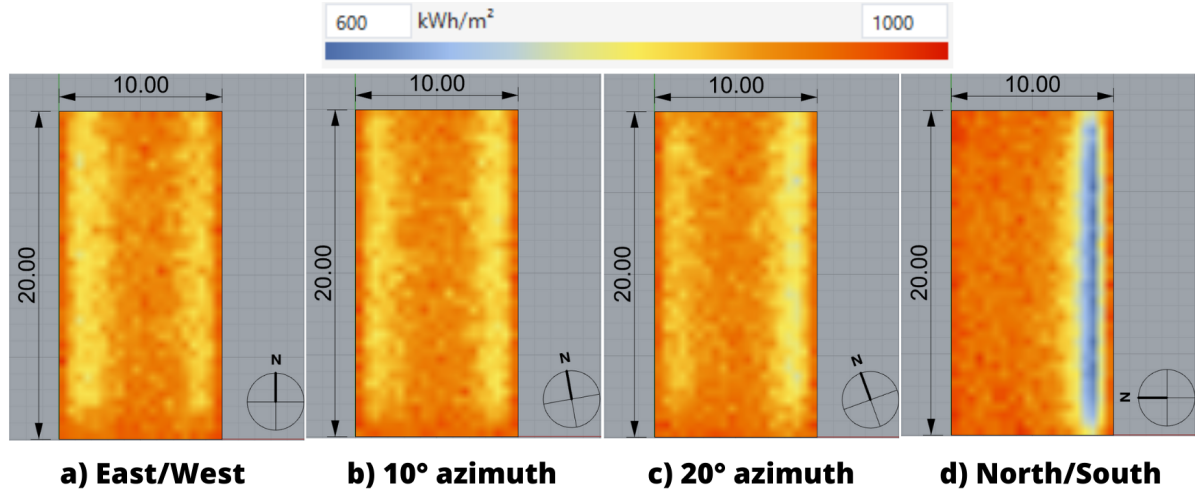

(c) H = 1 m, M=1 m

Figure 62: Total (Beam + Diffuse) solar exposure between rows of vertical bifacial agrivoltaic system. Panels orientation: a), b), c), d) in above pictures, Row Spacing(P)=10 m, Row length(R)=20 m.

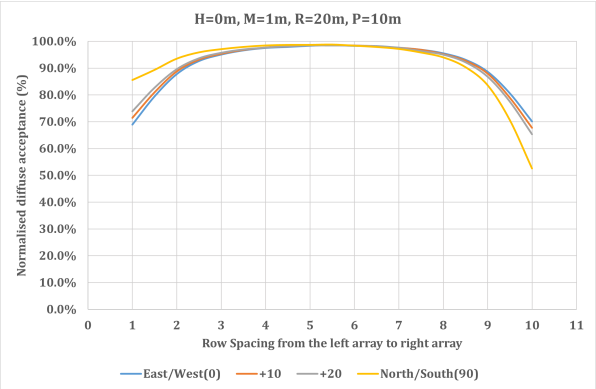

(a) H = 0 m, M=1 m

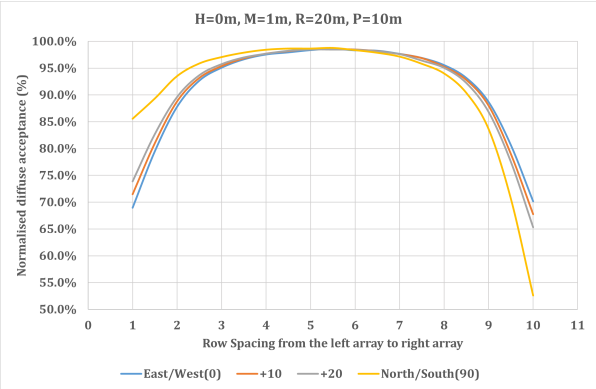

(b) H = 0 m, M=1 m (Zoomed)

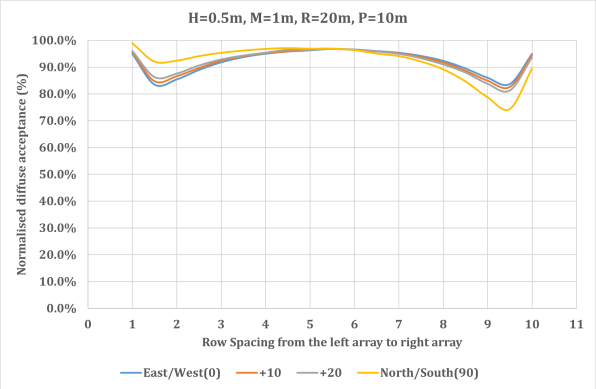

(c) H = 0.5 m, M=1 m

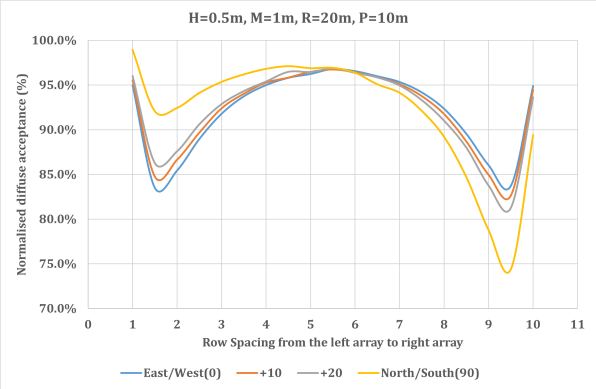

(d) H = 0.5 m, M=1 m (Zoomed)

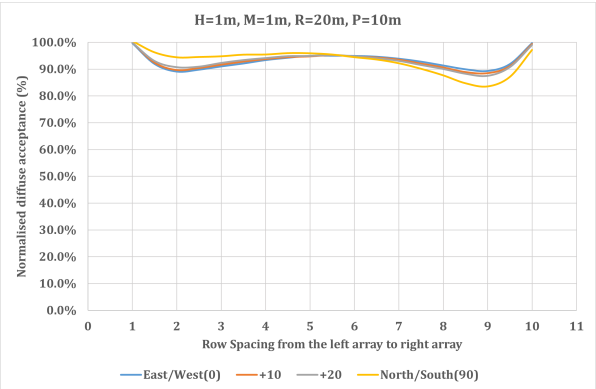

(e) H = 1 m, M=1 m

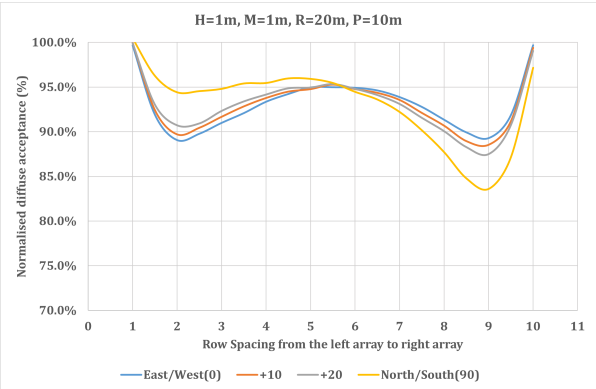

(f) H = 1 m, M=1 m (Zoomed)

Figure 63: Diffuse acceptance percentage between rows of vertical bifacial agrivoltaic system oriented at different azimuths.

In Figure 64 radiation maps for same system with module height (M) = 2 m are presented. At H = 0 m, there is a large drop in solar exposure along the edges as shown in Figure 64a. This is due to an increase in the 'M' value. This combination of 'M' and 'H' is not desirable for the crops in any orientation (azimuth). At H = 0.5 m in Figure 64b, the solar exposure is comparatively less than in the previous combination. However, if Figure 64b compared with Figure 62b for same 'H' value and different 'M' values, some regions still have lower values of solar exposure in Figure 64b. Hence, there will not be uniformity in light energy distribution.
At H = 1 m in Figure 64c, between East/West and 10° there is a possibility of having uniform distribution of solar exposure similar to same azimuths in Figure 62c. Of course, there will be a marginal decrease in the light energy values. The marginal decrease is shown in Figure 65.
Figure 65 shows extracted results from above radiation maps. The diffuse acceptance percentage at each grid point between row spacing is plotted for different ground clearance heights in Figure 65a, 65c and 65e respectively.
At H = 0 m and M = 2 m, there is only 70%-80% diffuse acceptance percentage available up to 3.5 m from left and right array for azimuth values. This gives an non-uniform light energy (solar exposure) to the crops. There is much better and symmetric distribution of solar exposure at H = 1 m than H = 0.5 m for East/West and 10° azimuth. North/South azimuth shows asymmetric distribution in all combination of 'H' and 'M'.
Figure 66 compares diffuse acceptance percentages at H = 1 m for M = 1 m & 2 m. The average drop in the diffuse acceptance percentage values in both cases is 6% only. That means it is possible to have two PV panels stacked instead of one without compromising the light energy available to the crops.

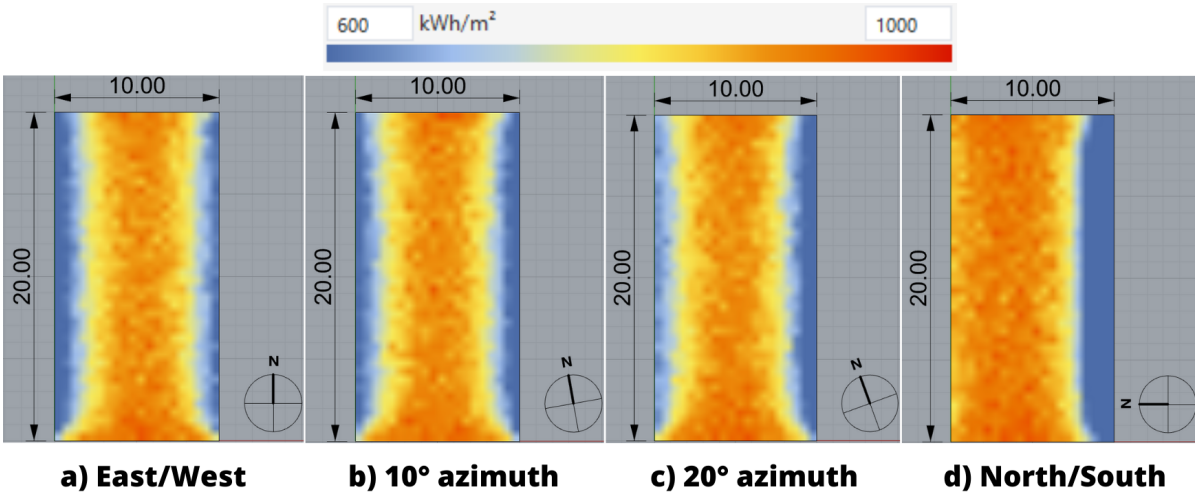

(a) H = 0 m, M=2 m

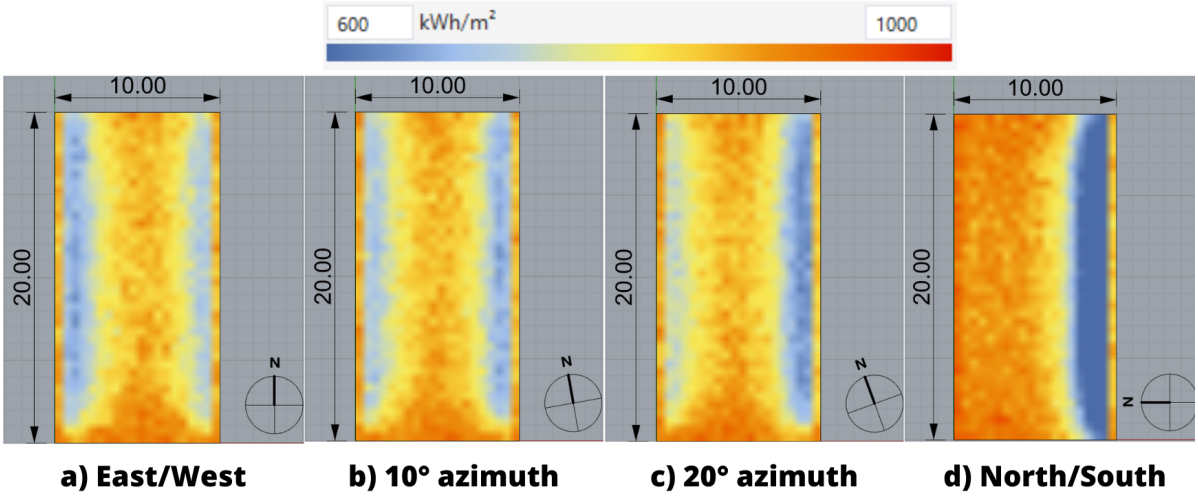

(b) H = 0.5 m, M=2 m

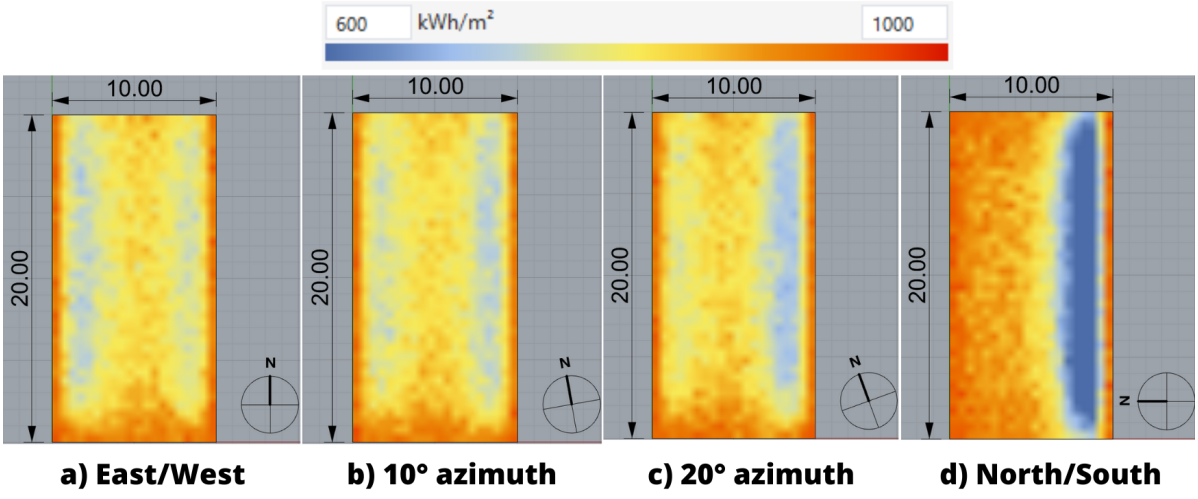

(c) H = 1 m, M=2 m

Figure 64: Total (Beam + Diffuse) solar exposure between rows of vertical bifacial agrivoltaic system. Panels orientation: a), b), c), d) in above pictures, Row Spacing(P)=10 m, Row length(R)=20 m. 87

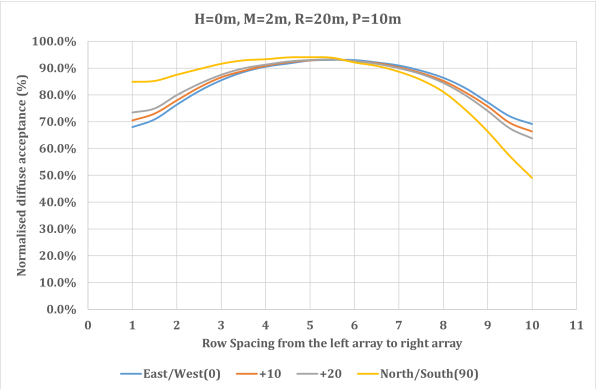

(a) H = 0 m, M = 2 m

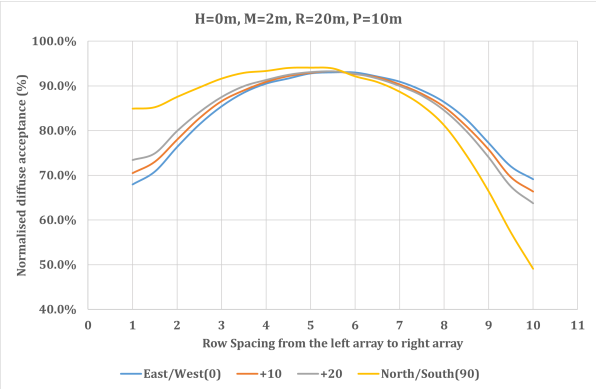

(b) H = 0 m, M = 2 m (Zoomed)

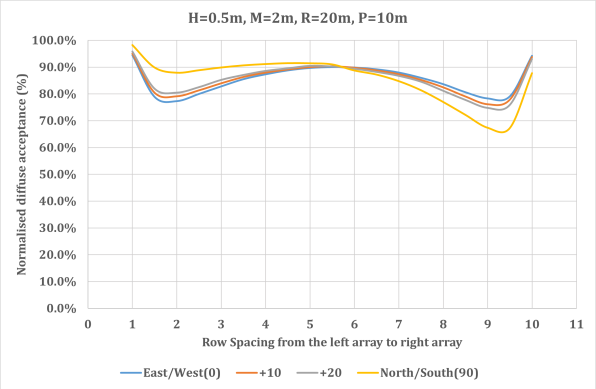

(c) H = 0.5 m, M = 2 m

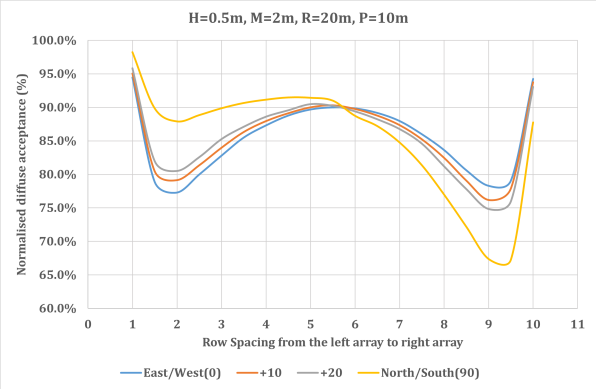

(d) H = 0.5 m, M = 2 m (Zoomed)

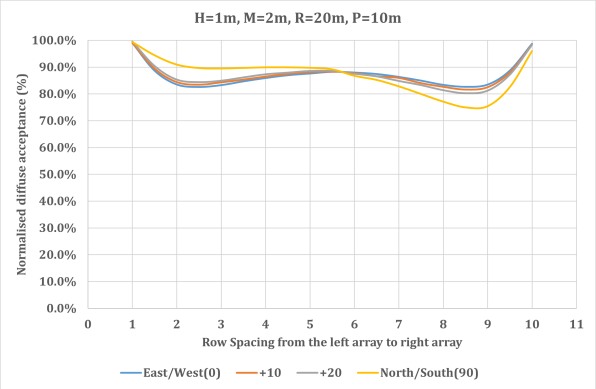

(e) H = 1 m, M = 2 m

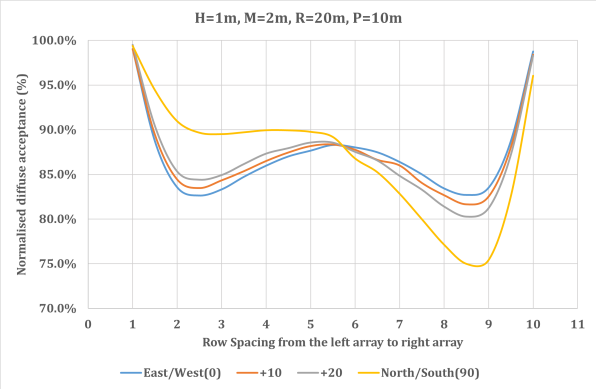

(f) H = 1 m, M = 2 m (Zoomed)

Figure 65: Diffuse acceptance percentage between rows of vertical bifacial agrivoltaic system oriented at different azimuths.

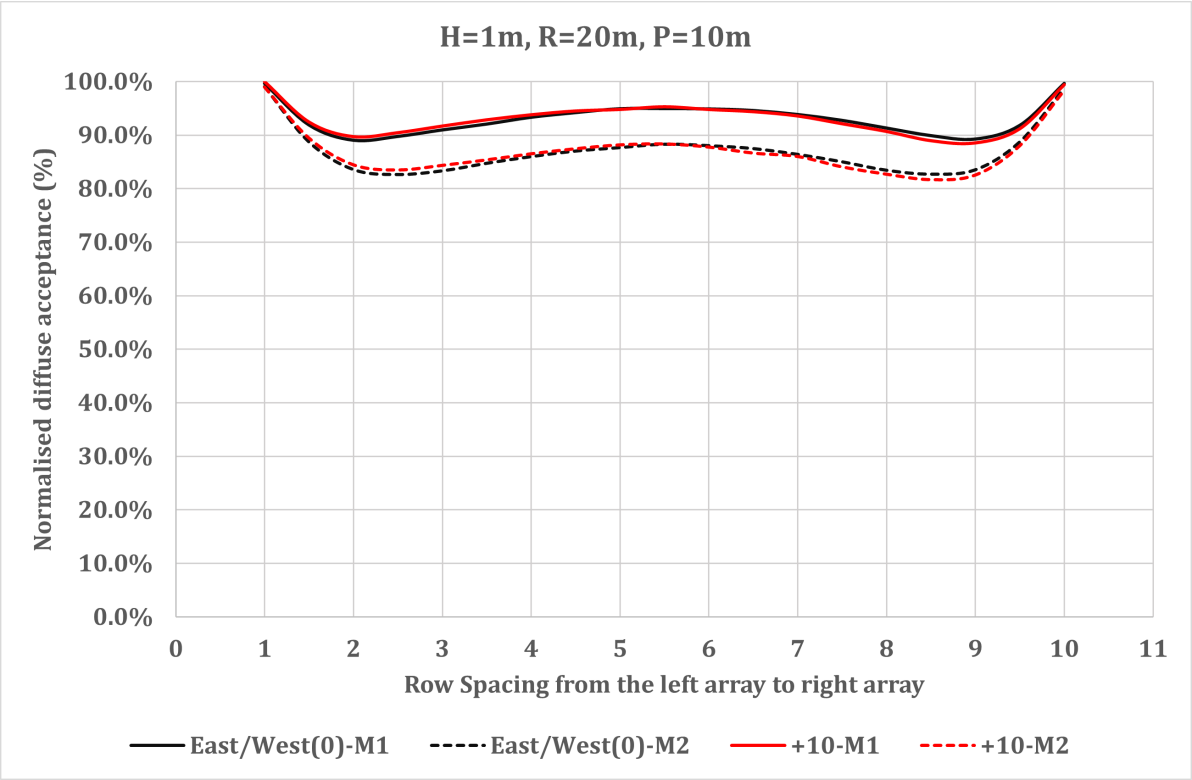

Figure 66: Comparing diffuse acceptance percentage for two different module heights at same ground clearance height.

4.2.3 Edge effects on crops

Figure 67 shows results from both Ladybug-sun hour analysis and ClimateStudio-radiation map process for different row length(R). The results presented here are for an entire year at Trondheim (N63°49.24′ E10°39.45′), Norway, and in East/West orientation. In both Figure 67a and 67b a different shading pattern is observed near the Southern edges of PV modules on crops as opposed to their internal rows. As the sun's elevation changes throughout the day, the pattern of shading under PV modules changes as well. Longer row lengths are preferable to short row lengths to avoid severe non-uniformity in shade distribution, leading to non-uniformity in crop yields. Near the Southern edges, more light energy (sun hours or total solar exposure) is present than in internal rows of PV panels; at shorter row lengths, leading to a non-uniform growth of crops. In another sense, the crops that receive more energy near the Southern edges either grow faster or get punished by severe sun heat. This could happen in short and long rows, but the crop yield loss is not comparative. This is quite challenging if the farmer does not own a larger field area because the farmer will not have the option to extend row lengths. However, a total economic evaluation (cost+revenue) comparison of crop and electricity production from all these different systems could eliminate this barrier.

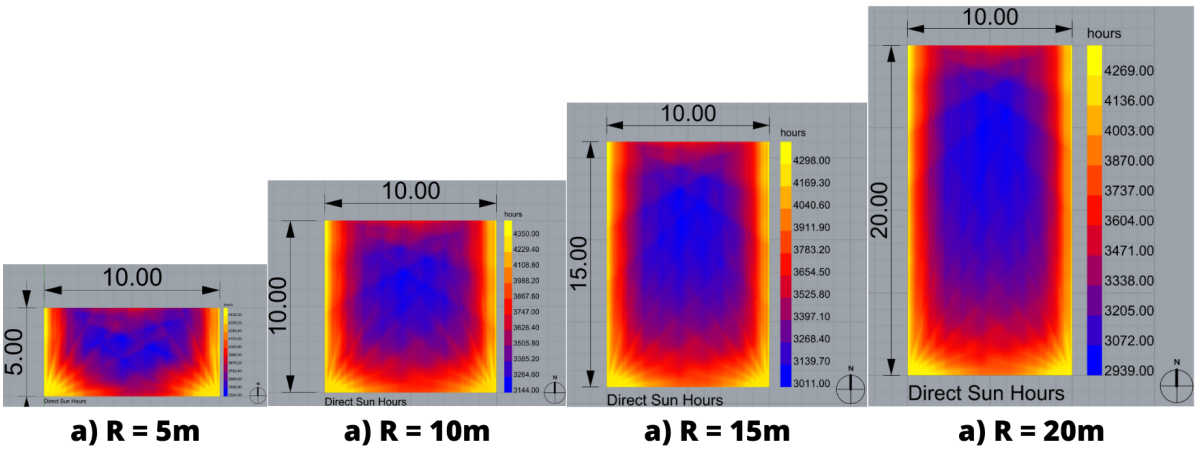

(a) Sun hour analysis using Ladybug for different row lengths.

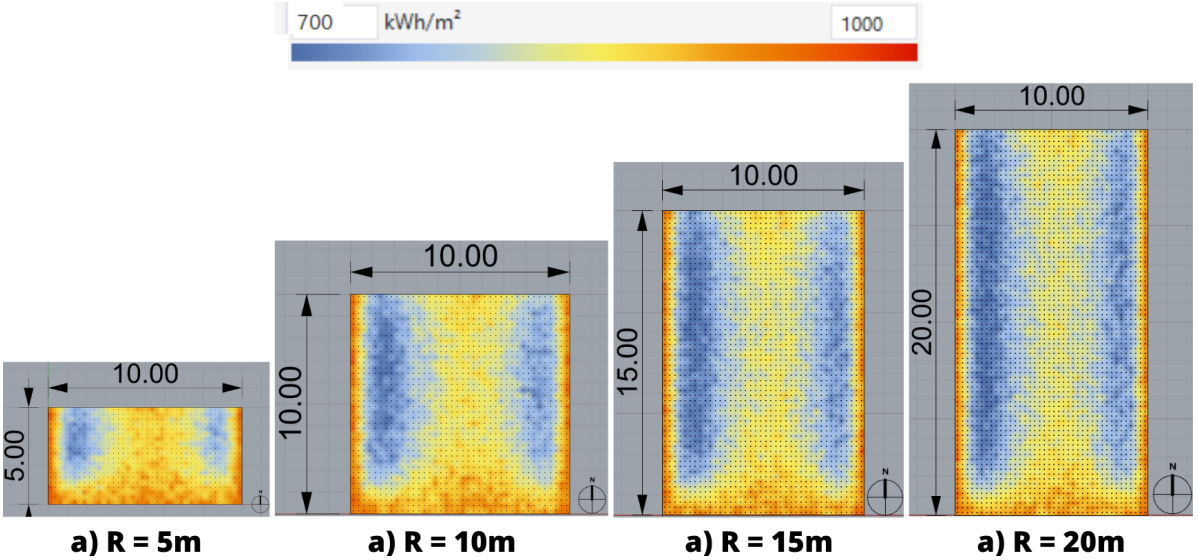

(b) Radiation maps from ClimateStudio for different row lengths.

Figure 67: Distribution of sun hours and radiation maps for entire year at Trondheim when row length 'R' is varied. Panels orientation: East/West, Row Spacing(P)=10 m, Ground clearance height(H)=0.8 m, Module height(M)=2 m.

4.3 Case study

The nominal PV power capacity of this agrivoltaic system is 53.3 kWp, maximum PV power is 40.1 kWDC and Nominal AC power is 50 kwAC.

4.3.1 PV performance and energy yield

The total system production is 54.1 MWh/yr at a specific production of 1015 kWh/kWp/yr. The average performance ratio (PR) of 1.493 and normalised production of 2.78 kWh/kWp/day

is obtained for this system. In order to calculate LER values, only the PV systems' annual energy yield (kWh/m^2/year) from the energy analysis is considered. However, a few important results from this analysis are presented here. A detailed report consisting of loss diagrams and performance curves is available in Appendix- 8.2.
The specific production of the system is lower than the earlier estimated value for the same orientation (East facing) in Figure 53e. This is due to the changes in the location, weather data considerations, and horizon profiles. Still this value is relatively more for bifacial systems in Norway because the expected specific production values are between 700 and 1000 kWh/kWp/year[92].
PV modules are usually evaluated for their performance by the performance ratio (PR). Figure 68 shows the performance ratio for each month and the energy yield curve. The energy yield is highest during the summer and spring months. As expected, it is lowest in the winter months. The average PR value is lowest in winter (December-February) and highest in Spring (March-May). In winters, the sun's elevation and azimuth are more diminutive and have short daylight time. In spring, it is quite the opposite. Note: The procedure followed in PVsyst for estimating PR for bifacial systems is available in Appendix.

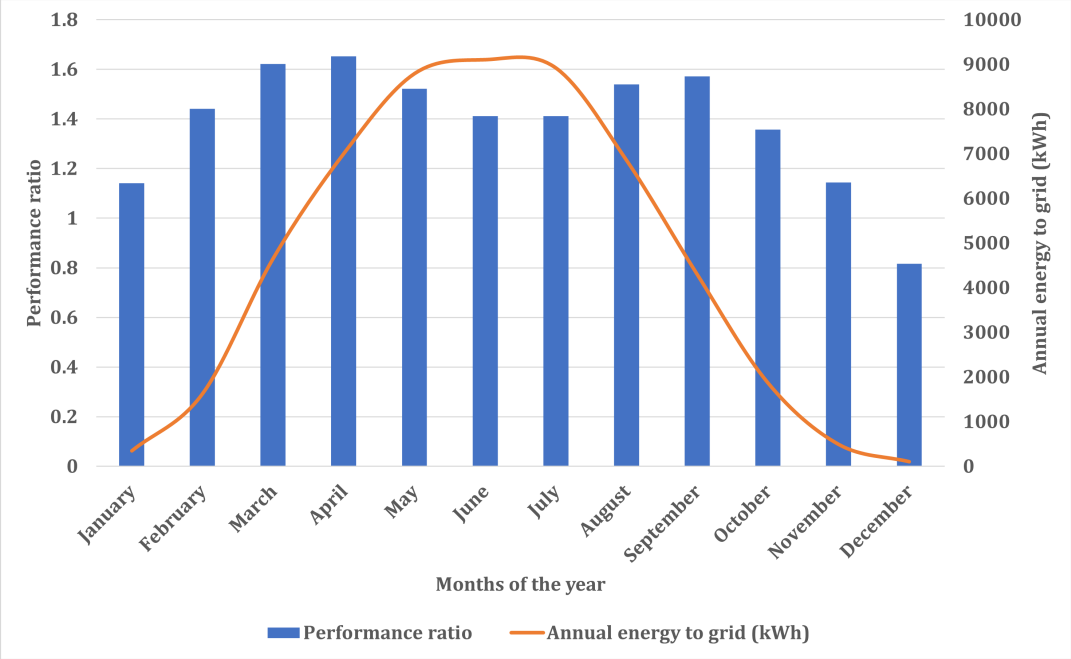

Figure 68: Performance ratio and energy yield value for each month in 53.3 kWp PV system at Skjetlein.

4.3.2 Crop yield

Figure 69 shows the radiation map of the entire agrivoltaic system. The shade distribution is the same as the system with only two-panel rows.

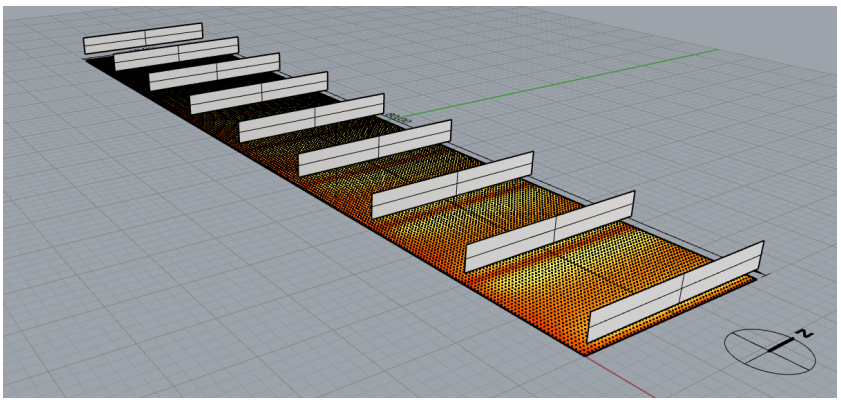

(a) Isometric view of 53.3 kWp agrivoltaic system

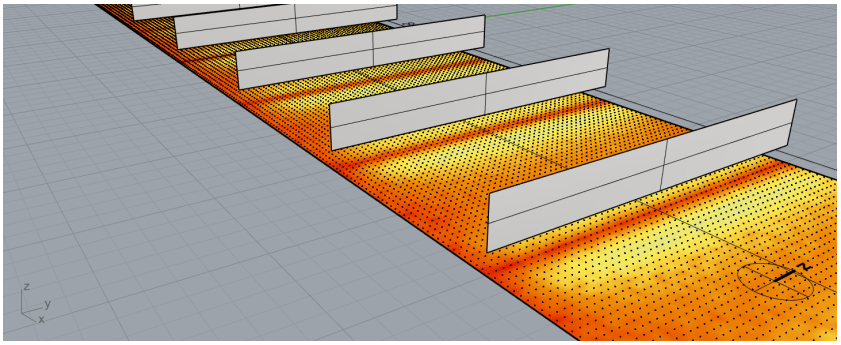

(b) Section of 53.3 kWp agrivoltaic system showing solar exposure and grid points

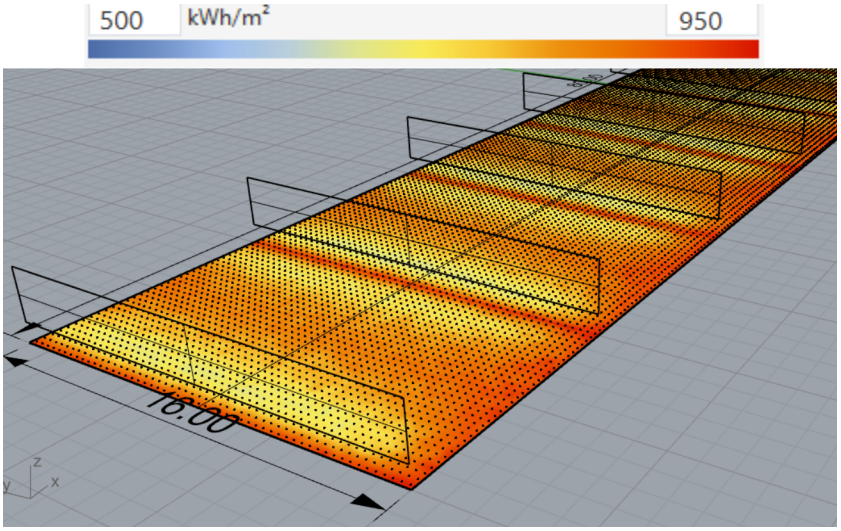

(c) Section of 53.3 kWp agrivoltaic system showing solar exposure and grid points

Figure 69: Total (Beam + Diffuse) solar exposure between rows of a 53.3 kWp vertical bifacial agrivoltaic system.

Figure 70 shows the average timothy crop yield between vertical rows of PV panels. This is the output obtained from the CATIMO crop model. It can be observed that the

nature of the crop growth curve follows the irradiation trend. The reduction in irradiation due to shading agrees with the results discussed earlier in the light management section.

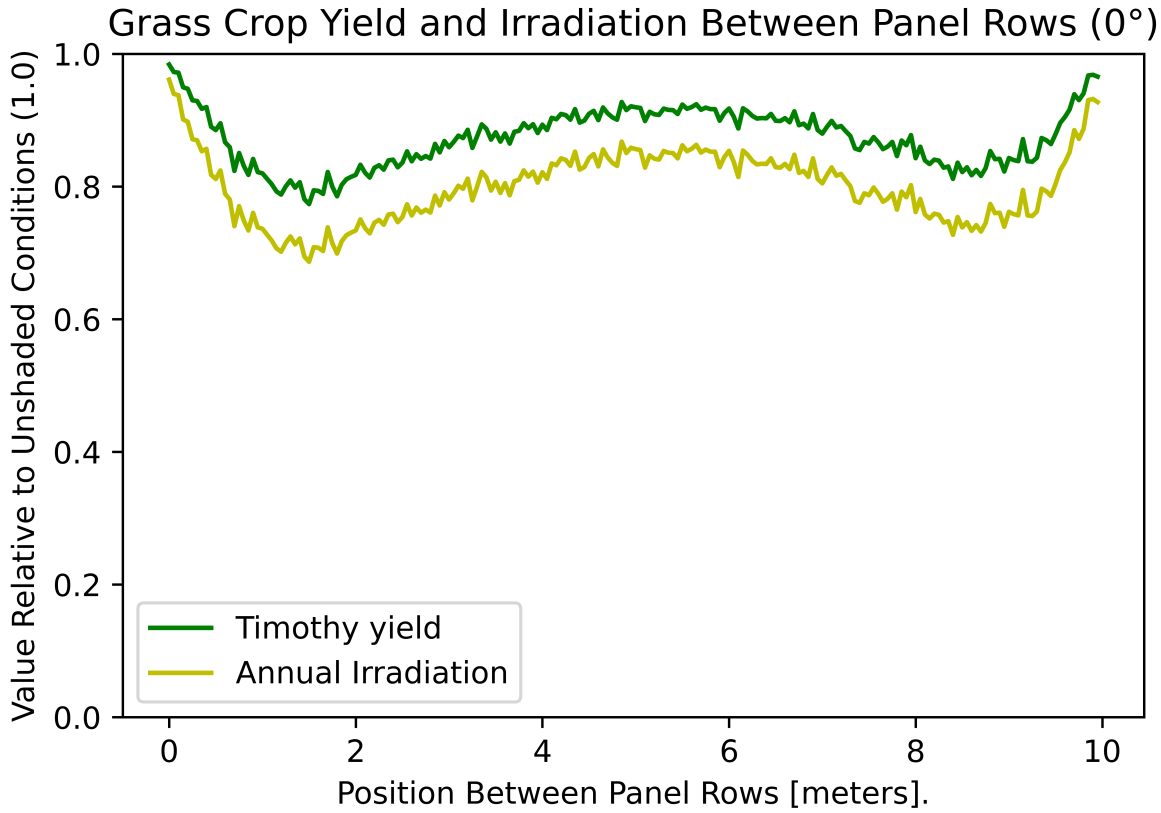

Figure 70: Grass crop yield and irradiation between vertical bifacial East/West oriented agrivoltaic system.

A total average loss in irradiation is 15.75% due to shades from the bifacial panels. The resulted specific yield for the entire agrivoltaic area is 786.25 kg/decare (0.786 g/m^2). This is a 9.38% reduction in crop growth or a factor of 0.906 when compared to unshaded (open-field) conditions of 1. In the most shaded areas in the system, the available irradiation for the crop growth is reduced by 29.73% as compared with less shaded places. At these areas, the specific crop yield is 684.44 kg/decare. However, a different result is obtained when considering the required safety distance of 50 cm between the panel rows and the tractor. For 10 m row spacing and East/West azimuth, the specific crop yield (excluding unharvested area) is 707.54 kg/decare, which means a relative of 0.815 when compared with unshaded conditions. The relative ratio is calculated by comparing agrivoltaic setup yield with open field yield.

4.3.3 LER

In order to estimate LER, a reference PV energy production and crop yield is needed. The reference PV system energy is estimated by designing a South oriented ground-mounted bifacial PV system tilted at 49° (Optimal tilt for the location) in the same land area as occupied by the agrivoltaic PV system. That area occupied by the agrivoltaic system is 1280 m^2. In the same area, the PV arrays at 5 m row spacing at 49° and facing due South is mounted. From this analysis, PV energy production of 192 kWh/m^2/year ($Y_{electricityPV}$) and specific production of 1051 kWh/kWp/day is obtained. The PV area is 583 m^2.
The crop yield in an open field i.e., in an conventional farmland without PV panels, is 0.8678 g/m^2 ($Y_{monocrop}$). This is estimated again using the CATIMO crop model.
The PV energy from agrivoltaic system ($Y_{electricityAVS}$) is 185 kWh/m^2/year (ratio of total system production 54.1 MWh/yr and PV system area 291 m^2) and corresponding crop yield ($Y_{cropAVS}$) is 0.707 54 g/m^2.
The estimated LER value is 1.79 i.e 0.815(crop)+0.9635(PV). That means it is possible to obtain 81.5% crop yield in an agrivoltaic system compared to open-field farming. In addition to crop yield, electricity is generated in the same land area. The increase in land-use efficiency is 79%. The loss of around 18.5% crop yield from this agrivoltaic system is equivalent to 96.36% additional electricity output from the PV system, which is nil in open field farming. In other words, it is possible to reap extra benefits from the same land area at the cost of marginal loss in the crop yield. Comparing the loss in crop yield with the gain in energy yield is a debatable hypothesis and always has to be validated by constructing a physical agrivoltaic system.

5 Discussion

This chapter presents the reflections drawn from the results and analysis. Two main aspects concerning the objectives of this thesis, i.e., the performance of a vertical bifacial system in an agrivoltaic scenario and crop yields from the same agrivoltaic system, are discussed. Apart from this, a discussion of results from the case study at Skjetlein videregående skole (N63°34.12′ E10°30.16′) is also reported here.

5.1 Vertical bifacial system

According to Vyas et al., the configuration with the least LCR and highest PLR is most competitive in terms of land area occupancy [81]. Among three agrivoltaic system configurations, the elevated agrivoltaic system (EAPV) has the smallest LCR after the vertical agrivoltaic system (VAPV). Lower LCR means building a PV structure in EAPV takes less land area out of the total land area compared with VAPV, or more area is available for farming purposes in EAPV than in VAPV.
The installed system cost for different dual-use PV systems has been mentioned in National Renewable Energy Lab (NREL) report (2020) [93]. The installation cost of vertical agrivoltaic system is 1.83 $/Wp, Tracker Stilt (elevated) agrivoltaic system 2.09 $/Wp and reinforced regular agrivoltaic system is 2.33 $/Wp. It implies elevated systems (with a tracker) costs slightly higher than vertical agrivoltaic systems. Therefore, vertical bifacial agrivoltaic systems (VAPV) are beneficial for the farmland owners as compared to an elevated agrivoltaic system (EAPV).
Riedel-Lyngskær, Nicholas, et al. (2022) [94] reported that the performance of bifacial systems is highly influenced by albedo. In a fixed system above green vegetation shown as high as 1.2 rear-side spectral impact and with snow cover it is as low as 0.98. The albedo of green vegetation is usually 0.25-0.3 and this variation is due to waxy nature of leaf surface. Also Trondheim (N63°40.95′ E10°44.77′) receives months-long snowfall. The analysis showed that a vertical East/West bifacial systems receive higher ground reflection on the rear-side as compared to a North/South system for the same albedo. Literature and results agree that vertical East/West bifacial systems benefit from grass albedo and snow albedo.
A vertically mounted bifacial module performed better than conventionally mounted monofacial module in higher latitude areas as reported by S Guo et al. (2013) [33]. One reason was higher bifacial gains at lower albedo values. With respect to latitude of a place, rear-side bifacial gain and energy yields at Trondheim, Norway (N63°40.95′ E10°44.77′) compared with Phoenix, USA (N33°44.99′ E−112°6.74′). At Trondheim, vertically mounted East facing bifacial modules outperform vertically mounted South facing monofacial modules. This is possible only if module with higher bifaciality is used.
Analysis showed that at lower bifaciality, the South facing vertically mounted bifacial PV system performs better than the East or West facing ones. This analysis was done for the location of Trondheim, which is located in high latitude. For better performance, choosing a bifacial module with higher bifaciality is more advisable at higher latitude

locations.
Drawing Tregenza skydome for analysing a vertical East/West oriented PV system in an agrivoltaic scenario is a first of its kind. The skydome analysis has revealed significant results to understand the direction of energy coming from the sky and its usefulness for the crops.
The diffuse acceptance results from PVsyst bifacial model has helped to compare results obtained in Ladybug and ClimateStudio. ClimateStudio formerly known as Diva is used in greenhouse energy analysis studies [95]. However, the ray-tracer algorithm on which ClimateStudio works has been used in agrivoltaic system studies as well. Ladybug tool is usually used in building energy modelling [78]. These two tools are combined for light management analysis in an agrivoltaic systems.
The energy yield results in SAM showed that East-facing vertical bifacial PV systems are suitable for Trondheim. These results have been validated with PVsyst results.
Overall results from this part of the study show that vertical bifacial PV systems perform well in terms of PV energy yield at Trondheim compared to conventional tilted monofacial PV systems. The vertical bifacial PV systems' geometry, orientation, and tilt ensure the availability of light to the crops. The methodology followed so far is satisfactory, and the results align with the literature.

5.2 Light management

From both sun hour and radiation map analyses, it is found that between East/West oriented and 10° azimuth, a spatial uniformity of light energy for the crops. Through modelling studies Riaz, Muhammad Hussnain, et al.(2021) [29] reported that East/West orientation bifacial panels gives a uniform shade distribution on the crops. Multi-scale modelling approach by Katsikogiannis, Odysseas Alexandros, et al. (2022) [21] has shown enhanced distribution and intensity of light in vertical East/West oriented bifacial systems. In both studies, the ground clearance height, row spacing and module height have shown significant effects on shade distribution on crops. This has been investigated thoroughly in this thesis.
The results obtained in this part of the thesis are in good agreement with the initial analysis. Combining these two methodologies forms an overall new procedure for analysing and optimising vertical bifacial agrivoltaic systems. This procedure can even be applied for elevated agrivoltaic system, ground mounted agrivoltaic system and greenhouses.

5.3 Case study

The energy analysis shows that the average performance ratio in the summer (June-August) is smaller than in spring. The probable reason could be more ground-reflected light and low PV cell temperature during the spring as against the summer. Riise, Heine Nygard, et al.(2021) [92] measured the performance of building-integrated bifacial systems in Norway, and their PR analysis also showed a similar trend. The measured PR value from their analysis is 1.01±0.06, and at STC, 0.93±0.05.

A relative reduction in irradiation will not result in same reduction in crop yield i.e. in this case a 15.75% reduction in irradiation results in corresponding crop reduction of 9.36%. Note: this includes all the crop grown in agrivoltaic area even the crop below the rows.
The final relative crop yield (excluding unharvested areas) is 0.815 as compared with open field harvest. This sums up to to average 19% reduction. However, the unharvested crop (region where tractors cannot reach) is usually eaten by sheep or cattle. Additionally, there will loss in final yield during harvesting and storage.
Whether or not this much reduction in crop yield is within acceptable limits has to be verified with the ministry of agriculture and food, Norway. In any case, there is need for certain norms, legal frameworks, and policies to understand the limits of agrivoltaic system installations in Norway. Countries like Japan [96], Germany [97], France [98], and Italy [99] already have such frameworks for agrivoltaics.
The estimated LER of 1.79 is high as compared with estimated value of 1.2 for similar system at Västerås, Sweden (N59°61.33′ E16°54.47′) reported in [19]. The higher value is might be due to high ratio of PV energy part. This has to be further investigated.

5.4 Limitations of the study

Following are the limitations of this thesis.

- There is no discussion of the economics of agrivoltaic systems.
- The waxy nature of leafs improves the reflection of light, but for the tested timothy grass crop, information about leaf surface is not available. Therefore it is not evaluated in the results.
- In agrivoltaic research, Ladybug and ClimateStudio were utilized to analyze shade distribution. Although there is no literature to compare and validate this new combination study, the results were compared with PVsyst.
- Based on sun hour data, the sun hour analysis in Ladybug appeared promising to estimate light energy for crops. However, this method does not take into account reflections from surrounding objects, and edge effects still have a significant effect on crops. Considering a larger grid size and larger geometry, the computational time is quite long.
- It took several weeks and hours to understand these tools. A deep understanding of how they work behind the scenes has not been explored. One advantage of these tools is that the background code can be re-written in Python and made into a new open-source tool exclusively for agrivoltaic system research.
- The weather data used in this thesis is from a typical meteorological year. The crop yield obtained in this thesis must be validated with actual data or a crop model. There are commercial and open-source crop modelling tools available. However, these models are not calibrated or tested for the crop 'timothy.' Therefore, the CATIMO crop model exclusively developed for this grass species and validated for Norwegian weather conditions have been used in this thesis.

6 Conclusions

This thesis work presents a detailed methodology for designing a vertical bifacial agrivoltaic system suitable for the Norwegian conditions. As a case study, a 53.3 kWp system is modelled, and its results are discussed. The results are in good agreement with the literature and our expectations. For the location of Trondheim (N63°49.24′ E10°39.45′), the PV collector azimuth between 10° $\leq$ azimuth $\geq$ 0°(East/West), ground clearance height between 0.5-1 m, and module height around 2 m is suggested for homogeneous shade (or light that is available to the crops) distribution. With this combination of PV system geometry, even the energy yields are within good limits. The row spacing and length depend on the tractor's dimensions and the PV system's capacity. Longer row lengths are recommended to overcome non-uniform shading due to edge effects.
As agrivoltaic researchers and sustainable engineering students, ensuring similar crop yields between agrivoltaic systems and open field farming is necessary. There are events where the crop yield, even in the open field, would have reduced due to drought season, climate change, and pest attack. Agrivoltaic systems offer long-term benefit of mitigating climate change [7] in the agriculture sector. Therefore, farmers should hold workshops and social awareness campaigns more often to promote this method. Following are the highlights of this work:

- The potential of software programs under agrivoltaic research has been explored. The functionalities identified and used in this thesis work are simple, easy to use, and learn. The functionalities like sun hour analysis, sun path diagrams, radiation map, bifacial model, sky dome, etc., are convenient in agrivoltaic system modelling.
- Theoretical analysis of the performance of vertical bifacial systems for Norwegian conditions agrees with the literature. A Vertical East/West oriented PV system gives a homogeneous distribution of light than a conventional South oriented PV system in an agrivoltaic scenario.
- A different shading pattern is observed near the edges of PV modules on crops compared to their internal rows. As the sun's elevation changes throughout the day, the way of shading under PV modules changes as well. Thus, winter crops (of course, no winter crops in most regions of Norway due to snow cover) may be affected differently by the shadow effect of solar panels than summer crops. The East/West facing agrivoltaic systems may be better suited than fixed South-facing ones due to their low shadow duration and uniform irradiance distribution.
- The solar exposure or radiation map analysis is applied in shade distribution studies in an agrivoltaic system for the first time. ClimateStudio offers quick and accurate results that enable testing of a variety agrivoltaic configurations in short order.
- The crop yield for modelled vertical bifacial agrivoltaic test system is 0.707 54 g/m^2 as against a yield of 0.8678 g/m^2 in an open field farming. The reduction in crop yield is attributed to shading caused by PV panels.
- The estimated land equivalent ratio for the test system is 1.79. That means a 79% increase in the land-use efficiency.

The results obtained above and discussed in previous chapters are computed for a typical meteorological year. That means the weather data has not accounted for drought and

rainy year data. As many agrivoltaic studies indicated, the soil moisture retention rate has been one of the advantages of agrivoltaic systems; therefore, in a drought year, the crops under agrivoltaic system might have better yield than open field crops. All these hypotheses have to be tested in a real system.

7 Future work

In most of the literature about agrivoltaics, the phrase 'food-water-energy' nexus is mentioned. From the above-discussed modelling procedure, it can be understood that how food and energy potentials are realised in agrivoltaic systems. However, the aspect of water and its connection with food-energy in an agrivoltaic system is not modelled in this thesis.

Therefore the installation of a physical agrivoltaic test system similar to the one discussed in the case study is proposed at the premises of Skjetlein videregående skole (VGS) (N63°34.12′ E10°30.16′). This location is one of the best places to have an agrivoltaic test and research facility. The teachers and the students posses knowledge about organic farming and renewable energy systems.

If this test system were to be installed, it would be the first agrivoltaic research facility in Norway. Here is some detail regarding the future scope of works in relevance to agrivoltaic research in Norway:

- Setting up data collection points at a real test system. The data that have to be recorded and monitored are divided into three categories: PV, Crop, and Microclimate. This is briefly described in Figure 71.
- Selection of appropriate sensors for collecting above mentioned data and optimally locating the sensors both in the open fields and in the agrivoltaic system area.
- Validation of modelled system with real-time data.
- Adding other crops like potato, barely, berries in addition to grass.
- Microclimate modelling in agrivoltaic systems using EnviMet and ArcGis.
- Wind and temperature studies using computational fluid dynamic method.
- Explore the potential of elevated agrivoltaic system (EAPV) for other regions of Norway where they grow berries, apples.
- Create a map showing potential grasslands where vertical agrivoltaic systems can be effectively installed in parts of Norway.

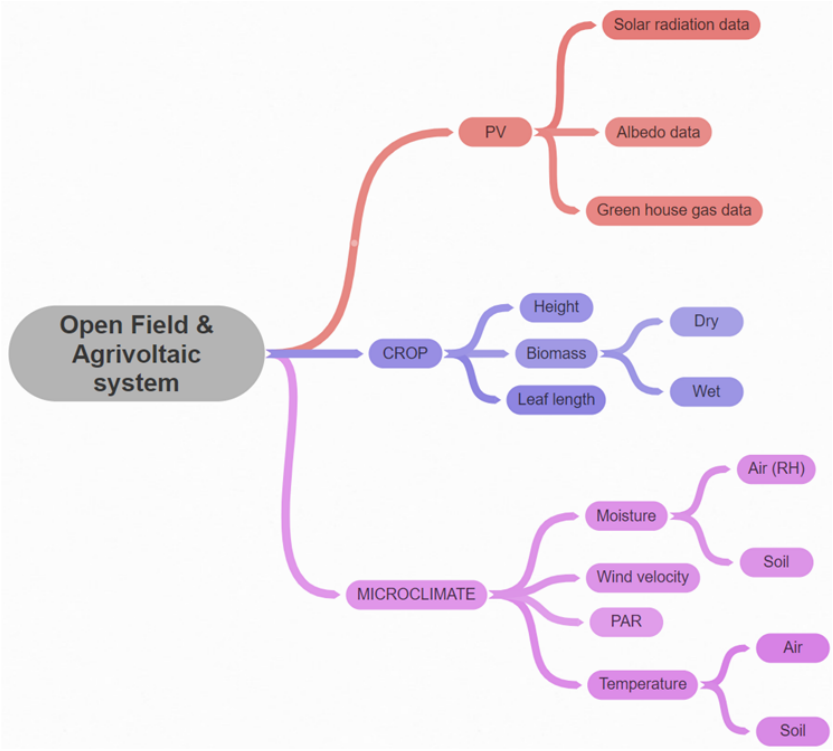

Figure 71: List of parameters that has to be monitored and recorded in an agrivoltaic setup. The collected data is used for validating modelling results.

References

[1] European Commission. *REPowerEU: Joint European action for more affordable, secure and sustainable energy*. 2022. URL: https://ec.europa.eu/commission/presscorner/detail/en/ip_22_1511.

[2] Kate Abnett. *EU will do 'whatever it takes' to rebuild solar energy manufacturing in Europe*. Mar. 2022. URL: https://www.reuters.com/business/sustainable-business/eu-will-do-whatever-it-takes-bring-solar-energy-manufacturing-back-europe-2022-03-31/.

[3] The World Bank. *Arable land (% of land area) - European Union*. 2018. URL: https://data.worldbank.org/indicator/AG.LND.ARBL.ZS?locations=EU.

[4] Solar resource data: Solargis. 2020 The World Bank Source: Global Solar Atlas 2.0. *Solar resource maps of Norway*. URL: https://solargis.com/maps-and-gis-data/download/norway.

[5] Solar resource data: Solargis. The World Bank Source: Global Solar Atlas 2.0. *Solar resource maps of Sweden*. 2020. URL: https://solargis.com/maps-and-gis-data/download/sweden.

[6] Solar resource data: Solargis. The World Bank Source: Global Solar Atlas 2.0. *Solar resource maps of Spain*. URL: https://solargis.com/maps-and-gis-data/download/spain.

[7] Mohammad Abdullah Al Mamun et al. "A review of research on agrivoltaic systems". In: *Renewable and Sustainable Energy Reviews* 161 (2022), p. 112351. ISSN: 1364-0321.

[8] C. Dupraz et al. "Combining solar photovoltaic panels and food crops for optimising land use: Towards new agrivoltaic schemes". In: *Renewable Energy* 36.10 (Oct. 2011), pp. 2725–2732. ISSN: 0960-1481. DOI: 10.1016/J.RENENE.2011.03.005.

[9] Greg A. Barron-Gafford et al. "Agrivoltaics provide mutual benefits across the food–energy–water nexus in drylands". In: *Nature Sustainability* 2.9 (2019), pp. 848–855. ISSN: 23989629. DOI: 10.1038/s41893-019-0364-5. URL: http://dx.doi.org/10.1038/s41893-019-0364-5.

[10] Adolf Goetzberger and A Zastrow. "On the coexistence of solar-energy conversion and plant cultivation". In: *International Journal of Solar Energy* 1.1 (1982), pp. 55–69.

[11] T. Akira Nagashima Sekiyama. "Sunlight Power Generation System Patent No. 2005-277038". In: (2005).

[12] Brecht Willockx et al. "A Standardized Classification and Performance Indicators of Agrivoltaic Systems". In: *Eu Pvsec 2020* (2020), pp. 1–4. URL: https://www.eupvsec-planner.com/presentations/c49900/a_standardized_classification_and_performance_indicators_of_agrivoltaic_systems.htm.

[13] Alexander Nassar. “Improving productivity of cropland through agrivoltaics”. In: (2020), pp. 4–5.

[14] Fraunhofer-ISE. *Agrivoltaics: Opportunities for Agriculture and Energy Transition.* URL: https://agri-pv.org/en/.

[15] Shiva Gorjian et al. “Progress and challenges of crop production and electricity generation in agrivoltaic systems using semi-transparent photovoltaic technology”. In: *Renewable and Sustainable Energy Reviews* 158 (2022), p. 112126. ISSN: 1364-0321.

[16] Hassan Imran and Muhammad Hussnain Riaz. “Investigating the potential of east/west vertical bifacial photovoltaic farm for agrivoltaic systems”. In: *Journal of Renewable and Sustainable Energy* 13.3 (2021), p. 33502. ISSN: 1941-7012.

[17] Zamen Tahir and Nauman Zafar Butt. “Implications of spatial-temporal shading in agrivoltaics under fixed tilt & tracking bifacial photovoltaic panels”. In: *Renewable Energy* (2022). ISSN: 0960-1481.

[18] Ramachandran Ammapet Vijayan, Jeevalakshmi Sivanarul, and Muthubalan Varadharajaperumal. “Optimizing the spectral sharing in a vertical bifacial agrivoltaics farm”. In: *Journal of Physics D: Applied Physics* 54.30 (2021), p. 304004. ISSN: 0022-3727.

[19] Pietro Elia Campana et al. “Optimization of vertically mounted agrivoltaic systems”. In: *arXiv preprint arXiv:2104.02124* (2021).

[20] F Johansson et al. “3D-thermal modelling of a bifacial agrivoltaic system: a photovoltaic module perspective”. In: *Energy Nexus* 5 (2022), p. 100052. ISSN: 2772-4271.

[21] Odysseas Alexandros Katsikogiannis, Hesan Ziar, and Olindo Isabella. “Integration of bifacial photovoltaics in agrivoltaic systems: A synergistic design approach”. In: *Applied Energy* 309 (2022), p. 118475. ISSN: 0306-2619.

[22] Muhammad Hussnain Riaz et al. “Crop-Specific Optimization of Bifacial PV Arrays for Agrivoltaic Food-Energy Production: The Light-Productivity-Factor Approach”. In: *IEEE Journal of Photovoltaics* (2022). ISSN: 2156-3381.

[23] Max Trommsdorff et al. “Potential of agrivoltaics to contribute to socio-economic sustainability: A case study in Maharashtra/India”. In: *AIP Conference Proceedings* 2361.1 (2021), p. 40001.

[24] Prannay R Malu, Utkarsh S Sharma, and Joshua M Pearce. “Agrivoltaic potential on grape farms in India”. In: *Sustainable Energy Technologies and Assessments* 23 (2017), pp. 104–110. DOI: 10.1016/j.seta.2017.08.004.

[25] T. Harinarayana and K. Sri Venkata Vasavi. “Solar Energy Generation Using Agriculture Cultivated Lands”. In: *Smart Grid and Renewable Energy* 05.02 (2014), pp. 31–42. ISSN: 2151-481X. DOI: 10.4236/sgre.2014.52004.

[26] Deng Wang et al. “Analysis of light environment under solar panels and crop layout”. In: *2017 IEEE 44th Photovoltaic Specialist Conference (PVSC)*. IEEE, 2017, pp. 2048–2053. ISBN: 150905605X.

[27] Atsutaka Yamada and Seichi Ogata. "Potential evaluation of agrivoltaic case of Kyoto prefecture Japan". In: *AIP Conference Proceedings* 2361.1 (2021), p. 20003.

[28] Martin Elborg. "Reducing land competition for agriculture and photovoltaic energy generation–A comparison of two agro-photovoltaic plants in Japan". In: *International Conference on Sustainable and Renewable Energy Development and Design (SREDD2017)*. Vol. 3. 2017, p. 5.

[29] Muhammad Hussnain Riaz et al. "The optimization of vertical bifacial photovoltaic farms for efficient agrivoltaic systems". In: *Solar Energy* 230 (2021), pp. 1004–1012. ISSN: 0038-092X.

[30] David Jung, Alois Salmon, and Patricia Gese. "Agrivoltaics for farmers with shadow and electricity demand: Results of a pre-feasibility study under net billing in central Chile". In: *AIP conference proceedings*. Vol. 2361. 1. AIP Publishing LLC, 2021, p. 30001. ISBN: 0735441049.

[31] Jesús Robledo et al. "Lessons learned from simulating the energy yield of an agrivoltaic project with vertical bifacial photovoltaic modules in France". In: *38th European Photovoltaic Solar Energy Conference and Exhibition (EU PVSEC)* (2021).

[32] VDMA.org. *International Technology Roadmap for Photovoltaics (ITRPV)*. Tech. rep., pp. 1–81. URL: https://www.vdma.org/international-technology-roadmap-photovoltaic.

[33] Siyu Guo, Timothy Michael Walsh, and Marius Peters. "Vertically mounted bifacial photovoltaic modules: A global analysis". In: *Energy* 61 (2013), pp. 447–454. ISSN: 0360-5442.

[34] Sami Jouttijärvi et al. "Benefits of bifacial solar cells combined with low voltage power grids at high latitudes". In: *Renewable and Sustainable Energy Reviews* 161 (2022), p. 112354. ISSN: 1364-0321.

[35] H. Marrou et al. "Microclimate under agrivoltaic systems: Is crop growth rate affected in the partial shade of solar panels?" In: *Agricultural and Forest Meteorology* 177 (2013), pp. 117–132. ISSN: 01681923. DOI: 10.1016/j.agrformet.2013.04.012. URL: http://dx.doi.org/10.1016/j.agrformet.2013.04.012.

[36] Hélène Marrou, Lydie Dufour, and Jacques Wery. "How does a shelter of solar panels influence water flows in a soil–crop system?" In: *European Journal of Agronomy* 50 (2013), pp. 38–51. ISSN: 1161-0301.

[37] H. Marrou et al. "Productivity and radiation use efficiency of lettuces grown in the partial shade of photovoltaic panels". In: *European Journal of Agronomy* 44 (Jan. 2013), pp. 54–66. ISSN: 1161-0301. DOI: 10.1016/J.EJA.2012.08.003.

[38] Jianan Zheng et al. "Increasing the comprehensive economic benefits of farmland with Even-lighting Agrivoltaic Systems". In: *Plos one* 16.7 (2021), e0254482. ISSN: 1932-6203.

[39] Jaiyoung Cho et al. “Application of Photovoltaic Systems for Agriculture: A Study on the Relationship between Power Generation and Farming for the Improvement of Photovoltaic Applications in Agriculture”. In: *Energies* 13.18 (2020), p. 4815.

[40] Rakeshkumar Mahto et al. “Agrivoltaics: A Climate-Smart Agriculture Approach for Indian Farmers”. In: *Land* 10.11 (2021), p. 1277.

[41] EMILIANO BELLINI. *Giant agrivoltaic project in China*. 2020. URL: https://www.pv-magazine.com/2020/09/03/giant-agrivoltaic-project-in-china/.

[42] Hassan Imran, Muhammad Hussnain Riaz, and Nauman Zafar Butt. “Optimization of single-axis tracking of photovoltaic modules for agrivoltaic systems”. In: *2020 47th IEEE Photovoltaic Specialists Conference (PVSC)*. IEEE, 2020, pp. 1353–1356. ISBN: 1728161150.

[43] SASCHA KRAUSE-TÜNKER HEIKO HILDEBRANDT. “Next2Sun GmbH”. In: (2014). URL: https://www.next2sun.de/en/homepage/.

[44] Heiko Hildebrandt et al. *Photovoltaic system and associated use*. May 2020.

[45] *Next2Sun reference Agrivoltaics systems*. URL: https://www.next2sun.de/en/references/.

[46] “Global Photovoltaic Power Potential by Country”. In: *Global Photovoltaic Power Potential by Country* June (2020). DOI: 10.1596/34102.

[47] Dejene Assefa Hagos, Alemayehu Gebremedhin, and Björn Zethraeus. “Solar water heating as a potential source for inland Norway energy mix”. In: *Journal of Renewable Energy* 2014 (2014). ISSN: 2314-4386.

[48] Renewable Energy World. *New utility-scale solar needs far less land than a decade ago, LBNL says*. 2022. URL: https://www.renewableenergyworld.com/news/new-utility-scale-solar-needs-far-less-land-than-a-decade-ago-lbnl-says/#gref.

[49] På oppdrag fra Solenergiklyngen. *Status update on the Norwegian solar PV market 2020*. 2021. URL: https://www.solenergiklyngen.no/2021/06/24/status-update-on-the-norwegian-solar-pv-market-2020/.

[50] Multiconsult og Asplan Viak and På oppdrag fra Solenergiklyngen. *Solcellesystemer og sol i systemet*. Tech. rep. 2018, pp. 1–88. URL: https://288856-www.web.tornado-node.net/wp-content/uploads/2021/02/180313-rapport_solkraft-markedsutvikling-2017-endelig.pdf.

[51] Multiconsult. *Markedstall for ny solenergi som er koblet til det norske kraftsystemet i løpet av 2018*. Tech. rep. 2018. URL: https://288856-www.web.tornado-node.net/wp-content/uploads/2021/02/20190301_oppsummering_markedstall_2018-1.pdf.

[52] Multiconsult. *Assessment of the Norwegian Solar PV Market in 2019*. Tech. rep. 2019. URL: https://288856-www.web.tornado-node.net/wp-content/uploads/2021/02/10218328-tvf-not-001_norway-2019-solar-pv-market-sizing_english-summary.pdf.

[53] EMILIANO BELLINI. "Norway deployed 65MW of solar in 2021". In: *pv magazine* (Jan. 2022). URL: https://www.pv-magazine.com/2022/01/19/norway-deployed-65mw-of-solar-in-2021/.

[54] KJERSTI KILDAHL. *Nine facts about Norwegian agriculture*. 2020. URL: https://www.nibio.no/en/news/nine-facts-about-norwegian-agriculture.

[55] H Steinshamn, L Nesheim, and A K Bakken. "Grassland production in Norway". In: *Proceedings of the 26th General Meeting of the European Grassland Federation, The Multiple Roles of Grassland in the European Bioeconomy, Trondheim, Norway, September*. 2016, pp. 4–8.

[56] NIBIO. *Norwegian Agriculture Status and Trends 2019*. 2020. URL: https://nibio.brage.unit.no/nibio-xmlui/handle/11250/2643268.

[57] Indexmundi. *Electricity consumption per capita*. 2020. URL: https://www.indexmundi.com/map/?v=81000.

[58] IEA. *Key energy statistics, 2020 of Norway*. 2020. URL: https://www.iea.org/countries/norway.

[59] statista.com. *Population in Norway from 2011 to 2021*. 2022. URL: https://www.statista.com/statistics/586331/total-population-in-norway/#:~:text=In%202021%2C%20the%20number%20of,more%20males%20living%20in%20Norway..

[60] The Norwegian Water Resources and Energy Directorate (NVE). *Electricity Consumption in Norway towards 2030*. 2018. URL: https://www.nve.no/energy-consumption-and-efficiency/energy-consumption-in-norway/electricity-consumption-in-norway-towards-2030/.

[61] Matthieu Chiodetti et al. "PV bifacial yield simulation with a variable albedo model". In: *the sun* 1 (2016), p. 4.

[62] Deutsche Gesellschaft für Sonnenenergie (DGS). *Planning and installing photovoltaic systems: a guide for installers, architects and engineers*. Routledge, 2013. ISBN: 1136528237.

[63] Stuart Bowden and Christiana Honsberg. *PVCDROM*. URL: https://www.pveducation.org/.

[64] Jinsuk Kang and C Reise. "Practical Comparison Between view factor method and raytracing method for bifacial PV system yield prediction". In: *36th European PV Solar Energy Conference and Exhibition*. 2019.

[65] Enrico M Vitucci et al. "Bifacial_radiance: a python package for modeling bifacial solar photovoltaic systems". In: *Solar Energy* 5.NREL/JA-5K00-75222 (2018), pp. 412–438. ISSN: 0038-092X.

[66] Stanford.edu. *Types of Ray Tracing*. URL: https://cs.stanford.edu/people/eroberts/courses/soco/projects/1997-98/ray-tracing/types.html.

[67] Christiana Honsberg, Bowden, and Stuart. *Typical Meteorological Year Data (TMY).* URL: https://www.pveducation.org/pvcdrom/properties-of-sunlight/typical-meteorological-year-data-tmy.

[68] S. Wilcox and W. Marion. *Users Manual for TMY3 Data Sets:Technical Report NREL/TP-581-43156.* Tech. rep. 2008, pp. 1–58. URL: https://www.nrel.gov/docs/fy08osti/43156.pdf.

[69] Climate Analytics. *EnergyPlus Weather File (EPW) Format.* URL: https://designbuilder.co.uk/cahelp/Content/EnergyPlusWeatherFileFormat.htm.

[70] Jose Chen Lopez. *Influence of Light on Crop Growth.* 2021. URL: https://www.pthorticulture.com/en/training-center/influence-of-light-on-crop-growth/.

[71] Christiana B. Honsberg et al. "Agrivoltaic Modules Co-Designed for Electrical and Crop Productivity". In: *Conference Record of the IEEE Photovoltaic Specialists Conference* (2021), pp. 2163–2166. ISSN: 01608371. DOI: 10.1109/PVSC43889.2021.9519011.

[72] Blokenearexeter. *Timothy grass (Phleum pratense L.) in Tiverton.* URL: https://commons.wikimedia.org/w/index.php?curid=20200543.

[73] 12 January 2007 (UTC) Kristian Peters – Fabelfroh 10:27. *Festuca pratensis.* URL: https://commons.wikimedia.org/w/index.php?curid=1554674.

[74] Ivar Leidus. *Trifolium pratense.* 2016. URL: https://commons.wikimedia.org/w/index.php?curid=50438310.

[75] Rasbak. *Lolium perenne.* URL: https://commons.wikimedia.org/w/index.php?curid=138144.

[76] M B Jones. "Plant microclimate". In: *Techniques in bioproductivity and photosynthesis.* Elsevier, 1985, pp. 26–40.

[77] *System Advisor Model Version 2021.12.02 (SAM 2021.12.02). National Renewable Energy Laboratory. Golden, CO. Accessed Feb 17, 2022.*

[78] Mostapha Sadeghipour Roudsari, Michelle Pak, and Adrian Smith. "Ladybug: a parametric environmental plugin for grasshopper to help designers create an environmentally-conscious design". In: *Proceedings of the 13th international IBPSA conference held in Lyon, France Aug.* 2013, pp. 3128–3135.

[79] Michelle Sadeghipour Roudsari Mostapha; Pak. *Ladybug tool EPW map.* 2013. URL: https://www.ladybug.tools/epwmap/.

[80] Jeff Oppong. *How to Use ArcGIS Pro to Calculate Land Surface Temperature (LST) from Landsat Imagery.* 2021. URL: https://www.gislounge.com/how-to-use-arcgis-pro-to-calculate-land-surface-temperature-lst-from-landsat-imagery/.

[81] Maharshi Vyas et al. "Solar Photovoltaic Tree: Urban PV power plants to increase power to land occupancy ratio". In: *Renewable Energy* 190 (May 2022), pp. 283–293. ISSN: 0960-1481. DOI: 10.1016/J.RENENE.2022.03.129.

[82] Amy Lindsay et al. “Key elements in the design of bifacial PV power plants”. In: *31st European photovoltaic solar energy conference and exhibition*. 2015, pp. 1764–1769.

[83] EMILIANO BELLINI. “Japan’s first vertical agrivoltaic project”. In: *pv magazine* (2022). URL: https://www.pv-magazine.com/2022/04/26/japans-first-vertical-agrivoltaic-project/.

[84] Ian Ashdown and Greg Ward. *gendaymtx - generate an annual Perez sky matrix from a weather tape*. Tech. rep. 2013, pp. 1–2. URL: https://www.radiance-online.org//learning/documentation/manual-pages/pdfs/gendaymtx.pdf.

[85] Silvana Ayala Pelaez et al. “Comparison of bifacial solar irradiance model predictions with field validation”. In: *IEEE Journal of Photovoltaics* 9.1 (2018), pp. 82–88. ISSN: 2156-3381.

[86] Edward Georg Hagen. *Info about Skjetlein*. URL: https://web.trondelagfylke.no/skjetlein-videregaende-skole/om-skolen/kort-info-om-skjetlein/.

[87] Ulrik Vieth Rør. “Analysis of discrepancies between simulated and actual energy production for a photovoltaic system in Norway”. PhD thesis. Norwegian University of Life Sciences, 2016.

[88] Helge Bonesmo and Gilles Bélanger. “Timothy yield and nutritive value by the CATIMO model: I. Growth and nitrogen”. In: *Agronomy Journal* 94.2 (2002), pp. 337–345. ISSN: 0002-1962.

[89] Tomas Persson et al. “Simulation of timothy nutritive value: A comparison of three process-based models”. In: *Field Crops Research* 231 (2019), pp. 81–92. ISSN: 0378-4290.

[90] Xingshu Sun et al. “Optimization and performance of bifacial solar modules: A global perspective”. In: *Applied energy* 212 (2018), pp. 1601–1610. ISSN: 0306-2619.

[91] Elin Molin et al. “Experimental yield study of bifacial PV modules in nordic conditions”. In: *IEEE Journal of Photovoltaics* 8.6 (2018), pp. 1457–1463. ISSN: 2156-3381.

[92] Heine Nygard Riise et al. “Performance analysis of a BAPV bifacial system in Norway”. In: *2021 IEEE 48th Photovoltaic Specialists Conference (PVSC)*. IEEE, 2021, pp. 1304–1308. ISBN: 1665419229.

[93] Kelsey Horowitz et al. *Capital Costs for Dual-Use Photovoltaic Installations: 2020 Benchmark for Ground-Mounted PV Systems with Pollinator-Friendly Vegetation, Grazing, and Crops*. Tech. rep. 2020.

[94] Nicholas Riedel-Lyngskær et al. “The effect of spectral albedo in bifacial photovoltaic performance”. In: *Solar Energy* 231 (2022), pp. 921–935. ISSN: 0038-092X.

[95] Amir Vadiee. *Energy analysis of the closed greenhouse concept: Towards a sustainable energy pathway*. 2011.

[96] Makoto Tajima and Tetsunari Iida. “Evolution of agrivoltaic farms in Japan”. In: *AIP Conference Proceedings* 2361.1 (2021), p. 30002.

[97] Jens Vollprecht, Max Trommsdorff, and Charis Hermann. “Legal framework of agrivoltaics in Germany”. In: *AIP Conference Proceedings*. Vol. 2361. 1. AIP Publishing LLC, 2021, p. 20002. ISBN: 0735441049.

[98] EMILIANO BELLINI. “France defines standards for agrivoltaics”. In: *pv magazine* (2022). URL: https://www.pv-magazine.com/2022/04/28/france-defines-standards-for-agrivoltaics/.

[99] EMILIANO BELLINI. “Italian solar sector defines standards for agrivoltaics”. In: *pv magazine* (2022). URL: https://www.pv-magazine.com/2022/03/11/italian-solar-sector-defines-standards-for-agrivoltaics/.

8 Appendix

8.1 Sun Hours Python script

Please find the python scripts by clicking here

8.2 PVsyst documentation of 50 kWp agrivoltaic system

By clicking on following bullet points, various reports and details can we viewed:

- PVsyst simulation report can accessed by clicking here.
- How is the PR (Performance Ratio) calculated ?

8.3 Animations of shade analysis

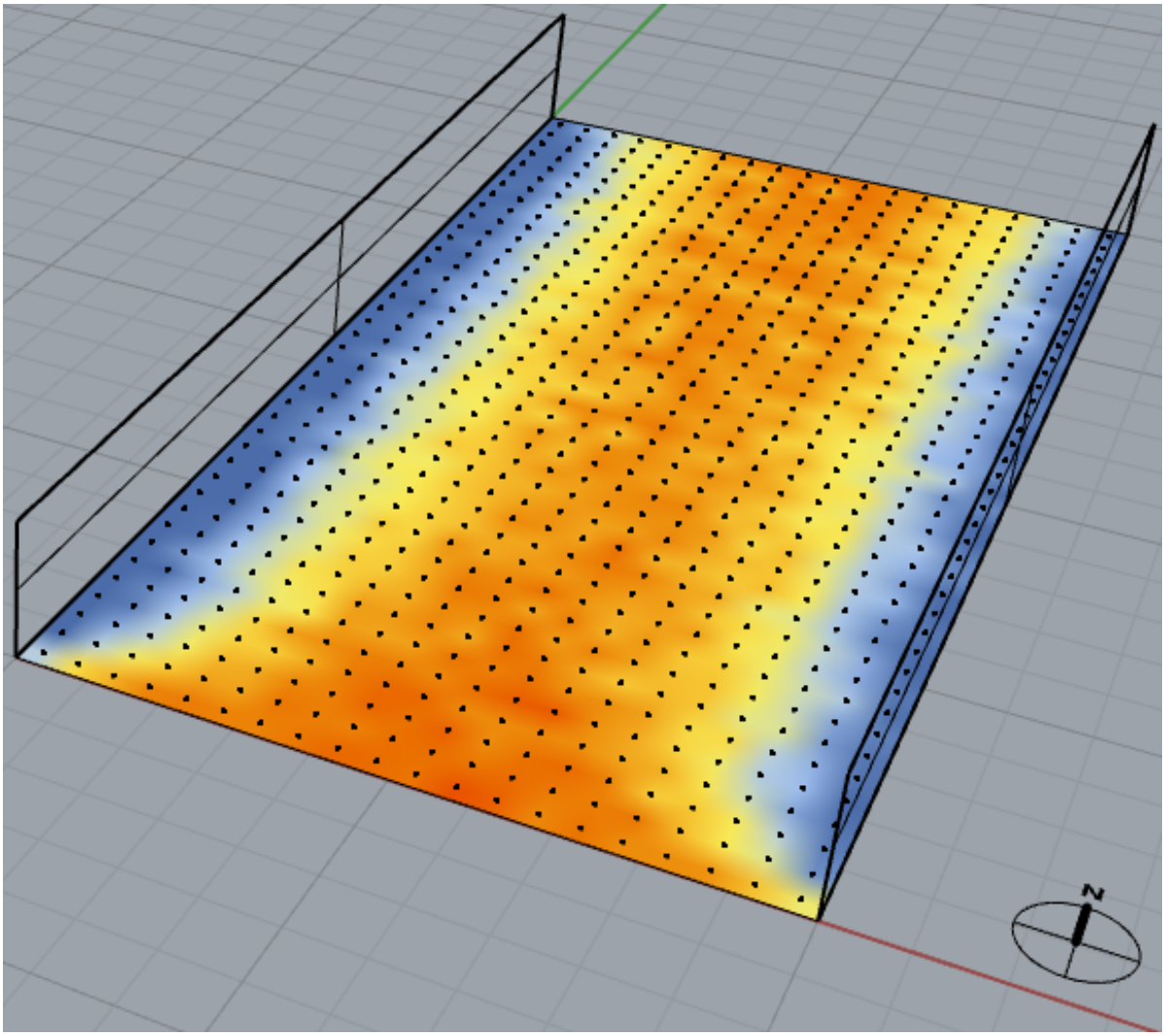

Figure 72: Animation showing distribution of shade as azimuth is changed from E/W to N/S. Dimensions of the geometry: P=10 m, R=20 m, M=2 m, H=0 m.

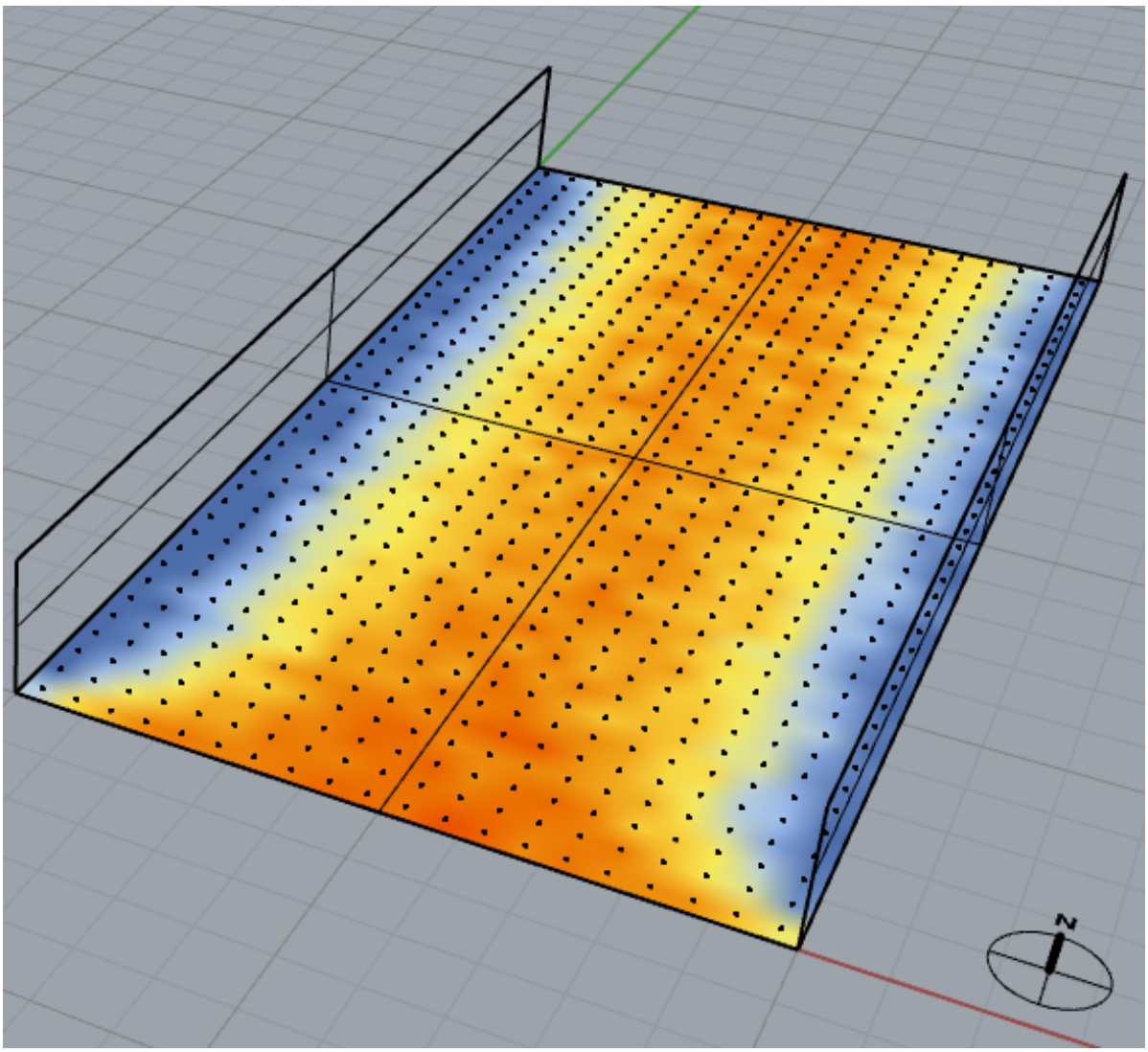

Figure 73: Animation showing distribution of shade as ground clearance height(H) is changed from 0 m to 2 m at interval of 0.5. Dimensions of the geometry: P=10 m, R=20 m, M=2 m.

8.4 Flow chart of Methodology

Figure 74 gives an illustration of flow chart representing overall workflow of the thesis.

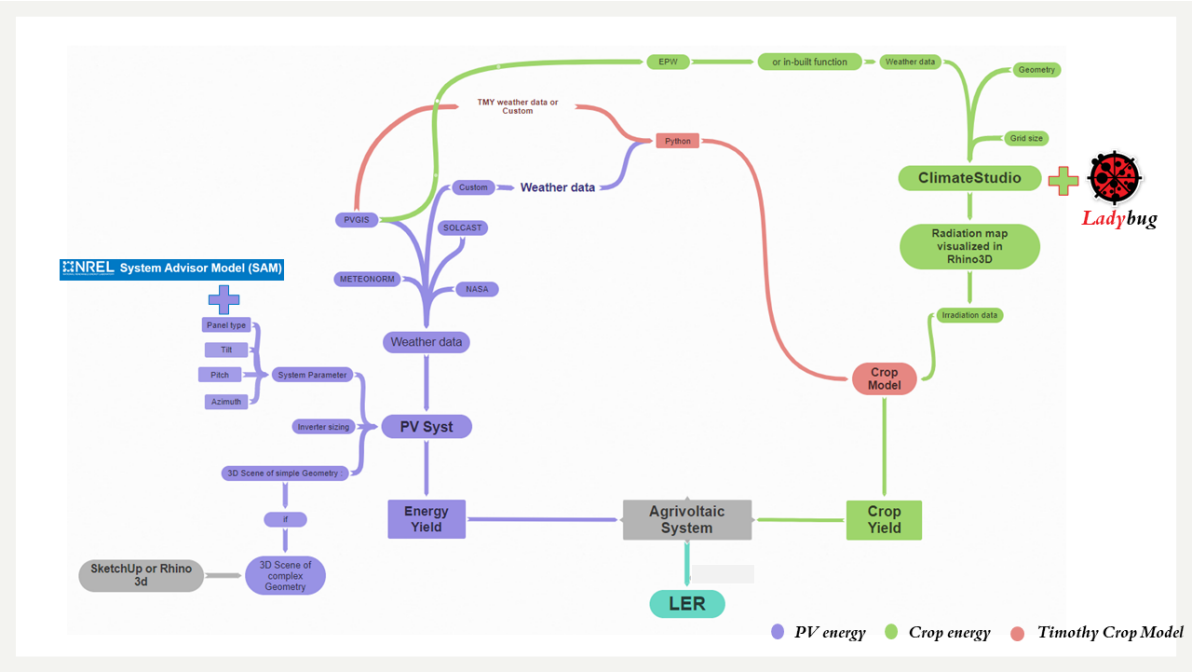

Figure 74: Flow chart describing the process followed to design a vertical bifacial East/West agrivoltaic system.

NTNU
Norwegian University of
Science and Technology

DTU